C^{12}/C^{13} RATIO FROM CN BANDS IN THE NEAR INFRA-RED SPECTRA OF SOME CARBON STARS

by

JOHN THOMAS HOLTS

B.Sc. University of Victoria, 1969.

A THESIS SUBMITTED IN PARTIAL FULFILLMENT
OF THE REQUIREMENTS FOR THE DEGREE OF
MASTER OF SCIENCE
in the Department
of
Physics

We accept this thesis as conforming
to the required standard

[redacted]

UNIVERSITY OF VICTORIA

June, 1972.

Supervisor: Dr. J. L. Climenhaga

ABSTRACT

Synthetic spectra were produced in order to study the C^{12}/C^{13} ratio from CN bands in carbon stars. All the lines of $C^{12}N^{14}$ and $C^{13}N^{14}$ were included in the region from λ8000 A to λ8300 A. A Voigt profile was assumed and various turbulent velocities were used in the calculations. Three temperatures were used in making the theoretical calculations, 3150, 2800 and 2400 K.

Two methods were used to determine the isotope ratio. The first involved the matching of the synthetic spectra to the observed spectra of the star. The second method was a modification of Fujita's empirical pseudo-curve of growth method (Fujita, 1970).

The results of the empirical pseudo-curve of growth method were much lower than those found by Fujita (1970) but agreed well with the results of the other method. The averages of both methods for the assumed excitation temperature are:

Star	Temperature	C^{12}/C^{13}
19 Psc	2800 K	6.0
DS Peg	2800	8.6
Y CVn	3150	4.2
UX Dra	2800	6.4

[redacted]

ACKNOWLEDGEMENTS

I wish to express my gratitude to my supervisor Dr. J. L. Climenhaga, Dean of Arts and Science, for his suggestion of the problem and his continued help throughout this work. I also wish to thank Dr. J. B. Tatum and the other members of the committee for their many helpful suggestions. I wish to thank Dr. Wright for the use of the facilities and equipment at the Observatory. Finally I am grateful for the University of Victoria Graduate Scholarship which I received in 1969/70 and 1970/71 and also the National Research Council for the Bursary held in 1971/72.

TABLE OF CONTENTS

LIST OF TABLES

LIST OF FIGURES

CHAPTER 1

INTRODUCTION

1.1 General introduction.

The abundance of the more common form of carbon, C^{12}, relative to another of its isotopic forms, C^{13}, is of particular interest to astrophysicists as C^{13} is a byproduct of the CNO bi-cycle. The C^{13} that is produced in the star's interior is brought to the surface by convection currents. It is thought that the equilibrium value of the abundance ratio C^{12}/C^{13} is about four (Caughlin, 1965) for the CNO bi-cycle. However before equilibrium is reached the ratio may be as low as three.

One variation of C^{13} production, proposed by Hayashi (1964), allows the C^{13} to become even more abundant. If the abundance of hydrogen is sufficiently low, in an intermediate helium zone, C^{12} will be converted into N^{13} which decays to C^{13}. The next step in the CNO bi-cycle does not take place because the hydrogen abundance is too low. The end product of the reaction is C^{13} and its abundance continues to increase.

The lower limit of the abundance ratio one would expect to observe may be less than three while the upper limit may possibly approach or exceed the terrestrial value of ninety. Depending on the amount of mixing within the star the observed abundance ratio could be any value in this range, assuming the CNO bi-cycle is operating. Studies of the rate of mixing (Caughlin, 1965) indicate that the ratio would be of the order of ten or less. If the observed C^{13} abundance is near the terrestrial value the only explanations would be that the CNO nuclei could not have gone through hydrogen burning for any length of time, that the C^{13} that

was created was destroyed by some other process or that the C^{13} was not brought to the surface by convection.

If the relative abundances of these two carbon isotopes, (C^{12}/C^{13}), can be determined in a star's atmosphere, then the amount of mixing taking place and the presence of the CNO bi-cycle would be indicated. The spectrum of atomic carbon is unsuitable for the study of the isotopic abundances as the isotopic shift in wavelength is negligible for such massive nuclei as carbon. The isotopic shift of molecular lines is a function of the reduced masses of the two molecules containing the different isotopes and is large enough to resolve the C^{12} and C^{13} features easily. The prominent C_2 and CN bands in the carbon stars are suitable for studying the C^{12}/C^{13} abundance ratio.

1.2 Early work.

The first reported observations of C^{13} were made in 1929 (Sanford, 1929) when the (1,0) band head of the Swan $C^{12}C^{13}$ system was recognized at 4745.2 A. Another band head at 4752.7 A was first thought to be $C^{12}C^{14}$ but was later found to agree better with the calculated position of $C^{13}C^{13}$ (Menzel, 1930). These early spectrograms had a very low dispersion and only a very rough estimate of the C^{12}/C^{13} ratio could be made. The estimated value from these early spectrograms was from three to five with an upper limit of ten.

Shajn (1942) studied several N type carbon stars, again at a low dispersion, using not only the (1,0) band but also the (0,1) and (0,2) bands of the Swan system of C_2. He found a variation in the abundance ratio between 2 and 20 from the ratios of the intensities of the $C^{12}C^{12}$ and $C^{12}C^{13}$ band heads. The spectrograms were suitable for photometric measurements and the intensities were measured from microphotometer tracings.

Only in one star did he find definite evidence of $C^{13}C^{13}$ (Y CVn) and in R CrB there was no trace of the isotopic bands of $C^{12}C^{13}$ and $C^{13}C^{13}$. This was the first indication of a possible range in the abundance of C^{13}. However it was uncertain at first whether the difference in intensities of the different isotopic bands was due only to a difference in abundance or was due to the conditions of excitation. It was found that the ratio of intensities of $C^{12}C^{13}$ bands to $C^{12}C^{12}$ bands increased enormously between laboratory measurements using an arc and those using a furnace, for the same mixture of $C^{12}C^{12}$ and $C^{12}C^{13}$. Fortunately one can check the accuracy of the abundance ratio determined from $C^{12}C^{13}$ and $C^{12}C^{12}$ bands with that obtained from $C^{13}C^{13}$ and $C^{12}C^{12}$ bands. The ratios found by Shajn (1942) for Y CVn using these bands agreed within experimental error.

1.3 Extensive studies by McKellar.

The earlier works were concentrated mainly on a small number of N type stars and used different methods to determine the relative intensities of the bands and thereby the C^{12}/C^{13} ratio. McKellar (1948, 1949) instigated an observing program designed to cover a large sample of both N and R type carbon stars with several spectrograms of each star. A total of twenty-one R stars was studied at dispersions of 42 and 70 A/mm. An attempt was made to account for the overlapping of isotopic bands of the C_2(1,0) band by lowering the continuum by an appropriate amount, determined from those stars in the study which showed little or no evidence of $C^{12}C^{13}$ bands. Also an attempt was made to remove the effects of atomic and other molecular lines by subtracting the intensities observed in the same regions of the spectra of the sun and Arcturus from the

measured intensity. Curve of growth effects were assumed to be small for fifteen of the twenty-one stars and the abundance ratio was determined from the relative intensities of the $C^{12}C^{12}$, $C^{12}C^{13}$ and $C^{13}C^{13}$ bands. If this assumption is valid then the material through which the light has passed is optically thin and the intensity (equivalent width) is a linear function of the number of molecules. A more complete description of the curve of growth effect will be given in a later chapter of this thesis. Of the fifteen stars the abundance for three was found to be greater than thirty and for the other twelve the average abundance ratio obtained was 3.4 .

For the other stars the $C^{12}C^{12}$ bands were probably saturated while the $C^{12}C^{13}$ bands were not. If the equivalent widths of these bands had been used directly, the abundance ratio determined would have been a lower limit because the actual number of $C^{12}C^{12}$ molecules giving rise to the band would have been greater than the number supposed.

At the time, this survey (McKellar, 1948) was the best available because it treated a large number of stars with as high a dispersion as was feasible. In the band head regions studied (7.5 A wide) there were as many as seventy lines blended together. To study the band structure a much higher dispersion was necessary. It appeared that carbon stars could be separated into two groups with different C^{13} abundances, one group with a small C^{13} abundance approaching the terrestrial value and the other with a high C^{13} abundance. Although this is what one might expect from current theories (Caughlin, 1965) it was in conflict with theories held at the time. The theoretical equilibrium C^{12}/C^{13} ratio was thought to be seventy and the initial ratio before the onset of

the CNO bi-cycle would have had to be near three (McKellar, 1948) to account for the observations. This was completely opposite to the current theoretical work on the CNO bi-cycle stated earlier in this thesis.

1.4 Recent surveys.

Wyller (1957) attempted to deal with the overlapping of bands in a different way. He became aware of the problem of overlapping bands when the rotational temperature derived from the intensity ratios of four C_2 bands showed a large variation. The cause of this discrepancy was the additional absorption due to $C^{12}C^{13}$ and $C^{13}C^{13}$ bands overlapping the measured $C^{12}C^{12}$ bands. The effect of blending was considered dy calculating theoretically the ratio of the contribution of these bands and the strength of the P_2 band head as a function of temperature. From such a graph, for a given temperature, the intensity ratio could be found. By multiplying this ratio by the observed equivalent width of the P_2 branch band head, the actual contribution to the other regions could be found. The effects of the curve of growth were still not taken into account as direct intensities were used to form the theoretical ratios, not equivalent widths.

In more recent work (Wyller 1959, 1960) a different region was studied and the CN molecule was included. The contribution of other bands to the $C^{12}C^{13}$ bands and to the $C^{13}N^{14}$ bands was removed as before. Also the observed equivalent width was reduced to account for atomic absorption. After both of these corrections had been applied to the obseved equivalent widths the abundance ratio was calculated. One disadvantage of the method was that once again curve of growth effects

were omitted. Another source of error in the final value was the size of the correction applied to some of the equivalent widths. In one case (19 Psc) the unreduced (0,2) $C^{12}C^{13}$ equivalent width was 4.12 Angstroms and after corrections were applied it was only 0.95 Angstroms. The resulting error in this value would be the compounded errors in the choice of excitation temperature, contribution of blending and to atomic absorption.

Since the red system of CN had not been extensively studied the line positions were calculated using theoretical formulas and constants determined from a best fit to laboratory measurements that were available. Extensive tables of the CN red system (Davis and Phillips, 1963) had not yet been published. When the earlier calculated positions used by Wyller were compared to these tables there was a difference of from 0,5 A to 0.8 A in the band head regions. The accuracy was sufficient if only small regions were studied as this error was almost constant for low rotational quantum numbers (lines near the band head). In order to study a large region with overlapping bands either the tabulated line postions or a better fit of the theoretical equations to these observed line postions would be necessary. Also if the constants for $C^{12}N^{14}$ were known the constants for $C^{13}N^{14}$ could be calculated by relations in Herzberg (1950, p.141).

Climenhaga (1960) computed theoretical profiles of the C_2 Swan bands by summing the absorption coefficients as had Wyller but then accounted for curve of growth effects by using Minnaert's semi-empirical formula (Aller, 1953, p.372),

$$\frac{1}{R_\lambda} = \frac{1}{R_c} + \frac{1}{N\alpha_\lambda} \qquad 1.1$$

where R_λ is the depth of a spectral line at wavelength λ,

R_c is the limiting depth of a line, typically 0.94 to 0.98, N is the number of molecules per unit area in the line of sight and α_λ is the molecular absorption coefficient.

The theoretical equivalent widths of the band heads were then plotted as a function of a quantity that was proportional to N, the number of molecules. Using the measured equivalent widths the ratio of the number of absorbing molecules of both $C^{12}C^{12}$ and $C^{12}C^{13}$ could be determined from these graphs. As lines of $C^{12}C^{12}$, $C^{12}C^{13}$ and $C^{13}C^{13}$ occured in the same region a combination of these lines had to be included. Different abundance ratios ranging from four to one hundred were used when calculating the profiles, covering the expected range in the abundance ratio. The results are given in column D of Table I for two of the stars studied. Two of the twelve stars studied showed no measurable amount of C^{13}, as McKellar had noted (McKellar, 1948). If the measured equivalent widths were compared directly (ignoring curve of growth effects) the calculated C^{12}/C^{13} ratio would have been decreased by 75%. The $C^{12}C^{12}$ bands were saturated while the $C^{12}C^{13}$ and $C^{13}C^{13}$ bands were not. This gave rise to the large difference.

When the calculations were extended to the red region (Climenhaga, 1966) a different method was adopted. Since the band heads of the CN red system were not as well defined, individual lines were studied. Profiles of the (4,0) CN, (2,0) CN and (0,2) C_2 bands were calculated by the same method as in the earlier paper (Climenhaga, 1960). The strength variable, a combination of the constant terms in intensity and the number of molecules, was varied until there was good agreement between the theoretical profiles and the observed intensity tracings in regions where there were lines of $C^{12}N^{14}$ and $C^{12}C^{12}$ only. Lines resulting from molecules containing C^{13}

Table I

Comparison of C^{12}/C^{13} ratio for selected stars, (by various authors).

Star	A	B	C	D	E	F	G	H	I
19 Psc	2.0		9.8	8.1	7.5		22		6.0
DS Peg		4.4		16.1	8.8		27		8.6
Y CVn	1.68	1.8	5.5		3:8		2		4.2
UX Dra		1.9						4.1	
WZ Cas		1.7				7.9		4.3	

Authors

A Wyller, 1957

B Mannino, 1957

C Wyller, 1960

D Climenhaga, 1960

E Climenhaga, 1966

F Hirai, 1969

G Fujita, 1970

H Climenhaga, Holts and Smolinski, 1971

I This thesis

were then chosen which were relatively free of atomic absorption and well separated from other molecular lines. The theoretical depths for abundance ratios of 100, 20 and 4 and the observed depths were measured for each line. The theoretical line depths were then corrected for instrumental broadening using the formula

$$I_0 = \frac{\int f(\xi)\ \Phi(x-\xi)\ d\xi}{\int \Phi(\xi)\ d\xi} \qquad 1.2$$

where $f(\xi)$ is the uncorrected profile,

$\Phi(x-\xi)$ is the observed instrumental profile

and I_0 is the corrected line depth.

The use of this formula will be described in more detail later in the section on instrumental profiles. When the corrected depths were plotted as a function of the abundance ratio, the observed abundance ratio was determined for the observed line depth.

A second method, which made use of the equivalent widths of the lines instead of depths, was also used. When a group of lines of $C^{12}N^{14}$ or $C^{12}C^{12}$ coincided in wavelength and were unblended with other lines and the corresponding lines of $C^{13}N^{14}$ or $C^{13}C^{12}$ also coincided and were unblended, then the two groups of lines were treated in the same way that the band heads were in the previous paper. The average value found from both of the methods for these bands is given in column E of table I.

A more extensive study of carbon stars was being carried out during this time by Fujita and his colleagues. Their work included classification (Fujita, 1965, 1967a, 1967b, Yamashita, 1970) and line identification (Utsumi, 1963, 1967). The whole problem of the interpretation of the spectra of carbon stars was discussed. The region from λ7800 A to λ8300 A was investigated for $C^{13}N^{14}$ features and many lines were noted

TABLE II

Comparison of empirical pseudo-curve of growth results with this thesis.

		T=	3150	2800	2520	2400	2100	1800	K
		θ=	1.6	1.8	2.0	2.1	2.4	2.8	
Star									
	1		20.0	22.0*	30.0	38.0*	70.0	80.0	
19 Psc	2		15.9	6.3		20.0			
	3		12.4	5.6		15.3			
	1		20.0	27.0*	40.0	50.0*	100.0	150.0	
DS Peg	2		12.6	7.0		17.8			
	3		23.1	10.1		26.5			
	1		2.0	3.0*	5.0	6.0*	10.0	20.0	
Y CVn	2		2.8	2.0		3.2			
	3		5.5	2.4		6.2			

1 Fujita, (1970), empirical pseudo-curve of growth method

2 This thesis, empirical pseudo-curve of growth method

3 This thesis, depths method

* interpolation from Fujita, (1970)

(tables in Fujita, 1964, 1965, 1966, 1968a, 1968b and 1970, Fujita and Utsumi, 1963, Fujita, Tsuji and Maehara, 1966). Fujita developed a method which accounts for curve of growth effects without making an assumption about the form of the relation between the number of molecules and the line depth. A description of his method as well as how it has been applied to this study is given in the section on the empirical pseudo-curve of growth method. The results obtained using this method were found by Fujita to be highly dependent on the choice of excitation temperature (Fujita, 1970, Fujita, Tsuji and Maehara, 1966). Some of the values in table II (those of Fujita) are interpolations for the temperatures used in this study. The results in column G of table I are for the excitation temperature chosen from Utsumi (1970).

The present study was the continuation of the work of Climenhaga (1966) in the red region. It was decided to extend the earlier calculations on the CN(2,0) band into the region from λ8000 A to λ8300 A and to include the CN(3,1) band. In order to consider the overlapping of two vibrational bands it was necessary to use the complete expressions for line strengths instead of simply the Hönl-London factors used previously. Those lines of the CN(2,0) band that fell in the region were as strong as those of the CN(3,1) band so that the correct intensity variation between vibrational bands had to be included. In view of the different results obtained by various authors, see table I, for the same stars it was decided to use two methods, the depths method and a modification of Fujita's method. Also as two different dispersions were employed it was possible to study the effects of an instrumental profile on the results obtained.

CHAPTER 2

EQUATIONS and METHODS

2.1 Introduction.

The computation of theoretical profiles may be broken into several parts. The first is to obtain accurate wavelengths or wavenumbers for the transitions of the atoms and molecules to be considered. Secondly an expression for the intensity of the lines as a function of temperature must be found. Next the effect of several line broadening mechanisms must be applied to the intensity. The broadening of spectral lines may arise from Doppler effects, natural broadening and collisional broadening. After the intensity as a function of wavelength is computed by summing contributions from all lines, it must be converted to a profile by use of a relation equating the intensity with line depth.

The formulae and constants used to generate the $C^{12}N^{14}$ and $C^{13}N^{14}$ line positions are discussed in section 2.2 . The intensity factors and populations of the energy levels are described in sections 2.3 and 2.4. A discussion of the absorption coefficient and broadening mechanisms is found in sections 2.5 and 2.6 . The calculation of actual line profiles as well as the addition of an instrumental profile is discussed in sections 2.7 and 2.8 . A brief description of the photographic plates follows. In the final sections the two methods used to evaluate the C^{12}/C^{13} ratio are outlined.

2.2 Line positions and notation.

Accurate positions for all lines to be studied must be obtained before a profile can be calcualted. Laboratory spectra may be measured and the line positions tabulated for future reference. Several problems

arise however. For molecular spectra the number of line positions becomes so large, (for each vibrational band there are about 600 lines in the case of CN), that using the tabulated values becomes impractical. Also tables of wavelengths often omit positions of some lines which are blended in band heads. Whole band systems are often omitted if they are weak. They contribute to the overall absorption but the individual lines cannot be identified because of blending with stronger lines. A better way to represent the tabulated data is to fit an analytical expression, which is derived from theoretical considerations of diatomic molecules, to the available observational data. The positions of unmeasured linescan then be predicted. Another advantage of the analytical formula is that once the constants are calculated for one isotopic species of a molecule, the positions for all other molecular species may be predicted. The constants need only be transformed by formulae given in Herzberg (1950, p.106) and Fay, Marenin and van Citters (1971).

Early attempts to fit an analytical formula to the observed positions of CN. (Weinard, 1955 and Godfrind, 1959). were only moderately successful for two reasons. They did not have a large number of observational data and the expressions used were only first approximations to the actual energy levels. Calculations of the constants were based on the study of only one or two vibrational band systems. The equations used did not consider the spin-orbit doubling of the lower state or the Λ doubling of the upper state.

Once extensive tables of line positions were published for CN (Davis and Phillips, 1963), Poletto and Rigutti (1965) made a least squares fit of more accurate formulae to these tables. Their results when used to predict the positions of the observed lines of high

TABLE III

Molecular Constants for $C^{12}N^{14}$, $(A^2\Pi\text{-}X^2\Sigma)$

i=	0	1	2	3	4	5
ω_i'	———	1813.474	-12.8272	5.610×10^{-3}	-4.192×10^{-4}	
ω_i''	———	2068.435	-12.9765	-3.082×10^{-2}	1.228×10^{-3}	
b_i'	1.71547	-1.73452×10^{-2}	9.583×10^{-6}	-2.756×10^{-6}	4.323×10^{-8}	-3.324×10^{-9}
	$b_6'= 1.6\times10^{-10}$	$b_7'= 3\times10^{-12}$				
b_i''	1.89931	-1.72786×10^{-2}	-4.740×10^{-5}	4.512×10^{-7}	3.533×10^{-10}	7.87×10^{-12}
d_i'	6.1534×10^{-6}	7.81×10^{-9}	6.83×10^{-10}	1.164×10^{-10}		
d_i''	6.3782×10^{-6}	4.39×10^{-8}	-9.65×10^{-9}	6.90×10^{-10}		
h_i'	7.47×10^{-12}	-8.0×10^{-14}				
h_i''	8.07×10^{-12}	-5.0×10^{-14}				
a_i'	-52.694	8.4652×10^{-2}	3.5089×10^{-3}			
p_i'	-6.4968×10^{-3}	1.6160×10^{-4}	-9.3257×10^{-5}			
q_i'	3.3115×10^{-4}	9.470×10^{-7}	2.332×10^{-6}			
γ_i''	1.5687×10^{-2}	-2.835×10^{-4}	1.9084×10^{-4}	-1.9352×10^{-5}		
$T_e'=$	9240.041	$T_e''=$ 0.0				

rotational quantum number yield an error of up to 0.8 A. This indicates that the equations used did not account correctly for the interaction between the rotational and vibrational motion of the molecule.

The rotational and vibrational constants and expressions for the energy levels used in this thesis were obtained from Faÿ, Marenin and van Citters (1971). They made a χ^2 fit to obtain constants based on the positions of about 1300 lines from 21 vibrational bands for N". (the rotational quantum number of the lower state) up to 100. The accuracy is said to be 0.1 A or better for lines of lower vibrational bands and N" < 80, while for bands of higher vibrational quantum number the accuracy was maintained for N" < 50.

The degree of accuracy obtained by Faÿ et al. required more adequate notation than that previously used. For example (Herzberg, 1950, p.106) the expansion of B_v as a function of v is usually taken to three terms while in Faÿ's paper the expansion is carried to eight terms in the case of the upper state and six terms for the lower state. In this thesis their notation has been adapted so that there is as little conflict with previous notation as possible and yet it is able to represent the increased number of constants. The capital letters have been used for the rotational and vibrational constants while for the coefficients of the expansion as a function of the vibrational quantum number the corresponding small letter has been used. This required changing the notation for the constants for Λ doubling and γ doubling from that used in Faÿ's paper. Also Γ_v has been used in this thesis for the γ doubling constant, while Fay used g_v and Herzberg (1950) used γ.

Instead of expressing the lambda doubling terms separately and

Figure 1.

Energy Levels CN $(A^2\Pi\text{-}X^2\Sigma)$

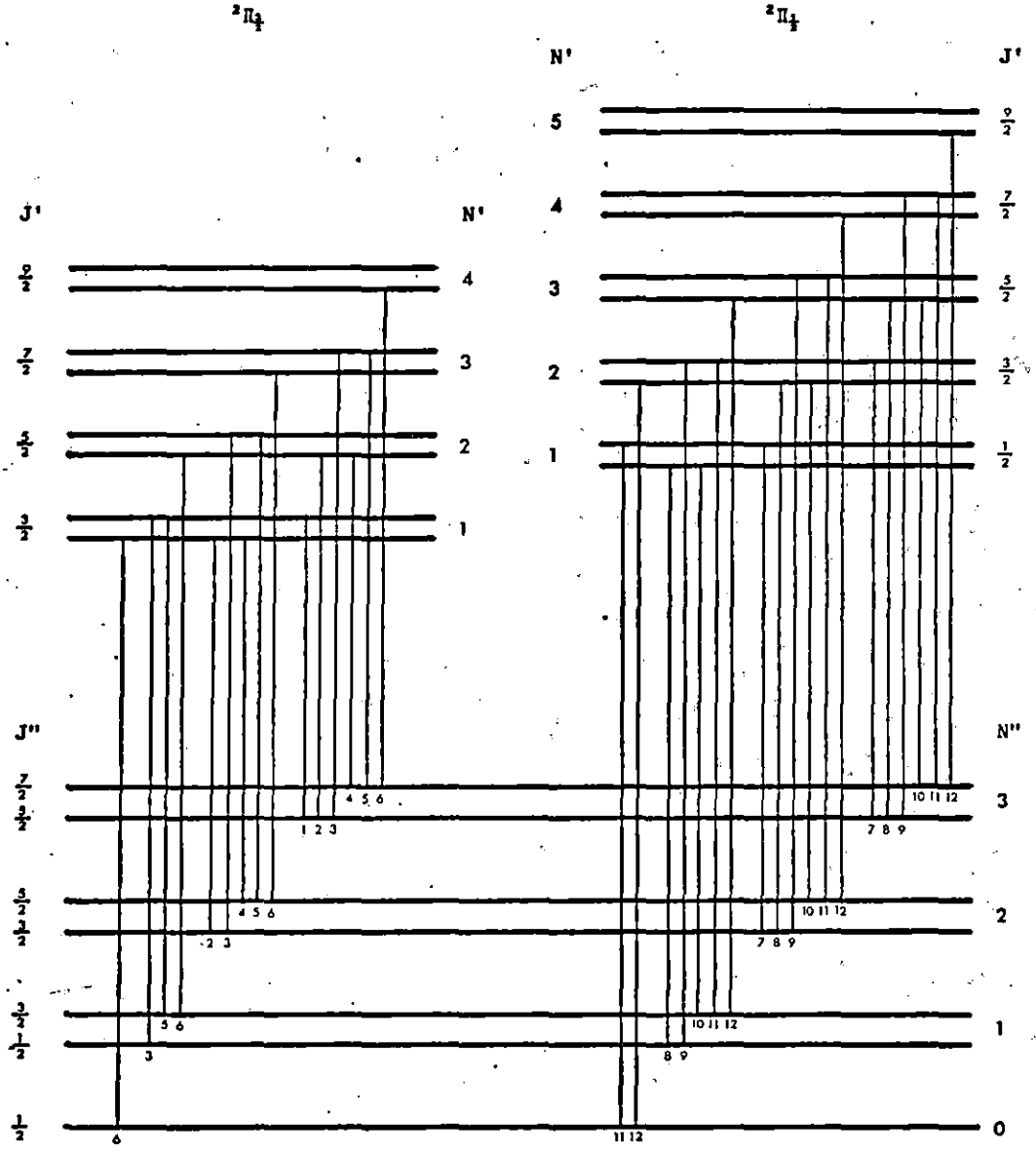

Branches

1 P_{12}	4 P_1	7 P_2	10 P_{21}
2 Q_{12}	5 Q_1	8 Q_2	11 Q_{21}
3 R_{12}	6 R_1	9 R_2	12 R_{21}

applying them to the expressions for the branches, as Faÿ et al. did, in this work they have been included in the expressions for the upper levels. Faÿ et al. use four expressions, two for the upper levels and two for the lower. Actually there are four levels, two for each rotational quantum number for each of the two upper states, and two lower levels. The different levels are indicated in diagram 1. The symbols used to denote the levels are F'_{1C}, F'_{1D}, F'_{2C}, F'_{2D}, F''_1 and F''_2. Slightly different notation was used to describe the Λ doubling terms. Herzberg uses Φ_c and Φ_d associated with F'_C and F'_D. However in this case there are four different possibilities Φ_{1C}, Φ_{2C}, Φ_{1D} and Φ_{2D}, formed by the combination of three different functions k_1, k_2 and k_3. These three functions are defined by Faÿ et al. (1971) and are from Mulliken and Christy (1931).

The formulae for both the six main and six satellite branches are included in this thesis. In figure 1 the energy level diagram for the $A^2\Pi_{inv}$-$X^2\Sigma$ transition is shown. The splitting in the upper $^2\Pi$ state is due to spin uncoupling into $^2\Pi_{1/2}$ and $^2\Pi_{3/2}$. The $^2\Pi_{3/2}$ lies lower than the $^2\Pi_{1/2}$ hence the level is inverted. That is, the spin splitting constant, A, is negative. Furthermore for each value of the upper state rotational quantum number J' there are two closely spaced levels. This splitting is caused by the interaction between the rotation of the nuclei and $\vec{L}$, the orbital electronic angular momentum vector, and is called Λ doubling. Expressed in terms of the upper state rotational quantum number, J', and with the revised notation, the formulae for the rotational energy are (Faÿ et al., 1971);

Rotational terms for the $^2\Pi$ state

$$F'_{1C}(J')=B_{v'}\{(J'+\tfrac{1}{2})^2-1-S(J')\}-D_{v'}J'^4+H_{v'}J'^6+\Phi_{1C}(J')$$

$$F'_{1D}(J')=B_{v'}\{(J'+\tfrac{1}{2})^2-1-S(J')\}-D_{v'}J'^4+H_{v'}J'^6+\Phi_{1D}(J') \qquad 2.1$$

$$F'_{2C}(J')=B_{v'}\{(J'+\tfrac{1}{2})^2-1+S(J')\}-D_{v'}(J'+1)^4+H_{v'}(J'+1)^6+\Phi_{2C}(J')$$

$$F'_{2D}(J')=B_{v'}\{(J'+\tfrac{1}{2})^2-1+S(J')\}-D_{v'}(J'+1)^4+H_{v'}(J'+1)^6+\Phi_{2D}(J')$$

where $S(J')=\tfrac{1}{2}\sqrt{4(J'+\tfrac{1}{2})^2+Y_{v'}(Y_{v'}-4)}$ 2.2

and $Y_{v'}=A_{v'}/B_{v'}$

The four terms for Λ doubling are (Fay et al., 1971);

$$\Phi_{1C}(J')= -k_1(J') -k_2(J') +k_3(J')$$

$$\Phi_{1D}(J')= k_1(J') -k_2(J') -k_3(J') \qquad 2.3$$

$$\Phi_{2C}(J')= k_1(J') +k_2(J') +k_3(J')$$

$$\Phi_{2D}(J')= -k_1(J') +k_2(J') -k_3(J')$$

and the three functions k_1, k_2 and k_3 are

$$k_1(J')=\tfrac{1}{2}\{(1-\tfrac{1}{2}Y_{v'})(\tfrac{1}{2}P_{v'}+Q_{v'})+Q_{v'}(J'-\tfrac{1}{2})(J'+\tfrac{3}{2})\}(J'+\tfrac{1}{2})/S(J')$$

$$k_2(J')=\tfrac{1}{2}(\tfrac{1}{2}P_{v'}+Q_{v'})(J'-\tfrac{1}{2})(J'+\tfrac{3}{2})/S(J') \qquad 2.4$$

$$k_3(J')=\tfrac{1}{2}(\tfrac{1}{2}P_{v'}+Q_{v'})(J'+\tfrac{1}{2})$$

The rotational constants $B_{v'}$, $D_{v'}$, $H_{v'}$, $P_{v'}$, $Q_{v'}$ and $A_{v'}$ may be expanded in terms of the vibrational quantum number v' in order to account for the interaction between the rotation and vibration of the molecule. Also the isotopic effect on the constants may be included by multiplying each term of the expansion by an appropriate power of ρ

where $\rho=\sqrt{\mu/\mu_i}$ 2.5

μ is the reduced mass of the molecule $C^{12}N^{14}$

and μ_i is the reduced mass of the molecule $C^{13}N^{14}$.

In the case of $C^{12}N^{14}$, ρ is equal to 1 in the following expansions

$$A_{v'} = \sum_{i=0}^{2} \rho^{i} \, a_i' \, (v'+\tfrac{1}{2})^i$$

$$B_{v'} = \sum_{i=0}^{7} \rho^{i+2} \, b_i' \, (v'+\tfrac{1}{2})^i$$

$$D_{v'} = \sum_{i=0}^{3} \rho^{i+4} \, d_i' \, (v'+\tfrac{1}{2})^i \qquad 2.6$$

$$H_{v'} = \sum_{i=0}^{1} \rho^{i+6} \, h_i' \, (v'+\tfrac{1}{2})^i$$

$$P_{v'} = \sum_{i=0}^{2} \rho^{i+2} \, p_i' \, (v'+\tfrac{1}{2})^i$$

$$Q_{v'} = \sum_{i=0}^{2} \rho^{i+4} \, q_i' \, (v'+\tfrac{1}{2})^i$$

The values for a_i', b_i', d_i', h_i', p_i' and q_i' are given in table III. Following convention the units of all constants are cm^{-1}. All constants for the upper state are primed, ('), even though there may not be a corresponding constant for the lower state.

The levels of the lower $^2\Sigma$ state are split by γ type doubling (Herzberg, 1950, p.222) except in the case of N"=0 for which there is only one level, (F_1''). The rotational energy levels for the lower state, expressed in terms of the quantum number N" are;

Rotational terms for the $^2\Sigma$ state

$$F_1''(N'') = B_{v''}N''(N''+1) - D_{v''}(N'')^2(N''+1)^2 + H_{v''}(N'')^3(N''+1)^3 + \tfrac{1}{2}\Gamma_{v''}N''$$

$$F_2''(N'') = B_{v''}N''(N''+1) - D_{v''}(N'')^2(N''+1)^2 + H_{v''}(N'')^3(N''+1)^3 - \tfrac{1}{2}\Gamma_{v''}(N''+1) \qquad 2.7$$

The rotational constants of the lower state may be expanded in the same way as those of the upper state;

$$\Gamma_{v''} = \sum_{i=0}^{3} \rho^{i}\, \gamma_i''\, (v''+\tfrac{1}{2})^{i}$$

$$B_{v''} = \sum_{i=0}^{5} \rho^{i+2}\, b_i''\, (v''+\tfrac{1}{2})^{i}$$

$$D_{v''} = \sum_{i=0}^{3} \rho^{i+4}\, d_i''\, (v''+\tfrac{1}{2})^{i} \qquad 2.8$$

$$H_{v''} = \sum_{i=0}^{1} \rho^{i+6}\, h_i''\, (v''+\tfrac{1}{2})^{i}$$

Note that the γ doubling constant is $\Gamma_{v''}$ instead of the customary γ. The change was necessary to maintain the use of lower case characters for the expansions and capitals for the constants. This is the only serious conflict with established notation.

These expansions for the rotational energy levels may be combined to form the twelve branches as shown in figure 1. The designation of the lines of each branch refers to the lower state quantum number N". The term values of each of the twelve branches can be calculated from the following equations;

with $J_1''=N''+\tfrac{1}{2}$ and $J_2''=N''-\tfrac{1}{2}$

Main branches

$$P_1(N'') = \nu_{oo} + F_{1C}'(J_1''-1) - F_1''(N'')$$

$$P_2(N'') = \nu_{oo} + F_{2D}'(J_2''-1) - F_2''(N'')$$

$$Q_1(N'') = \nu_{oo} + F_{1D}'(J_1'') - F_1''(N'') \qquad 2.9$$

$$Q_2(N'') = \nu_{oo} + F_{2C}'(J_2'') - F_2''(N'')$$

$$R_1(N'') = \nu_{oo} + F_{1C}'(J_1''+1) - F_1''(N'')$$

$$R_2(N'') = \nu_{oo} + F_{2D}'(J_2''+1) - F_2''(N'')$$

Satellite branches

$$P_{12}(N'')=\nu_{oo}+F'_{1D}(J''_2-1)-F''_2(N'')$$

$$P_{21}(N'')=\nu_{oo}+F'_{2C}(J''_1-1)-F''_1(N'')$$

$$Q_{12}(N'')=\nu_{oo}+F'_{1C}(J''_2)-F''_2(N'') \qquad 2.10$$

$$Q_{21}(N'')=\nu_{oo}+F'_{2D}(J''_1)-F''_1(N'')$$

$$R_{12}(N'')=\nu_{oo}+F'_{1D}(J''_2+1)-F''_2(N'')$$

$$R_{21}(N'')=\nu_{oo}+F'_{2C}(J''_1+1)-F''_1(N'')$$

where ν_{oo} is the band origin and is the difference of the electronic, T_e, and vibrational, $G(v)$, energy terms for the upper and lower states.

$$\nu_{oo}=(T'_e-T''_e)+(G'(v')-G''(v''))+(G'_e-G''_e) \qquad 2.11$$

The constants T'_e and T''_e are given in table III. $G'(v')$ and $G''(v'')$ are found from the expansions;

$$G'(v')=\sum_{i=1}^{4}\rho^i\,\omega'_i\,(v'+\tfrac{1}{2})^i$$

$$G''(v'')=\sum_{i=1}^{4}\rho^i\,\omega''_i\,(v''+\tfrac{1}{2})^i \qquad 2.12$$

There is a final term G_e for the electronic shift due to the isotope effect on the electronic levels (see Dieke, 1935). For the upper electronic state;

$$G'_e=B_{v'}\{L(L+1)-\Lambda^2\}+\frac{b'_0\rho^2}{8}\left\{3c'_2-\frac{7}{4}(c'_1)^2\right\} \qquad 2.13$$

where

$$c'_2=\frac{2\,\omega'^2_e}{3\,b'_0}+\frac{5}{4}(c'_1)^2 \qquad 2.14$$

$$c'_1=\frac{b'_1\,\omega'_e}{6(b'_0)^2}-1$$

The orbital electronic angular momentum, L, and its projection on the internuclear axis Λ were found from the free-atom approximation. When the values L=1, Λ=1 were used to predict the $C^{13}N^{14}$ positions a systematic difference was noted (Fay et. al., 1971). If L=2 was used the agreement for $C^{13}N^{14}$ was found to be better. Dieke (1935) noted that in cases of doubt the value of L could be found using formula 2.13 and the observed shifts. The constants for the lower state were calculated using the values for ω_2'', ω_1'', b_0'', b_1'' and $B_{v''}$ in equation 2.13 along with L=1 and Λ=0. In the terms c_1 and c_2 the ρ terms cancel for the isotopic molecule $C^{13}N^{14}$. That is

$$c_1 = \frac{(b_1'\rho^3)(\omega_1'\rho)}{6(b_0'\rho^2)^2} - 1 = \frac{b_1'\omega_1'}{6(b_0')^2} - 1 \qquad 2.15$$

but must be retained for the b_0' term in equation 2.13.

2.3 Line strengths.

In order to calculate an absorption profile for a line at wavelength λ the absorption oscillator strength, f_{12}, of the transition must be known. The 'f' value is related to the line strength S (Tatum, 1967) by

$$f_{12} = \frac{8\pi^2 mc}{3he^2\lambda\tilde{\omega}_1} S \qquad 2.16$$

where $\tilde{\omega}_1$ is the statistical weight of the lower level

h is Planck's constant

e is the electronic charge

m is the mass of an electron

and c is the velocity of light.

If the sum rule (equation 2.19) for the Hönl-London factors is obeyed, the statistical weight is the electronic statistical weight.

TABLE IV

Hönl-London Factors

$$P_2(J''_2)\ \Big\}\ P_{12}(J''_2) \qquad \frac{(2J''_2-1)^2 \pm (2J''_2-1)\times\{Y_v'^2,-4Y_{v'}+(2J''_2-1)^2\}^{-0.5}\times(4J''^2_2-4J''_2+1-2Y_{v'})}{16J''_2}$$

$$P_1(J''_1)\ \Big\}\ P_{21}(J''_1) \qquad \frac{(2J''_1-1)^2 \pm (2J''_1-1)\times\{Y_v'^2,-4Y_{v'}+(2J''_1-1)^2\}^{-0.5}\times(4J''^2_1-4J''_1-7+2Y_{v'})}{16J''_1}$$

$$Q_2(J''_2)\ \Big\}\ Q_{12}(J''_2) \qquad \frac{(2J''_2+1)\times[(4J''^2_2+4J''_2-1)\pm\{Y_v'^2,-4Y_{v'}+(2J''_2+1)^2\}^{-0.5}\times(8J''^3_2+12J''^2_2-2J''_2+1-2Y_{v'})]}{16J''_2\times(J''_2+1)}$$

$$Q_1(J''_1)\ \Big\}\ Q_{21}(J''_1) \qquad \frac{(2J''_1+1)\times[(4J''_1+4J''_1-1)\pm\{Y_v'^2,-4Y_{v'}+(2J''_1+1)^2\}^{-0.5}\times(8J''^3_1+12J''^2_1-2J''_1-7+2Y_{v'})]}{16J''_1\times(J''_1+1)}$$

$$R_2(J''_2)\ \Big\}\ R_{12}(J''_2) \qquad \frac{(2J''_2+3)^2 \pm (2J''_2+3)\times\{Y_v'^2,-4Y_{v'}+(2J''_2+3)^2\}^{-0.5}\times(4J''^2_2+12J''_2+1+2Y_{v'})}{16(J''_2+1)}$$

$$R_1(J''_1)\ \Big\}\ R_{21}(J''_1) \qquad \frac{(2J''_1+3)^2 \pm (2J''_1+3)\times\{Y_v'^2,-4Y_{v'}+(2J''_1+3)^2\}^{-0.5}\times(4J''^2_1+12J''_1+9-2Y_{v'})}{16(J''_1+1)}$$

When a transition arises from a single lower level then $\tilde{\omega}_1=1$.

The line strength, S, may in turn be found from the expression

$$S = \frac{\text{Hönl-London factor x Band strength}}{(2-\delta_{0,\Lambda})(2S+1)(2J+1)} \qquad 2.17$$

where $\delta_{0,\Lambda}$ is the Kronecker delta symbol and has the value 1 if $\Lambda=0$ and 0 if $\Lambda\neq0$. (Tatum, 1967).

S is the spin quantum number and equals ½ for doublet states

J is the rotational quantum number, (of the lower state for absorption).

When the spin quantum number and the value of the Kronecker delta symbol are applied equation 2.17 becomes;

$$S = \frac{\text{Hönl-London factor x Band strength}}{2(2J+1)} \qquad 2.18$$

The sum rule used for the Hönl-London factors is that, for all transitions with a common upper or lower level, the sum of the factors is (2J'+1) or (2J"+1) respectively. For example, denoting the Hönl-London factor for the R_2 state by $S(R_2)$, then

$$S(P_2)+S(P_{21})+S(Q_2)+S(Q_{21})+S(R_2)+S(R_{21})=2J'+1$$
$$\text{and } S(P_{12})+S(Q_{12})+S(R_{12})+S(P_2)+S(Q_2)+S(R_2)=2J''+1 \qquad 2.19$$

The relative Hönl-London factors for intermediate coupling between Hund's cases a and b were developed by Earls (1935). However his factors when summed as above yield (2J+1)/2. Therefore each factor was multiplied by two to obtain the absolute Hönl-London factors given in table IV. Also as suggested by Tatum (1967), the factors have been rewritten in terms of the lower quantum number J".

The band strength may be approximated as the product of the Franck-Condon factor $q_{v'v''}$ or $\int(v',v'')$ and the square of the electronic

transition moment $R_e^2(n',n'')$ or R_e^2.

2.4 Population of levels.

The population of a single level N(nvNJp) in relation to the total population N is tabulated by Tatum (1967). For the CN $^2\Sigma$-$^2\Pi$ transition in absorption the population of the lower level is required. The general formula is

$$\frac{N(nvNJp)}{N} = \frac{(2J''+1)2\phi}{Q_{el}\,Q_{vib}\,Q_{rot}}\, e^{-\{T_e+G(v'')+F(N'')\}\frac{hc}{kT}} \qquad 2.20$$

For a heteronuclear molecule such as CN, $\phi=\frac{1}{2}$ and equation 2.20 becomes

$$\frac{N(nvNJp)}{N} = \frac{(2J''+1)}{Q_{el}\,Q_{vib}\,Q_{rot}}\, e^{-\{T_e+G(v'')+F(N'')\}\frac{hc}{kT}} \qquad 2.21$$

where T_e is the energy of the lower electronic state ($^2\Sigma$)

$G(v'')$ is the energy of the lower vibrational level

$F(N'')$ is the energy of the lower rotational level

k is Boltzmann's constant

T is the molecular excitation temperature

h is Planck's constant

c is the velocity of light

Q_{el} is the electronic partition function

Q_{vib} is the vibrational partition function

and Q_{rot} is the rotational partition function.

2.5 Absorption coefficient.

To calculate line profiles one must calculate the line absorption coefficient, α_λ, including Doppler, natural and collisional broadening. The absorption coefficient at line center, α_0, is defined as (Aller,

1953, p.322 and Mihalas, 1970, p.250);

$$\alpha_0 = \frac{\sqrt{\pi}}{mc} e^2 f_{12} \lambda_0 \frac{1}{\xi_0} \frac{1}{4\pi\epsilon_0} \qquad 2.22$$

in MKS units, ($\frac{1}{4\pi\epsilon_0}$ has been added to the cgs expressions),

where e is the electronic charge

m is the electron mass

λ_0 is the line wavelength

f_{12} is the oscillator strength

c is the velocity of light

ϵ_0 is the permittivity of free space

and ξ_0 is the most probable velocity of the molecule.

Normally ξ_0 is assumed to be thermal, that is;

$$\xi_0 = \sqrt{\frac{2kT}{M}} \qquad 2.23$$

where k is Boltzmann's constant

T is the kinetic temperature

and M is the mass of the molecule.

However when microturbulence is present the microturbulent velocity ξ_t must be included, hence ξ_0 becomes;

$$\xi_0 = \sqrt{\frac{2kT}{M} + \xi_t^2} \qquad 2.24$$

The relationship between α_λ and α_0 is

$$\frac{\alpha_\lambda}{\alpha_0} = H(a,u) \qquad 2.25$$

where H(a,u) is known as the Hjerting or Voigt function, (Hjerting, 1938). It combines the effects of Doppler, natural and collisional broadening. It can be calculated from tables (Harris, 1948, Finn and Mugglestone, 1965) or from equations (Harris, 1948). The

Hjerting function can be expressed (Aller, 1953, p.323) as

$$H(a,u)=\frac{a}{\pi}\int_{-\infty}^{\infty}\frac{e^{-y^2}}{a^2+(u-y)^2}\,dy \qquad 2.26$$

where $a=\frac{\Gamma}{4\pi}\frac{\lambda^2}{\Delta\lambda_0 c}$

Γ is the effective damping constant

$\Delta\lambda_0=\frac{\lambda}{c}\xi_0$ the Doppler line width

c is the velocity of light

ξ_0 was defined previously, (equation 2.24)

$u=\frac{\lambda-\lambda_0}{\Delta\lambda_0}$

λ_0 is the wavelength of the line

and λ is the wavelength at which α_λ is being evaluated.

2.6 Voigt function evaluation.

The expression for the Voigt function (equation 2.26) may be expanded as a Taylor series for small values of a, (Aller, 1953, p.325);

$$H(a,u)=H_0(u)+aH_1(u)+a^2H_2(u)+a^3H_3(u)+a^4H_4(u)+\cdots \qquad 2.27$$

The usual method of evaluation is to use the tabulated values of H_0, H_1, H_2 and H_3 given in Harris (1948). However the table is limited to values of u between 0 and 12 in steps of 0.1 or 0.2. A step size of 0.1 in u corresponds to 0.02A at the wavelength being studied and a finer grid of values was desired so that interpolation would have been necessary if the tables were to be used.

As Harris had defined each of the terms it was possible to calculate them for any value of u so that as many points as desired could be used. The coefficients of equation 2.27 are (Harris, 1948);

$$H_0(u)=e^{-u^2}$$

$$H_1(u)= -\frac{2}{\sqrt{\pi}}\,(1-2uF(u))$$

$$H_2(u)=(1-2u^2)e^{-u^2}$$

$$H_3(u)= -\frac{2}{\sqrt{\pi}}\left\{\frac{2}{3}(1-u^2)-2u(1-\frac{2}{3}u^2)F(u)\right\} \qquad 2.28$$

$$H_4(u)=(\tfrac{1}{2}-2u^2+\frac{2}{3}u^4)e^{-u^2}$$

where $F(u)=e^{-u^2}\int_0^u e^{t^2}dt$ 2.29

Harris used tables of F(u) calculated by Miller and Gordon (1931) to evaluate the above functions, (equations 2.28). Miller and Gordon had used earlier tables of e^{-u} and $\int_0^u e^{t^2}$ for 0<u<2. For the range 2<u<6 their values were found from a complicated approximation made necessary by the lack of high speed calculating machines. For 6<u a semiconvergent series was used. For this study it was decided to recalculate F(u). Three series were found to be suitable. The first two, from Miller and Gordon (1931), are;

$$F(u)=u\left\{1-\frac{2}{3}u^2+\frac{4}{15}u^4-\frac{8}{105}u^6+\cdots+\frac{(-1)^{n+1}u^{2(n-1)}2^{n-1}}{(2n-1)(2n-3)\cdots3\cdot1}\cdots\right\} \quad 0<u<1 \qquad 2.30$$

$$F(u)=\frac{1}{2u}+\frac{1}{4u^3}+\frac{3}{8u^5}+\frac{15}{16u^7}+\cdots+\frac{(2n-3)(2n-5)\cdots3\cdot1}{2^n\,u^{2n-1}} \quad 7<u \qquad 2.31$$

For the range 1<u<7 it was decided to use an expansion for e^{t^2} in equation 2.29 and then integrate term by term. The expansion and the resulting series are;

$$F(u)=e^{-u^2}\int_0^u\left\{1+t^2+\frac{t^4}{2!}+\frac{t^6}{3!}+\cdots+\frac{t^{2n}}{n!}+\cdots\right\}dt$$

$$=e^{-u^2}\left\{u+\frac{u^3}{3}+\frac{u^5}{5\cdot2!}+\frac{u^7}{7\cdot3!}+\cdots+\frac{u^{2n+1}}{(2n+1)n!}+\cdots\right\} \qquad 2.32$$

TABLE V

Accuracy of function F(u)

Va Precision 10^{-16}

eqn.	u	n	F(u)	g_{n+1}/g_n	Maximum error
2.30	0.01	5	0.009999331274	0.000	
2.30	0.99	19	0.538794550160	-0.050	
2.32	1.00	19	0.538079506913	0.048	0.0498
2.32	6.99	122	0.072186467326	0.394	0.6469
2.31	7.00	21	0.072180974658	0.418	
2.31	15.00	10	0.033407906809	0.042	

Vb Precision 10^{-6}

eqn.	u	n	F(u)	g_{n+1}/g_n	Difference (Va-Vb)
2.30	0.01	3	0.009999331274	0.000	0.000
2.30	0.99	11	0.538794554924	-0.085	-0.000000004764
2.32	1.00	10	0.538079506479	0.083	0.000000000434
2.32	6.99	93	0.072186467087	0.514	0.000000000239
2.31	7.00	6	0.072180973688	0.112	0.000000000970
2.31	15.00	4	0.033407906722	0.016	0.000000000087

Vc

u	F(u) (Miller and Gordan, 1931)	F(u) (this thesis)
0.01	0.009999	0.009999
0.93	0.541025	0.541026
0.94	0.540910	0.540909
0.95	0.540688	0.540688
0.96	0.540363	0.540364
0.97	0.539938	0.539939
0.98	0.539414	0.539415
0.99	0.538793	0.538795
1.00	0.538080	0.538080
6.95	0.072711573	0.072711573
7.00	0.072180975	0.072180975
12.00	0.041812876	0.041812876

This series when carried to many terms will approximate F(u) to a desired accuracy for any value of u. As a test the summations for all three equations were ended when the last term was less than 10^{-16} times the sum to that point. With this accuracy the size of the last term, g_n, with respect to the first omitted term, g_{n+1}, is given in column five of table Va. For the series 2.32 the size of the maximum error is also given, expressed in terms of the last included term. The size of the error is determined from the equation, (Kaplan, 1952, p.329);

$$\text{maximum error} = \frac{u^2(2n+1)}{(n+1)(2n+3)\left\{1 - \frac{u^2(2n+3)}{(2n+5)(n+2)}\right\}} \qquad 2.33$$

As the first term omitted was less than 10^{-16} times the series total, the accuracy should be better than 15 significant figures. When the intensities were calculated the accuracy was only seven significant figures so that the series were terminated at 10^{-6}. In table Vb the calculations have been repeated using the lower accuracy. As can be seen by comparing tables Va and Vb the error, (given in column six, table Vb), is less than one in 10^{-7}. In column three the number of terms retained is given. It is easily seen that formula 2.31 requires many more terms for convergence for large u and would be impractical to use for all values of u even though valid.

The computed values of F(u) were compared with those tabulated by Miller and Gordon, (1931). Their values were tabulated to six, eight and nine significant figures whereas the new calculations were tabulated to 12 significant figures, (table Va, column 4). Some of the earlier tabulated values of F(u) did not agree with the corresponding calculated ones, (see table Vc). The difference was only ±2 in the last figure of the earlier calculations. This was quite possibly due to rounding and

truncation errors and the shortcuts which were made to save time in computing the earlier values. A table of F(u) was produced for future reference. Similarly the terms in the Voigt function expansion were evaluated and were found to agree with those of Harris (1948).

2.7 Optical depth and curve of growth effects.

The optical depth τ_λ which is necessary for the calculation of the line profile is the product of the number of absorbing molecules, N(nvNJp), and the molecular absorption coefficient, α_λ

$$\tau_\lambda = N(nvNJp)\alpha_\lambda \qquad 2.34$$

and can be calculated from previously defined equations.

Combining equations 2.16, 2.18, 2.21, 2.22, 2.26 and 2.34 One has the optical depth

$$\tau_\lambda = \frac{N\pi\sqrt{\pi}}{\varepsilon_0\ 3h\ Q_{el}\ Q_{vib}\ Q_{rot}}\ \frac{1}{\xi} \times \text{Hönl-London factor}$$

$$\times\ q_{v'v''}\ R_e^2 \times e^{-\{T''_e+G(v'')+F(N'')\}\frac{hc}{kT}} \times H(a,u) \qquad 2.35$$

For the evaluation of τ_λ the values for the combined partition function $Q=Q_{el}\ Q_{vib}\ Q_{rot}$ were taken from Tatum (1966). The Franck-Condon factors, $q_{v'v''}$, were taken from Spindler (1965) and the electronic transition moment, R_e, from Arnold, Whiting and Lyle (1969). Although not strictly true the same constants were used for both $C^{12}N^{14}$ and $C^{13}N^{14}$ as they would have been almost the same.

The relation between the optical depth and the actual line profile has been investigated by many authors. Two of the equations that have been used to produce theoretical curves of growth are (Aller, 1953, p.372);

$$R_\lambda = \frac{N\alpha_\lambda}{1+N\alpha_\lambda} = \frac{\tau_\lambda}{1+\tau_\lambda} \qquad 2.36$$

used by Menzel (1936) and

$$R_\lambda = \frac{R_c \tau_\lambda \, (\kappa_0/\kappa_\lambda)}{1+\tau_\lambda (\kappa_0/\kappa_\lambda)} \qquad 2.37$$

used by Bell, where κ_0/κ_λ allows for variation in the depth of the photosphere with wavelength. R_c is the continuum depth and represents the maximum line depth possible.

The form of the equation used in this study is

$$R_\lambda = \frac{R_c \, \tau_\lambda}{R_c+\tau_\lambda} \qquad 2.38$$

Minnaert's semi-empirical formula (Minnaert, 1935) as used by Unsöld.

Curve of growth effects arise because the intensity of a line is not a simple function of the number of atoms or molecules giving rise to the line. For weak lines the equivalent width is proportional to the number of atoms or molecules, for medium strength lines it is proportional to the square root of the logarithm of the number and for very strong lines it is proportional to the square root of the number and another term which is the result of natural and pressure broadening damping (see diagram, Aller, 1953, p.374).

Theoretical profiles can be produced by using equation 2.35 and one of 2.36, 2.37 or 2.38 for each line. If more than one line is considered then one must account for the overlapping which will occur. This may be done by summing the optical depth contributions of each line at a set of points in the region under study. In this study the sum is then used in equation 2.38 for τ_λ. The profile so produced does not take into account the finite resolving power of the spectrograph. The profile is what one would expect to see if the spectrograph had an infinitely narrow entrance slit.

2.8 Instrumental broadening.

The usual procedure in the case of instrumental broadening is to try to remove the instrumental profile from the observed profile. The integral equation to be solved has been stated many times (see Bracewell, 1955);

$$g(x)=\int_{-\infty}^{\infty}h(x-y)f(y)dy \qquad 2.39$$

where $f(x)$ is the unbroadened profile

$h(y)$ is the instrumental profile normalized so that

$\int_{-\infty}^{\infty}h(y)dy=1$

and $g(x)$ is the observed profile.

The problem is to find $f(y)$ when $g(x)$ and $h(x)$ are known. In this study for ease in calculating and because comparisons were to be made with calculated profiles it was decided to apply the instrumental broadening to the calculated profile. The instrumental profile may be found from the shape of weak emission lines of the comparison spectra on the photographic plates. When $h(x)$ and $f(x)$ are known the procedure becomes a straightforward integration over a finite, and generally quite small, range as the measured instrumental profile is not infinite in width. If the instrumental profile is not normalized to one then equation 2.39 can be rewritten in the form of equation 1.2, that is

$$g(x)=\frac{\int_{-\infty}^{\infty}h(x-y)f(y)dy}{\int_{-\infty}^{\infty}h(y)dy} \qquad 2.40$$

The instrumental profile used was assumed to be at most 1.5A wide so that equation 2.40 became in use,

$$g(\lambda)=\frac{\int_{-.75}^{.75}h(x)f(\lambda+x)dx}{\int_{-.75}^{.75}h(x)dx} \qquad 2.41$$

TABLE VI

Data on Photographic Plates Used

STAR	HD	Plate Number	Date	Julian Date	Camera	Emulsion	Dispersion
19 Psc	223075	1511	Sept 12/64	2438650.873	3262	I-N	7.9 A/mm
DS Peg	206570	1512	Sept 13/64	2438651.844	3262	I-N	7.9 A/mm
Y C Vn	110914	2412	Apr 3/66	2439218.865	3262	I-N	7.9 A/mm
UX Dra	183556	4763	July 13/69	2440415.781	3281-ISR	I-N	12.8 A/mm
19 Psc	223075	4970	Aug 31/69	2440464.993	3281-ISR	I-N	12.8 A/mm

where h(x) and f(λ+x) were tabulated and the integrals evaluated by Simpson's rule. The correction for instrumental broadening was applied to some of the computed profiles. The results will be described in chapter three.

2.9 General method.

The stellar spectrograms were taken with the 32 inch camera of the 48 inch D.A.O. telescope. For details of the spectrograph see Richardson (1968). The plates used are described in table VI. In the first two columns are the name and Henry Draper catalogue number of the star. The plate number is in column three. The date and Julian day are in the next two columns. The last three columns contain the camera number, emulsion and dispersion of the plates. The two different dispersions used made possible a check on the effects of instrumental broadening.

The plates were processed on the microphotometer at the D.A.O. giving an intensity tracing. The intensity tracing was converted to a constant continuum height on an intensitometer in order to compare the tracings with the computed profiles. A major problem arises in the measurement of spectra of late type stars. The continuum must be drawn on the intensity tracing before being reduced on the intensitometer. For cool stars the number of lines is so great that the observed profiles may never reach the continuum. Especially in the region of strong molecular bands the highest points observed may still not represent the continuum (Wright, 1962). For the two plates P:4763 and P:4970, the continuum was drawn through the highest three points in 600 A (from λ7800A to λ8400A). Although these points may not be on the continuum the error introduced is not large for either method used to evaluate the C^{12}/C^{13} ratio because

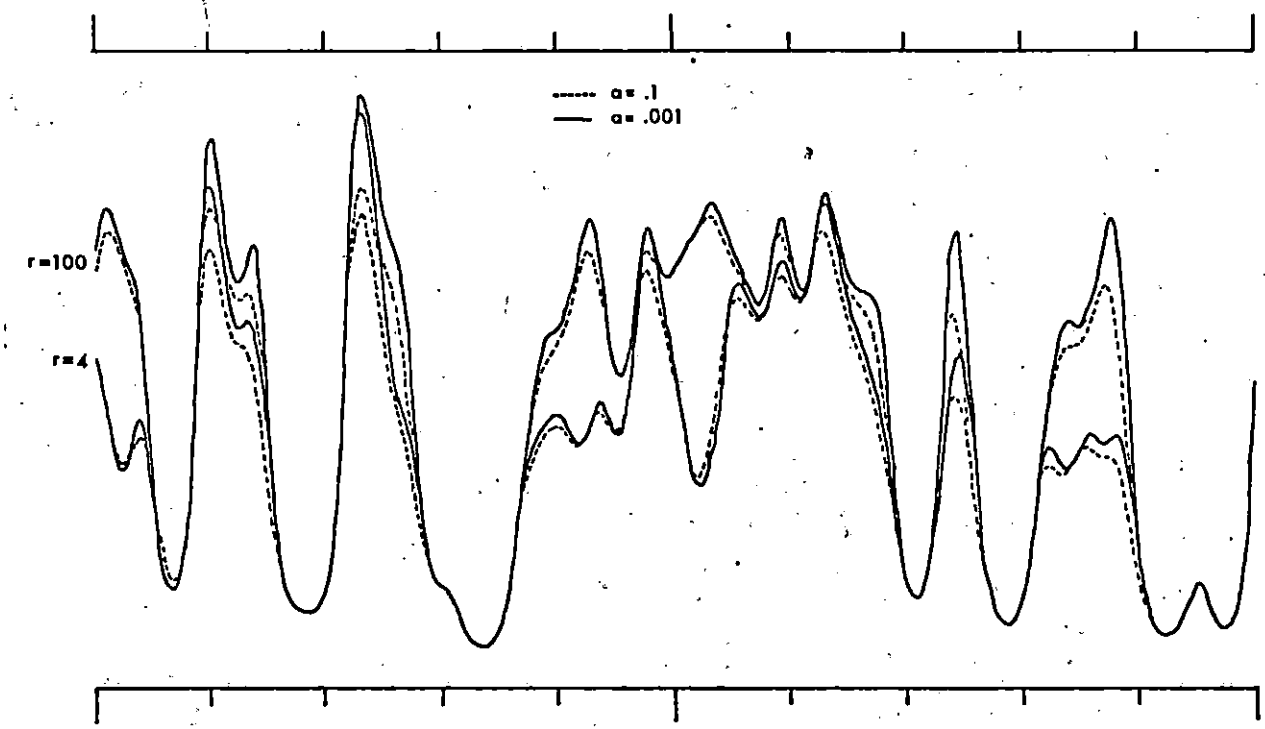

Figure 2. Comparison of profiles for different values of a.

the depths of fairly strong lines were measured. However if equivalent widths were measured any difference in the placement of the continuum would have had a large effect on the area in the wings of the line.

Once the wavelengths and intensities of the lines of $C^{12}N^{14}$ and $C^{13}N^{14}$ were calculated, the contributions of the absorption coefficient for each isotopic species were summed at intervals of 0.05A. Thus two sets of absorption coefficients were produced. These were then combined to form the total optical depth, τ_λ, as used in equation 2.38 by

$$\tau_\lambda = \tau_{\lambda_{C^{12}N^{14}}} + \frac{1}{r}\,\tau_{\lambda_{C^{13}N^{14}}} \qquad 2.42$$

where $\tau_{\lambda_{C^{12}N^{14}}}$ is the optical depth due to $C^{12}N^{14}$,

$\tau_{\lambda_{C^{13}N^{14}}}$ is the optical depth due to $C^{13}N^{14}$,

and r is the abundance ratio of C^{12} to C^{13}.

In the calculations an arbitrary constant was used in equation 2.35 for N. An additional factor was then applied when plotting profiles in order to obtain a close fit with the observed spectra. The value of the maximum line depth, R_c, was estimated for each tracing and was in the range 0.86 to 0.98 .

The choice of the ratio of damping constant to Doppler width, a, was more difficult. Climenhaga (1960) chose a=0.10 after using a=0.01 in a parallel set of calculations. In a study of the CN(4,0) band (Climenhaga, Holts and Smolinski, 1970) profiles were calculated using the values a=0.10 and a=0.001 as extremes in the possible values of a. These two profiles are compared in figure 2. The only difference appears in the wings of strong lines and has little effect on the depth of the lines. For the present study an intermediate value of 0.025 was used.

TABLE VIIA C12 N14 Line identifications

7846.30	7846.307	.1052	(5,3)	Q2(53)
	7846.346	.0290	(7,4)	R2(45)
7848.55	7848.556	.0883	(7,4)	Q2(38)
7850.40	7850.269	1.3952	(2,0)	R21(13)
	7850.270	1.3407	(2,0)	R21(14)
	7850.514	1.4434	(2,0)	R21(12)
	7850.519	1.2817	(2,0)	R21(15)
7851.00	7851.003	1.4832	(2,0)	R21(11)
	7851.019	1.2196	(2,0)	R21(16)
7851.75	7851.733	1.5122	(2,0)	R21(10)
	7851.772	1.1557	(2,0)	R21(17)
7852.75	7852.701	1.5275	(2,0)	R21(9)
	7852.779	1.0911	(2,0)	R21(18)
7853.95	7853.905	1.5261	(2,0)	R21(8)
	7854.043	1.0265	(2,0)	R21(19)
7855.35	7855.341	1.5043	(2,0)	R21(7)
7856.40	7856.325	.0826	(5,2)	P2(59)
	7856.457	.0830	(6,3)	P1(47)
7857.00	7857.006	1.4584	(2,0)	R21(6)
7858.90	7858.898	1.3842	(2,0)	R21(5)
7859.40	7859.390	.8393	(2,0)	R21(22)
7861.00	7861.014	1.2775	(2,0)	R21(4)
7861.70	7861.696	.7805	(2,0)	R21(23)
7863.35	7863.350	1.1339	(2,0)	R21(3)
7864.25	7864.267	.7240	(2,0)	R21(24)
7865.90	7865.903	.9491	(2,0)	R21(2)
7867.10	7867.103	.6699	(2,0)	R21(25)
7868.65	7868.673	.7176	(2,0)	R21(1)
7870.20	7870.207	.6184	(2,0)	R21(26)
7871.70	7871.557	.4285	(2,0)	R21(0)
	7871.679	.0787	(7,4)	Q2(40)
	7871.757	.0515	(7,4)	P2(34)
7872.80	7872.858	3.4870	(2,0)	P2(6)
	7872.887	1.7104	(2,0)	P2(3)
	7872.648	2.9842	(2,0)	P2(5)
	7872.659	2.2894	(2,0)	P2(4)
	7872.702	3.0416	(2,0)	Q21(5)
	7872.703	2.7768	(2,0)	Q21(4)
	7872.920	3.2332	(2,0)	Q21(6)
	7872.921	2.4324	(2,0)	Q21(3)
7874.00	7873.940	4.6841	(2,0)	P2(3)
	7873.999	1.5062	(2,0)	Q21(1)
	7874.031	3.4291	(2,0)	Q21(3)
	7873.994	.6125	(2,0)	P2(1)
7874.85	7874.837	5.2624	(2,0)	P2(9)
	7874.854	1.0369	(2,0)	Q21(0)
	7874.929	3.4479	(2,0)	Q21(9)
7876.00	7875.959	5.8173	(2,0)	P2(10)
	7876.061	3.4268	(2,0)	Q21(10)
7877.35	7877.317	6.3426	(2,0)	P2(11)
	7877.429	3.3720	(2,0)	Q21(11)
7878.00	7878.018	.0955	(6,3)	Q2(55)
7878.95	7878.915	6.8327	(2,0)	P2(12)
	7879.036	3.2902	(2,0)	Q21(12)
7880.80	7880.756	7.2829	(2,0)	P2(13)
	7880.887	3.1871	(2,0)	Q21(13)
7882.30	7882.284	3.7531	(2,0)	Q2(4)
	7882.328	1.3848	(2,0)	P21(4)
7882.90	7882.843	7.6896	(2,0)	P2(14)
	7882.984	3.0678	(2,0)	Q21(14)

TABLE VIIA C12 N14 (continued)

7884.40	7884.408	4.8412	(2,0)	Q2(5)
	7884.461	1.5647	(2,0)	P21(5)
7885.25	7885.179	8.0500	(2,0)	R2(15)
	7885.329	2.9368	(2,0)	Q21(15)
7886.75	7886.750	5.9530	(2,0)	Q2(6)
	7886.813	1.6995	(2,0)	P21(6)
7887.80	7887.765	8.3619	(2,0)	R2(16)
	7887.926	2.7976	(2,0)	Q21(16)
7889.35	7889.313	7.0803	(2,0)	Q2(7)
	7889.386	1.7939	(2,0)	P21(7)
7890.65	7890.606	8.6242	(2,0)	R2(17)
	7890.776	2.6533	(2,0)	Q21(17)
7892.10	7892.101	8.2056	(2,0)	Q2(8)
	7892.184	1.8530	(2,0)	P21(8)
7894.15	7894.031	1.9543	(2,0)	P2(5)
	7894.060	4.5651	(2,0)	R1(9)
	7894.169	6.0183	(2,0)	R1(8)
	7894.260	7.0842	(2,0)	R1(10)
7896.70	7896.694	8.4235	(2,0)	R1(13)
7898.35	7898.366	10.3854	(2,0)	Q2(10)
7899.80	7899.820	9.0970	(2,0)	R1(15)
7900.70	7900.675	9.1114	(2,0)	R2(20)
7901.85	7901.850	11.4110	(2,0)	Q2(11)
	7901.829	9.3609	(2,0)	R1(16)
	7901.962	1.8654	(2,0)	P21(11)
7903.20	7903.224	3.0046	(2,0)	P2(7)
7904.15	7904.133	9.5750	(2,0)	R1(17)
7905.60	7905.573	12.3769	(2,0)	Q2(12)
	7905.695	1.8292	(2,0)	P21(12)
7906.70	7906.731	9.7391	(2,0)	R1(18)
	7906.591	1.6453	(2,0)	R1(0)
7908.75	7908.570	1.7955	(2,0)	R12(3)
	7908.587	1.5282	(2,0)	R12(2)
	7908.605	3.6074	(2,0)	Q1(3)
	7909.611	2.4959	(2,0)	Q1(?)
	7908.698	9.1948	(2,0)	R2(22)
	7908.835	1.9341	(2,0)	R12(4)
	7908.918	1.9305	(2,0)	Q21(22)
	7908.929	4.7487	(2,0)	Q1(4)
	7908.936	1.4565	(2,0)	R12(1)
	7908.951	1.3905	(2,0)	Q1(1)
7909.60	7909.539	13.2729	(2,0)	Q2(13)
	7909.582	5.9152	(2,0)	Q1(5)
	7909.622	9.8536	(2,0)	R1(19)
	7909.671	1.7790	(2,0)	Q21(13)
7910.55	7910.560	7.0947	(2,0)	Q1(6)
	7910.495	2.1029	(2,0)	R12(5)
7911.85	7911.861	8.2723	(2,0)	Q1(7)
	7911.738	2.1383	(2,0)	R12(7)
7913.50	7913.432	9.4330	(2,0)	Q1(8)
	7913.399	2.1460	(2,0)	R12(3)
	7913.339	1.7954	(2,0)	Q21(23)
7915.40	7915.420	10.5619	(2,0)	Q1(9)
	7915.327	2.1301	(2,0)	R12(9)
7916.30	7916.281	9.9383	(2,0)	R1(21)
7918.20	7918.214	14.8230	(2,0)	Q2(15)
7920.20	7920.235	12.6710	(2,0)	Q1(11)
	7920.123	2.0428	(2,0)	R12(11)
7920.75	7920.727	2.5997	(2,0)	Q12(5)
	7920.781	1.8520	(2,0)	P1(5)
7922.95	7922.929	15.4654	(2,0)	Q2(16)
7924.10	7924.197	9.8426	(2,0)	R1(23)

TABLE VIIA C12 N14 (continued)

7925.15	7925.170	.5027	(2,0)	P12(4)
7926.30	7926.288	14.5077	(2,0)	Q1(13)
7927.15	7927.167	2.9743	(2,0)	P1(7)
	7927.094	3.0853	(2,0)	Q12(7)
7927.95	7927.900	16.0142	(2,0)	Q2(17)
	7927.963	8.8535	(2,0)	R2(26)
7928.45	7928.457	9.7330	(2,0)	R1(24)
7929.75	7929.773	15.3023	(2,0)	Q1(14)
7930.80	7930.768	3.2174	(2,0)	Q12(8)
	7930.852	3.5435	(2,0)	P1(8)
7933.45	7933.461	8.6784	(2,0)	R2(27)
	7933.410	1.7377	(2,0)	R12(15)
7934.80	7934.861	4.1061	(2,0)	P1(9)
	7934.767	3.2896	(2,0)	Q12(9)
7936.35	7936.361	6.0079	(2,0)	P2(13)
7937.65	7937.653	16.6159	(2,0)	Q1(16)
7939.20	7939.191	4.6541	(2,0)	P1(10)
	7939.236	8.4738	(2,0)	R2(28)
7942.05	7942.045	17.1283	(2,0)	Q1(17)
7944.40	7944.379	17.0878	(2,0)	Q2(20)
7945.30	7945.288	8.2429	(2,0)	R2(29)
7946.75	7946.737	17.5424	(2,0)	Q1(18)
7948.80	7948.773	8.9509	(2,0)	R1(28)
	7948.810	5.6781	(2,0)	P1(12)
7949.35	7949.365	6.7887	(2,0)	P2(15)
7950.40	7950.402	17.2571	(2,0)	Q2(21)
7951.70	7951.728	17.3586	(2,0)	Q1(19)
	7951.621	7.9892	(2,0)	R2(30)
7954.05	7954.094	6.1423	(2,0)	P1(13)
	7953.960	3.1558	(2,0)	Q12(13)
7954.60	7954.584	8.6856	(2,0)	R1(29)
7956.70	7956.695	17.3360	(2,0)	Q2(22)
7958.25	7958.235	7.7158	(2,0)	R2(31)
7959.70	7959.691	6.5582	(2,0)	P1(14)
7960.70	7960.688	8.3991	(2,0)	R1(30)
7962.60	7962.606	18.2031	(2,0)	Q1(21)
7963.35	7963.260	17.3284	(2,0)	Q2(23)
	7963.401	7.4034	(2,0)	P2(17)
7965.55	7965.601	6.0524	(2,0)	P1(15)
	7965.443	2.9356	(2,0)	Q12(15)
7967.10	7967.088	8.0947	(2,0)	R1(31)
7968.50	7968.494	18.2372	(2,0)	Q1(22)
7970.10	7970.100	17.2385	(2,0)	Q2(24)
7971.80	7971.823	7.2921	(2,0)	P1(16)
7972.35	7972.316	7.1233	(2,0)	R2(33)
	7972.423	1.2941	(2,0)	P12(12)
7973.80	7973.733	7.7756	(2,0)	R1(32)
7974.70	7974.679	18.1845	(2,0)	Q1(23)
7977.20	7977.217	17.0716	(2,0)	Q2(25)
7978.40	7978.354	7.5854	(2,0)	P1(17)
	7978.496	7.8381	(2,0)	P2(19)

TABLE VIIA C12 N14 (continued)

7979.80	7979.787	6.8104	(2,0)	R2(34)
	7979.812	1.2821	(2,0)	P12(13)
7981.15	7981.163	19.0497	(2,0)	Q1(24)
7984.60	7984.612	16.8331	(2,0)	Q2(26)
7986.45	7986.449	7.9868	(2,0)	P2(20)
7987.95	7987.947	17.8392	(2,0)	Q1(25)
7992.30	7992.290	16.5290	(2,0)	Q2(27)
7995.05	7995.030	17.5557	(2,0)	Q1(26)
8000.20	8000.250	16.1655	(2,0)	Q2(28)
	7999.805	8.1796	(2,0)	P1(20)
8002.40	8002.414	17.2085	(2,0)	Q1(27)
8003.20	8003.182	8.1500	(2,0)	P2(22)
8003.55	8003.542	6.4138	(2,0)	R1(36)
8005.50	8005.634	.0303	(8,5)	Q2(30)
	8005.412	.0144	(7,4)	R2(55)
8007.55	8007.573	8.2833	(2,0)	P1(21)
8008.50	8008.497	15.7490	(2,0)	Q2(29)
8010.10	8010.099	16.8029	(2,0)	Q1(28)
8011.85	8011.733	6.0660	(2,0)	R1(37)
	8011.968	8.1672	(2,0)	P2(23)
8012.60	8012.585	5.5137	(2,0)	R2(38)
	8012.597	1.1296	(2,0)	P12(17)
8015.65	8015.650	8.3415	(2,0)	P1(22)
8017.05	8017.033	15.2858	(2,0)	Q2(30)
8018.10	8018.086	16.3454	(2,0)	Q1(29)
8020.25	8020.228	5.7201	(2,0)	R1(38)
8021.05	8021.038	8.1439	(2,0)	P2(24)
8021.55	8021.523	5.1905	(2,0)	R2(39)
	8021.596	1.0766	(2,0)	P12(18)
8024.05	8024.037	8.3560	(2,0)	P1(23)
8025.85	8025.859	14.7825	(2,0)	Q2(31)
8026.40	8026.376	15.9427	(2,0)	Q1(30)
8029.05	8029.027	5.3782	(2,0)	R1(39)
8030.40	8030.393	8.0826	(2,0)	P2(25)
8030.80	8030.761	4.8719	(2,0)	R2(40)
	8030.915	1.0208	(2,0)	P12(19)
8032.75	8032.733	8.3291	(2,0)	P1(24)
8035.00	8034.971	15.3012	(2,0)	Q1(31)
	8034.978	14.2454	(2,0)	Q2(32)
8038.15	8038.134	5.0423	(2,0)	R1(40)
8039.10	8039.115	.0814	(2,0)	R21(47)
8040.15	8040.038	7.0857	(2,0)	P2(26)
	8040.301	4.5597	(2,0)	R2(41)
8041.75	8041.740	8.2632	(2,0)	P1(25)
8043.90	8043.872	14.7275	(2,0)	Q1(32)
8044.40	8044.392	13.6807	(2,0)	Q2(33)
8045.45	8045.452	.6868	(3,1)	R21(10)
8045.80	8045.803	.5277	(3,1)	R21(17)
8046.45	8046.426	.5932	(3,1)	R21(9)

TABLE VIIA C12 N14 (continued)

8047.60	8047.548	4.7141	(2,0)	R1(41)
	8047.646	.6920	(3,1)	R21(8)
8049.10	8049.112	.6816	(3,1)	R21(7)
8050.05	8049.975	7.8561	(2,0)	P2(27)
	8050.144	4.2553	(2,0)	R2(42)
8051.05	8051.058	8.1610	(2,0)	P1(26)
8053.10	8053.080	14.1277	(2,0)	Q1(33)
8054.10	8054.103	13.0944	(2,0)	Q2(34)
8054.95	8054.944	.5774	(3,1)	R21(4)
8057.25	8057.273	4.3948	(2,0)	R1(42)
8059.25	8059.236	.3322	(3,1)	R21(24)
8060.25	8060.207	7.6957	(2,0)	P2(28)
	8060.294	3.9600	(2,0)	R2(43)
8060.70	8060.689	8.0254	(2,0)	P1(27)
8062.60	8062.597	13.5079	(2,0)	Q1(34)
8063.40	8063.406	.0285	(6,3)	Q1(65)
8064.10	8064.115	12.4922	(2,0)	Q2(35)
8065.55	8065.564	.2842	(3,1)	R21(26)
8067.30	8067.263	.7684	(3,1)	R2(3)
	8067.283	1.5665	(3,1)	R2(6)
	8067.299	1.0971	(3,1)	Q21(3)
	8067.310	4.0869	(2,0)	R1(43)
	8067.349	1.4616	(3,1)	Q21(6)
8068.50	8068.467	2.1048	(3,1)	R2(8)
	8068.553	1.5522	(3,1)	Q21(8)
8069.45	8069.420	2.3651	(3,1)	R2(9)
	8069.517	1.5625	(3,1)	Q21(9)
8070.70	8070.618	2.6151	(3,1)	R2(10)
	8070.633	7.9505	(2,0)	P1(28)
	8070.725	1.5542	(3,1)	Q21(10)
	8070.736	7.5106	(2,0)	R2(29)
	8070.753	3.6750	(2,0)	R2(44)
8071.40	8071.397	.7923	(2,0)	P12(23)
8072.40	8072.424	12.8739	(2,0)	Q1(35)
8073.30	8073.271	.8069	(3,1)	Q2(2)
	8073.296	.3917	(3,1)	P21(2)
8073.80	8073.765	3.0734	(3,1)	R2(12)
	8073.892	1.4946	(3,1)	Q21(12)
8074.45	8074.429	11.8795	(2,0)	Q2(36)
8075.05	8075.043	1.2312	(3,1)	Q2(3)
	8075.079	.5204	(3,1)	P21(3)
8075.75	8075.719	3.2770	(3,1)	R2(13)
	8075.857	1.4489	(3,1)	Q21(13)
8077.05	8077.040	1.6915	(3,1)	Q2(4)
	8077.086	.6244	(3,1)	P21(4)
	8077.178	.2211	(3,1)	R21(29)
8077.80	8077.933	3.4513	(3,1)	R2(14)
	8077.662	3.7884	(2,0)	R1(44)
8079.30	8079.264	2.1758	(3,1)	Q2(5)
	8079.329	.7060	(3,1)	P21(5)
8080.50	8080.565	1.3371	(3,1)	Q21(15)
	8080.592	.4381	(3,1)	P2(3)
	8080.592	1.1223	(2,0)	Q12(29)
	8080.407	3.6249	(3,1)	R2(15)
8080.90	8080.893	7.6665	(2,0)	P1(29)
8081.60	8081.523	3.4011	(2,0)	R2(45)
	8081.566	7.3008	(2,0)	P2(30)
	8081.719	2.6754	(3,1)	Q2(6)

TABLE VIIA C12 N14 (continued)

8082.55	8082.563	12.2310	(2,0)	Q1(36)
8083.15	8083.146	3.7669	(3,1)	R2(16)
8084.40	8084.405	3.1821	(3,1)	Q2(7)
8085.05	8085.048	11.2614	(2,0)	Q2(37)
8086.20	8086.151	3.8868	(3,1)	R2(17)
	8086.330	1.2099	(3,1)	Q21(17)
8087.35	8087.329	3.6882	(3,1)	Q2(8)
8088.35	8088.330	3.5031	(2,0)	R1(45)
8089.70	8089.615	1.1438	(3,1)	Q21(18)
	8089.641	2.9519	(3,1)	R1(9)
	8089.731	2.7056	(3,1)	R1(8)
	8089.876	3.1861	(3,1)	R1(10)
8090.45	8090.433	3.4055	(3,1)	R1(11)
	8090.493	4.1363	(3,1)	Q2(9)
8091.45	8091.469	7.4495	(2,0)	P1(30)
8092.70	8092.698	7.0705	(2,0)	P2(31)
8093.00	8092.972	4.0592	(3,1)	R2(19)
	8093.016	11.5946	(2,0)	Q1(37)
8093.90	8093.901	4.6697	(3,1)	Q2(10)
	8093.941	1.1123	(3,1)	P2(6)
8095.15	8095.170	1.4060	(3,1)	R1(3)
8095.90	8095.974	10.6426	(2,0)	Q2(38)
	8095.831	4.0978	(3,1)	R1(15)
8096.80	8096.792	4.1122	(3,1)	R2(20)
8097.55	8097.558	5.1320	(3,1)	Q2(11)
8097.95	8097.964	4.2184	(3,1)	R1(16)
8099.30	8099.316	3.2306	(2,0)	R1(46)
8101.45	8101.466	5.5690	(3,1)	Q2(12)
8102.35	8102.363	7.2118	(2,0)	P1(31)
8103.15	8103.157	4.3925	(3,1)	R1(13)
8103.90	8103.784	10.9388	(2,0)	Q1(38)
	8104.137	6.8227	(2,0)	P2(32)
8105.65	8105.630	5.9730	(3,1)	Q2(13)
	8105.642	.2191	(3,1)	R12(5)
	8105.698	2.6580	(3,1)	Q1(6)
8107.20	8107.210	10.0273	(2,0)	Q2(39)
8108.10	8108.100	3.7175	(3,1)	Q1(7)
8109.85	8109.805	4.2397	(3,1)	Q1(8)
	8109.920	4.1448	(3,1)	R2(23)
8110.05	8110.053	6.3432	(3,1)	Q2(14)
8110.60	8110.624	2.9714	(2,0)	R1(47)
8111.85	8111.943	4.7479	(3,1)	Q1(9)
8113.50	8113.576	6.9565	(2,0)	P1(32)
	8113.255	4.4888	(3,1)	R1(21)
8114.85	8114.871	10.2983	(2,0)	Q1(39)
	8114.859	4.1167	(3,1)	P2(24)
	8114.738	6.6754	(3,1)	Q2(15)
8115.85	8115.994	6.5605	(2,0)	P2(33)
	8115.725	2.6527	(2,0)	R2(48)
8117.05	8116.993	5.5988	(3,1)	Q1(11)
	8117.234	4.4791	(3,1)	R1(22)
	8117.284	1.1736	(3,1)	Q12(5)
8118.75	8118.758	9.4195	(2,0)	Q2(40)
8119.85	8119.922	6.1311	(3,1)	Q1(12)
	8119.690	6.9675	(3,1)	Q2(16)
	8120.052	4.0710	(3,1)	R2(25)

TABLE VIIA C12 N14 (continued)

8120.95	8120.943	2.2887	(3,1)	P2(11)
8121.50	8121.520	4.4502	(3,1)	R1(23)
8122.25	8122.255	2.7258	(2,0)	R1(48)
8123.25	8123.262	6.5289	(3,1)	Q1(13)
8123.95	8123.935	1.3951	(3,1)	Q12(7)
	8124.012	1.3363	(3,1)	P1(7)
8125.00	8124.910	7.2178	(3,1)	Q2(17)
	8125.111	6.6868	(2,0)	P1(33)
8127.85	8127.765	2.4289	(2,0)	R2(49)
	8127.775	1.4560	(3,1)	Q12(8)
	8127.863	1.5923	(3,1)	P1(8)
	8127.942	6.2867	(2,0)	P2(34)
8130.55	8130.622	9.8226	(2,0)	Q2(41)
	8130.403	7.4254	(3,1)	Q2(18)
	8130.902	7.2087	(3,1)	Q1(15)
8132.00	8131.955	1.4899	(3,1)	Q12(9)
	8132.053	1.8454	(3,1)	P1(9)
8133.50	8133.501	2.7040	(3,1)	P2(13)
8134.20	8134.211	2.4941	(2,0)	R1(49)
8135.20	8135.199	7.4862	(3,1)	Q1(16)
8136.20	8136.171	7.5902	(3,1)	Q2(19)
	8136.213	4.2593	(3,1)	R1(26)
8138.00	8138.006	9.0480	(2,0)	Q1(41)
8140.20	8140.172	2.8894	(3,1)	P2(14)
	8140.315	6.0043	(2,0)	P2(35)
	8140.129	2.2182	(2,0)	R2(50)
	8139.818	7.7204	(3,1)	Q1(17)
8142.20	8142.217	7.7124	(3,1)	Q2(20)
8144.75	8144.740	7.9106	(3,1)	Q1(18)
8146.55	8146.496	2.2762	(2,0)	R1(50)
	8146.512	1.4697	(3,1)	Q12(12)
	8146.641	2.5539	(3,1)	P1(12)
8150.05	8149.982	8.0569	(3,1)	Q1(17)
	8150.059	8.4445	(2,0)	Q1(42)
8152.10	8152.169	2.7636	(3,1)	P1(13)
	8152.029	1.4340	(3,1)	Q12(13)
8152.90	8153.005	5.7159	(2,0)	P2(36)
	8152.821	2.0205	(2,0)	R2(51)
8155.30	8155.154	7.8325	(3,1)	Q2(22)
	8155.305	7.6734	(2,0)	Q2(43)
	8155.538	8.1598	(3,1)	Q1(20)
8156.80	8156.780	.5739	(3,1)	P12(10)
8157.50	8157.507	3.5053	(3,1)	R2(31)
8159.10	8159.111	2.0720	(2,0)	R1(51)
8160.10	8160.105	3.8136	(3,1)	R1(30)
8162.00	8162.050	7.8332	(3,1)	Q2(23)
	8161.806	3.3370	(3,1)	P2(17)
	8162.439	7.8591	(2,0)	Q1(43)
8164.15	8164.213	3.1304	(3,1)	P1(15)
	8164.051	1.3360	(3,1)	Q12(15)
8164.80	8164.777	3.3760	(3,1)	R2(32)
8166.00	8166.016	5.4239	(2,0)	P2(37)
	8165.842	1.8358	(2,0)	R2(52)
8166.85	8166.851	3.6779	(3,1)	R1(31)
8167.60	8167.591	8.2401	(3,1)	Q1(22)
8168.15	8168.131	7.1259	(2,0)	Q2(44)
8169.25	8169.235	7.7970	(3,1)	Q2(24)
	8169.573	3.4468	(3,1)	P2(13)

TABLE VIIA C12 N14 (continued)

8170.70	8170.725	3.2847	(3,1)	P1(16)
	8170.553	1.2781	(3,1)	Q12(16)
8172.30	8172.348	3.2407	(3,1)	R2(33)
	8172.061	1.8814	(2,0)	R1(52)
8174.00	8173.908	3.5354	(3,1)	R1(32)
	8174.089	8.2207	(3,1)	Q1(23)
8175.15	8175.148	7.2940	(2,0)	Q1(44)
8176.70	8176.711	7.7259	(3,1)	Q2(25)
8177.60	8177.564	3.4183	(3,1)	P1(17)
	8177.616	3.5361	(3,1)	P2(19)
8179.30	8179.349	5.1307	(2,0)	P2(38)
	8179.197	1.6637	(2,0)	R2(53)
8181.30	8181.277	3.3875	(3,1)	R1(33)
	8181.283	6.5992	(2,0)	Q2(45)
8183.90	8183.803	.0426	(3,1)	R21(45)
8184.50	8184.480	7.6225	(3,1)	Q2(26)
	8184.534	1.1528	(3,1)	Q12(18)
8185.35	8185.347	1.7040	(2,0)	R1(53)
8185.95	8185.947	3.6049	(3,1)	P2(20)
8188.10	8188.026	8.0732	(3,1)	Q1(25)
	8188.189	6.7509	(2,0)	Q1(45)
8188.95	8188.959	3.2356	(3,1)	R1(34)
8192.55	8192.546	7.4894	(3,1)	Q2(27)
8194.70	8194.764	6.0946	(2,0)	Q2(46)
	8194.547	3.6535	(3,1)	P2(21)
8195.45	8195.467	7.9501	(3,1)	Q1(26)
8196.90	8196.956	3.0810	(3,1)	R1(35)
	8196.882	2.9116	(3,1)	R2(36)
8198.95	8198.972	1.5395	(2,0)	R1(54)
8200.00	8200.030	3.6914	(3,1)	P1(20)
	8199.814	1.0230	(3,1)	Q12(20)
8201.20	8201.191	4.9221	(2,0)	P1(39)
8203.25	8203.224	7.7976	(3,1)	Q1(27)
	8203.480	3.6823	(3,1)	P2(22)
8204.10	8204.093	.5370	(3,1)	P12(16)
8205.65	8205.675	2.6649	(3,1)	R2(37)
8207.00	8206.999	4.5491	(2,0)	P2(40)
	8206.917	1.3561	(2,0)	R2(55)
8208.60	8208.578	5.6134	(2,0)	Q2(47)
8209.55	8209.575	7.1451	(3,1)	Q2(29)
8211.30	8211.298	7.6186	(3,1)	Q1(28)
8212.75	8212.940	1.3875	(2,0)	R1(55)
	8212.687	3.6921	(3,1)	P2(23)
8213.90	8213.901	2.7685	(3,1)	R1(37)
8215.20	8215.278	5.7363	(2,0)	Q1(47)
	8215.038	4.6263	(2,0)	P1(40)
8216.65	8216.630	3.7683	(3,1)	P1(22)
8218.55	8218.544	6.9396	(3,1)	Q2(30)
8219.70	8219.639	7.4160	(3,1)	Q1(29)
8221.30	8221.321	4.2643	(2,0)	P2(41)
	8221.289	1.2198	(2,0)	R2(56)
8222.80	8222.727	5.1563	(2,0)	Q2(48)
	8222.851	2.6128	(3,1)	R1(38)
8224.20	8224.196	2.3727	(3,1)	R2(39)
	8224.183	.2821	(2,0)	P12(35)

TABLE VIIA C12 N14 (continued)

8225.40	8225.418	3.7770	(3,1)	P1(23)
8229.25	8229.225	4.3354	(2,0)	P1(41)
	8229.332	5.2666	(2,0)	Q1(48)
8232.05	8232.000	3.6580	(3,1)	P2(25)
	8232.122	2.4587	(3,1)	R1(39)
8234.50	8234.532	3.7669	(3,1)	P1(24)
8236.00	8235.979	3.9856	(2,0)	P2(42)
	8236.007	1.0945	(2,0)	R2(57)
8237.35	8237.215	4.7238	(2,0)	Q2(49)
	8237.400	6.4763	(3,1)	Q2(32)
	8237.431	6.9517	(3,1)	Q1(31)
8242.10	8242.112	3.6163	(3,1)	P2(26)
8243.80	8243.728	4.3226	(2,0)	Q1(49)
	8243.754	4.0510	(2,0)	P1(42)
	8243.973	3.7393	(3,1)	P1(25)
	8243.979	2.0879	(3,1)	R2(41)
8246.80	8246.784	6.6957	(3,1)	Q1(32)
8247.30	8247.293	6.2241	(3,1)	Q2(33)
8251.00	8250.976	3.7144	(2,0)	P2(43)
8252.55	8252.530	3.5598	(3,1)	P2(27)
8253.75	8253.741	3.6952	(3,1)	P1(26)
8256.45	8256.460	6.4277	(3,1)	Q1(33)
8257.50	8257.500	5.9618	(3,1)	Q2(34)
8259.45	8258.471	4.4045	(2,0)	Q1(50)
	8258.630	3.7744	(2,0)	P1(43)
8260.75	8260.768	.1016	(4,2)	R21(23)
	8260.775	.1432	(4,2)	R21(3)
8261.90	8261.891	2.0144	(3,1)	R1(42)
8263.25	8263.259	3.4897	(3,1)	P2(28)
8265.05	8265.042	1.8166	(3,1)	R2(43)
8266.45	8266.451	6.1502	(3,1)	Q1(34)
	8266.316	3.4519	(2,0)	P2(44)
8267.20	8267.221	3.0337	(2,0)	Q2(51)
8270.00	8269.989	.2073	(2,0)	P12(33)
8271.00	8270.856	.2860	(4,2)	R2(4)
	8270.879	.3602	(4,2)	R2(5)
	8270.905	.3501	(4,2)	Q21(4)
	8270.939	.3341	(4,2)	Q21(5)
	8271.074	.2137	(4,2)	R2(3)
	8271.112	.3062	(4,2)	Q21(3)
	8271.147	.4355	(4,2)	R2(6)
	8271.218	.4090	(4,2)	Q21(6)
8272.45	8272.456	1.8746	(3,1)	R1(43)
	8272.430	.5854	(4,2)	R2(8)
8274.30	8274.266	3.5632	(3,1)	P1(28)
	8274.302	3.4075	(3,1)	P2(29)
8276.80	8276.798	5.8660	(3,1)	Q1(35)
8278.15	8278.083	.8556	(4,2)	R2(12)
	8278.218	.4202	(4,2)	Q21(12)
8278.85	8278.862	5.4170	(3,1)	Q2(36)
8280.20	8280.159	.9126	(4,2)	R2(13)
	8280.306	.4077	(4,2)	Q21(13)
8281.30	8281.257	.4706	(4,2)	Q2(4)
	8281.306	.1742	(4,2)	P21(4)
8282.75	8282.745	3.5757	(2,0)	Q2(52)
8285.05	8285.024	3.4780	(3,1)	P1(29)
	8285.131	1.0103	(4,2)	R2(15)
8285.65	8285.660	3.3146	(3,1)	P2(30)

TABLE VIIA C12 N14 (continued)

8286.10	8286.161	.7442	(4,2)	Q2(6)
	8286.097	.3381	(3,1)	P12(24)
	8286.232	.2145	(4,2)	P21(6)
8287.45	8287.445	5.5775	(3,1)	Q1(36)
	8287.407	1.5632	(3,1)	R2(45)
8289.00	8289.008	3.6456	(2,0)	Q1(52)
	8288.981	.8852	(4,2)	Q2(7)
8291.20	8291.214	1.0842	(4,2)	R2(17)
8292.05	8292.049	1.0261	(4,2)	Q2(8)
8294.70	8294.601	1.6102	(3,1)	R1(45)
	8294.679	1.1119	(4,2)	R2(18)
	8294.746	.3215	(4,2)	R1(7)
8298.50	8298.430	1.1334	(4,2)	R2(19)
	8298.431	5.2869	(3,1)	Q1(37)
	8298.622	3.2420	(2,0)	Q2(53)
8300.40	8300.395	.3912	(4,2)	R1(3)

TABLE VIIB C13 N14 Line identifications

7847.25	7847.240	0.1454	(6,3)	Q2(51)
7865.10	7865.122	0.0756	(4,1)	P1(68)
7916.95	7916.944	3.2787	(2,0)	R2(6)
7921.35	7921.294	5.9897	(2,0)	R2(11)
	7921.406	3.3353	(2,0)	Q21(11)
7931.45	7931.424	7.9628	(2,0)	R2(16)
7934.25	7934.174	8.2289	(2,0)	R2(17)
	7934.346	2.6827	(2,0)	Q21(17)
7935.60	7936.602	7.7358	(2,0)	Q2(8)
7940.40	7940.417	8.6223	(2,0)	R2(19)
7941.10	7941.029	4.0357	(2,0)	R1(5)
	7941.128	7.9941	(2,0)	R1(13)
7947.65	7947.664	8.8326	(2,0)	R2(21)
7952.55	7952.527	12.5798	(2,0)	Q2(13)
	7952.660	1.7627	(2,0)	P21(13)
7953.40	7953.478	9.4548	(2,0)	R1(19)
	7953.273	1.3137	(2,0)	Q1(1)
	7953.258	1.3854	(2,0)	R12(1)
	7953.220	4.4726	(2,0)	Q1(4)
7961.55	7961.572	10.9950	(2,0)	Q1(10)
	7961.468	2.0572	(2,0)	R12(10)
	7961.403	4.3369	(2,0)	P2(10)
7964.00	7964.031	11.9776	(2,0)	Q1(11)
	7963.917	2.0140	(2,0)	R12(11)
7975.45	7975.589	8.4838	(2,0)	R2(27)
	7975.570	1.4283	(2,0)	P21(18)
	7975.386	15.7496	(2,0)	Q2(18)
7975.95	7975.861	1.3705	(2,0)	Q21(27)
	7976.028	9.3291	(2,0)	R1(25)
7982.40	7982.347	3.2541	(2,0)	Q12(10)
	7982.451	4.3889	(2,0)	P1(10)
7983.70	7983.694	1.0076	(2,0)	P12(7)
7985.80	7985.798	8.9934	(2,0)	R1(27)
7989.50	7989.514	16.7827	(2,0)	Q1(18)
7991.10	7991.107	8.7825	(2,0)	R1(28)
	7991.114	6.4586	(2,0)	P2(15)
7993.10	7993.118	7.8788	(2,0)	R2(30)
7996.75	7996.679	3.1381	(2,0)	Q12(13)
	7996.699	8.5467	(2,0)	R1(29)
	7996.814	5.8159	(2,0)	P1(13)
7998.20	7998.191	16.7296	(2,0)	Q2(22)
8001.30	8001.298	1.2448	(2,0)	P12(10)
8004.70	8004.540	16.7632	(2,0)	Q2(23)
	8004.582	1.2286	(2,0)	R12(21)
	8004.711	7.0688	(2,0)	P2(17)
	8004.775	1.0453	(2,0)	P21(23)
	8004.797	17.5299	(2,0)	Q1(21)
8006.15	8006.157	7.3694	(2,0)	R2(32)
8011.15	8011.154	16.7185	(2,0)	Q2(24)
8013.85	8013.906	6.9413	(2,0)	P1(16)
	8013.740	2.8220	(2,0)	Q12(16)
8014.60	8014.620	1.2831	(2,0)	P12(12)
8016.45	8016.428	17.5962	(2,0)	Q1(23)
8019.35	8019.327	7.5143	(2,0)	P2(19)
8022.70	8022.676	17.5098	(2,0)	Q1(24)
8025.20	8025.182	16.4119	(2,0)	Q2(26)

TABLE VIIB C13 N14 (continued)

8026.80	8026.801	7.4848	(2,0)	P1(18)
8027.80	8027.781	6.5052	(2,0)	R2(35)
8033.65	8033.696	7.6907	(2,0)	P1(19)
	8033.500	2.4227	(2,0)	Q12(19)
8036.10	8036.039	17.1205	(2,0)	Q1(26)
	8036.236	6.7807	(2,0)	R1(35)
8036.95	8036.953	1.2262	(2,0)	P12(15)
8043.20	8043.155	16.8281	(2,0)	Q1(27)
	8043.216	7.8664	(2,0)	P2(22)
8048.30	8048.261	15.4864	(2,0)	Q2(29)
	8048.382	7.9703	(2,0)	P1(21)
	8048.164	2.1466	(2,0)	Q12(21)
8051.80	8051.715	7.9021	(2,0)	P2(23)
	8051.719	6.1260	(2,0)	R1(37)
	8051.926	5.5856	(2,0)	R2(38)
8056.50	8056.505	15.0761	(2,0)	Q2(30)
8058.25	8058.260	16.0761	(2,0)	Q1(29)
8065.05	8065.028	14.6246	(2,0)	Q2(31)
8066.25	8066.251	15.6283	(2,0)	Q1(30)
8078.80	8078.646	4.6722	(2,0)	R2(41)
	8078.856	7.7869	(2,0)	P2(26)
8129.30	8129.292	7.3450	(2,0)	P1(30)
8132.70	8132.699	10.7822	(2,0)	Q2(38)
8145.80	8145.825	5.8060	(3,1)	Q2(13)
8151.55	8151.535	10.4735	(2,0)	Q1(39)
8160.85	8160.830	5.9521	(3,1)	Q1(12)
8173.15	8173.163	6.3974	(2,0)	P1(34)
8176.10	8176.088	4.2609	(3,1)	R1(26)
8182.65	8182.649	3.7692	(3,1)	R2(29)
8189.85	8189.720	7.9207	(3,1)	Q1(19)
	8189.913	7.9264	(2,0)	Q2(43)
8193.65	8193.736	7.7500	(3,1)	Q2(22)
	8193.589	2.2178	(2,0)	R1(51)
8202.30	8202.276	7.3914	(2,0)	Q2(44)
8217.70	8217.699	3.1744	(3,1)	R2(34)
8223.50	8223.418	3.4605	(3,1)	P1(18)
	8223.558	3.5515	(3,1)	P2(20)
8226.40	8226.336	8.0503	(3,1)	Q1(25)
	8226.540	4.9205	(2,0)	P2(39)
8229.85	8229.850	7.5066	(3,1)	Q2(27)
8230.60	8230.633	3.5572	(3,1)	P1(19)
	8230.427	1.1337	(3,1)	Q12(19)
8235.05	8235.040	6.5191	(2,0)	Q1(46)
	8235.060	5.0042	(2,0)	P1(39)
8238.00	8238.161	3.6337	(3,1)	P1(20)
	8237.944	1.0697	(3,1)	Q12(20)
	8237.924	7.3668	(3,1)	Q2(28)
8239.10	8239.103	1.4798	(2,0)	R2(55)
8240.05	8240.031	4.6439	(2,0)	P2(40)
8241.10	8240.969	7.8173	(3,1)	Q1(27)
	8241.251	5.8979	(2,0)	Q2(47)
8245.40	8245.371	1.5144	(2,0)	R1(55)
8248.40	8248.401	4.7215	(2,0)	Q1(47)
8248.75	8248.743	7.6592	(3,1)	Q1(28)

TABLE VIIB C13 N14 (continued)

8249.40	8249.406	3.6627	(3,1)	P2(23)	8260.05	8260.064	2.4721	(3,1)	R2(39)
						8260.069	0.5113	(3,1)	P12(18)
8254.90	8254.881	5.4418	(2,0)	Q2(48)					
	8254.940	7.0160	(3,1)	Q2(30)	8262.65	8262.625	3.7445	(3,1)	P1(23)
8259.40	8259.404	2.7136	(3,1)	R1(38)	8268.85	8268.835	5.0081	(2,0)	Q2(49)
					8269.45	8269.437	2.3311	(3,1)	R2(40)

For each of three temperatures (T= 2400, 2800 and 3150 K) the absorption coefficient was calculated in steps of 0.05 A between wavelengths, λ7800 and λ8400 A. Three turbulent velocities (as found by Utsumi, 1970) were used in the calculations (V_t= 7.47, 7.9 and 9.5 km/sec), making a total of nine sets of data. The three temperatures covered the approximate range in temperature reported for the stars observed (Utsumi, 1970).

2.10 Method of line depths.

The multiplicative constant used when applying the absorption coefficients was varied for the calculated profile until the depths of the lines in regions free of $C^{13}N^{14}$ features matched the observed depths. The choice of suitable $C^{13}N^{14}$ features was made difficult by the presence in the region studied of the telluric H_2O band system. These lines were shifted with respect to the spectrum of the stars by varying amounts depending upon the change in radial velocity caused by the earth's rotation and revolution about the sun. A $C^{13}N^{14}$ feature which was present in one star would be blended with an H_2O line in another. It was decided to locate and list all $C^{13}N^{14}$ features on the theoretical profile and measure only those which showed little blending. A line was considered free of blending when the profile within approximately 0.5 A on either side matched fairly well the calculated profile. The effects of atomic lines were ignored except in the case of strong lines listed in 'The Solar Spectrum, 2935 A to 8770 A' (Moore, Minnaert and Houtgast, 1966). The wavelengths and identifications (vibrational band, branch and rotational quantum number) of these $C^{13}N^{14}$ features are given in table VIIb.

When the observed $C^{13}N^{14}$ line depths for a plate were measured the wavelengths to the nearest 0.05 A were recorded. The wavelengths and

depths of all measured lines as well as the strength constant used to produce the matching theoretical profile, were input to a computer program which then calculated the theoretical profiles for a short region on either side of the input wavelength for different C^{12}/C^{13} ratios. From the resulting carbon ratios and corresponding theoretical depths the observed C^{12}/C^{13} ratio was found by interpolation.

2.11 Method of empirical pseudo-curve of growth.

The empirical pseudo-curve of growth method used by Fujita (Fujita, Tsuji and Maehara, 1966 and Fujita, 1970, p.127) seemed to produce different results than found by other authors (see tables I and II). This method did not assume a specific form for the curve of growth relation but determined an empirical form. He measured the line depth, (instead of the equivalent width as is usual with curve of growth analyses), and plotted the logarithm of depth for both $C^{12}N^{14}$ and $C^{13}N^{14}$ as a function of a term $\log_{10}(K)$ where

$$\log_{10}(K)=\log_{10}(q_{v'v''})+\log_{10}(S^{J'p'}_{J''p''})-(\chi_{v''}+\chi_{r''})\theta_{ex} \qquad 2.43$$

K is the line strength factor omitting terms which are constant for the whole band

$q_{v'v''}$ is the Franck-Condon factor

$S^{J'p'}_{J''p''}$ is the Honl-London factor

$\chi_{v''}$ is the energy if the lower vibrational state

$\chi_{r''}$ is the energy of the lower rotational state, both energies measured in eV

θ_{ex} is the reciprocal excitation temperature, $(= \frac{5040}{T_{ex}})$.

The notation for the above terms has been changed from that of Fujita to agree with that used earlier in this paper. The horizontal shift in the graphs between the $C^{12}N^{14}$ data and the $C^{13}N^{14}$ data is the logarithm of the abundance ratio. Two assumptions were made to employ this method. The first assumption was that the observed absorption intensity was a monotonically increasing function of the number of absorbing molecules. The form of this function could be found empirically. The second assumption was that lines of the same intensity were produced by the same number of absorbing molecules. These two assumptions were unrestrictive. However the one drawback to this method as presented was that it did not take into account the effects of blending of many weak lines. As can be seen from tables VIIA and VIIB many lines sometimes occur within 0.2 A of each other. Fujita was using high dispersion plates, (3 A/mm), and the effect would appear to be less important than at the dispersions used in this paper. Still the contribution of neighbouring lines should not be omitted as the lines have a finite width and the wings of one line will contribute to the center of the next.

In this study the dispersion used, (8 A/mm), required blends to be considered. The effect of the finite width of the line was included by broadening the central line strength using a Voigt profile. Unfortunately one must assume a turbulent velocity as well. As a check on the effect of a possible wrong choice of the turbulent velocity one set of calculations was performed using a different turbulent velocity. The results are described in the discussion of the empirical pseudo-curve of growth method. The line strength with the Voigt function applied and summed at intervals for all the lines present was the same data as used for the depths method and the data was used for both methods.

At any wavelength there was a contribution from both $C^{12}N^{14}$ and $C^{13}N^{14}$. A problem arose in how to include the weaker component when doing calculations for one of the isotopic species. When $C^{12}N^{14}$ lines were considered the formula

$$K^{C^{12}} = \tau_{C^{12}N^{14}} + \frac{1}{r}\tau_{C^{13}N^{14}} \qquad 2.44$$

was used where r was the ratio C^{12}/C^{13} and $K^{C^{12}}$ is equivalent to K in equation 2.43 . Calculations were performed with r= 1, 4, 20 and 100, which covered the range of values that was expected for r in stellar atmospheres. The differences in the resulting graphs were very small and the value of 4 was chosen as it was close to the earlier determined values. The shift introduced by using r=1 and r=100 was included for a few points in three graphs (figures 6, 7 and 8) to indicate the maximum error introduced. One would expect little variation in the theoretical value of $K^{C^{12}}$ in equation 2.44 for the different values of r since only definite $C^{12}N^{14}$ lines were chosen so that the contribution of $C^{13}N^{14}$ was very small.

In the case of $C^{13}N^{14}$ lines formula 2.44 could not be used since the main contribution was from the $C^{13}N^{14}$ term and had to be free of the ratio r. Instead the equation

$$K^{C^{13}} = r\tau_{C^{12}N^{14}} + \tau_{C^{13}N^{14}} \qquad 2.45$$

was used where the minor contribution from $C^{12}N^{14}$ was properly accounted for in the total. The variation in the assumed value of r again affected the resulting graphs little. With r=4 the two sets of graphs were compared and the abundance ratio determined for each pair.

2.12 Effect of dispersion.

Several important points arose in the measurement of the abundance

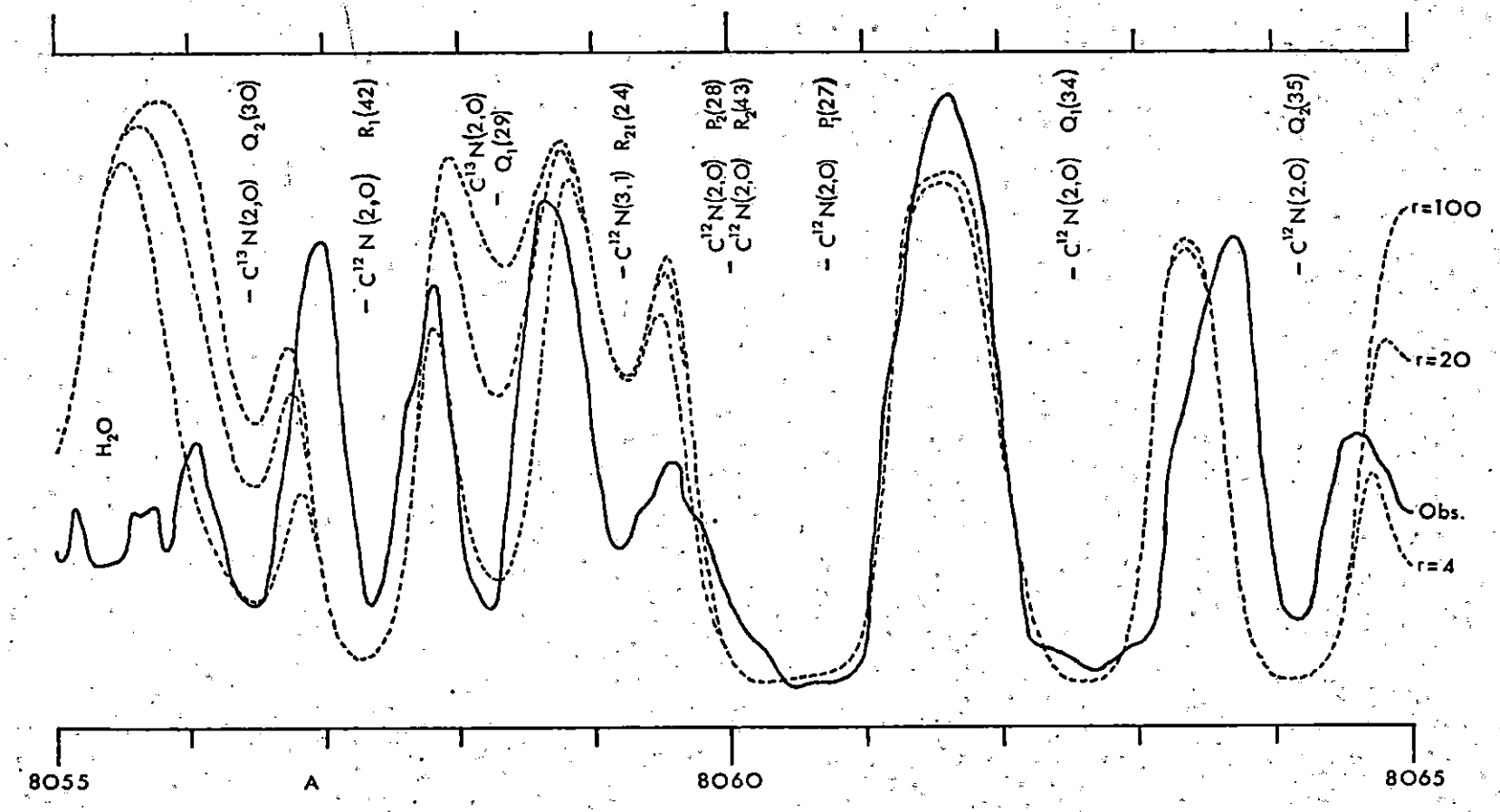

Figure 3. Comparison of theoretical and observed profiles. Theoretical: T=2800 K, V_t= 9.5 km/sec. Observed: 19 Psc, P:1511, Dispersion = 7.9 A/mm.

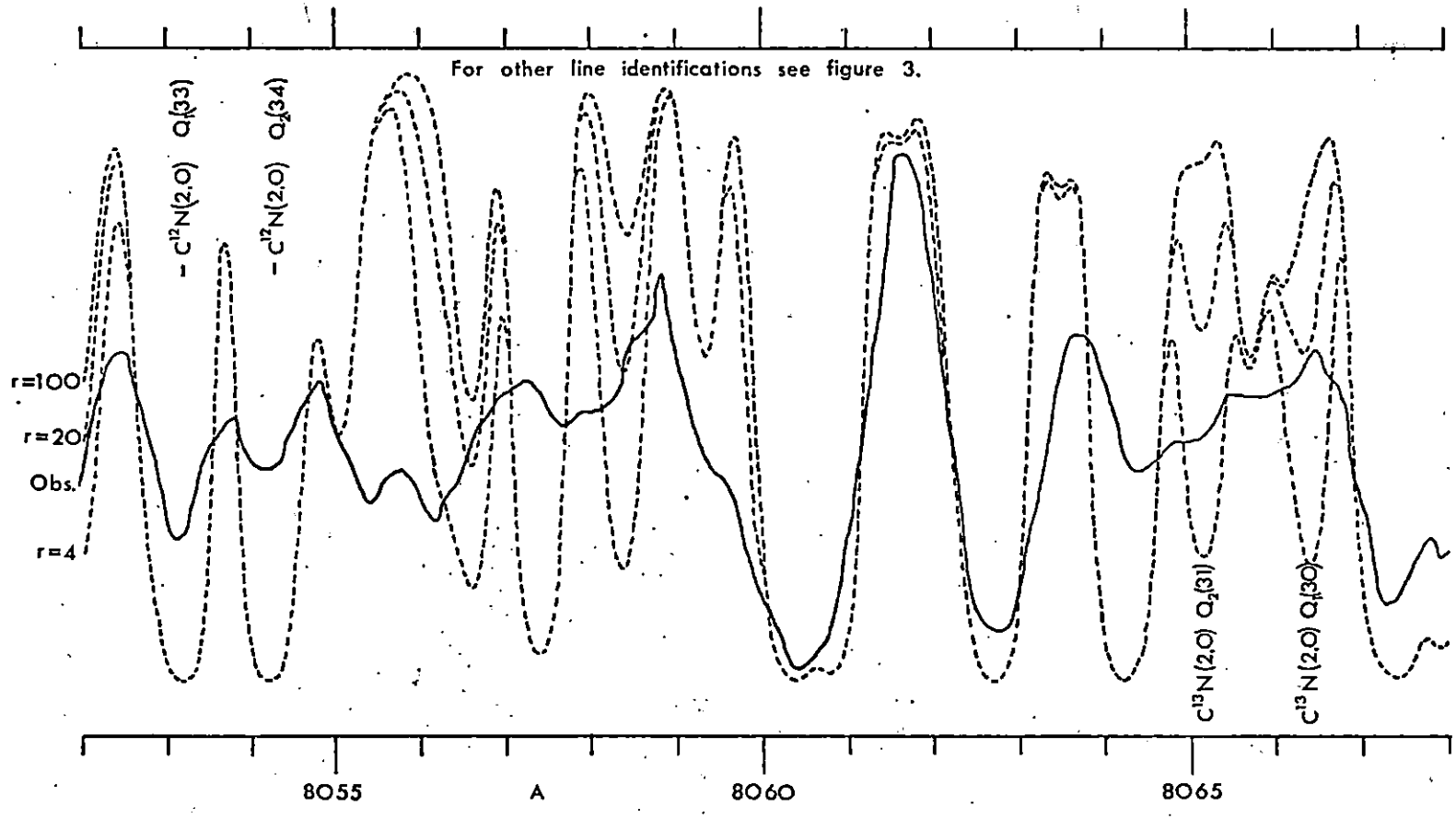

Figure 4. Comparison of theoretical and observed profiles. Theoretical: T = 2800 K, V_t = 9.5 km/sec. Observed: 19 Psc, P: 4970. Dispersion = 12.8 A/mm.

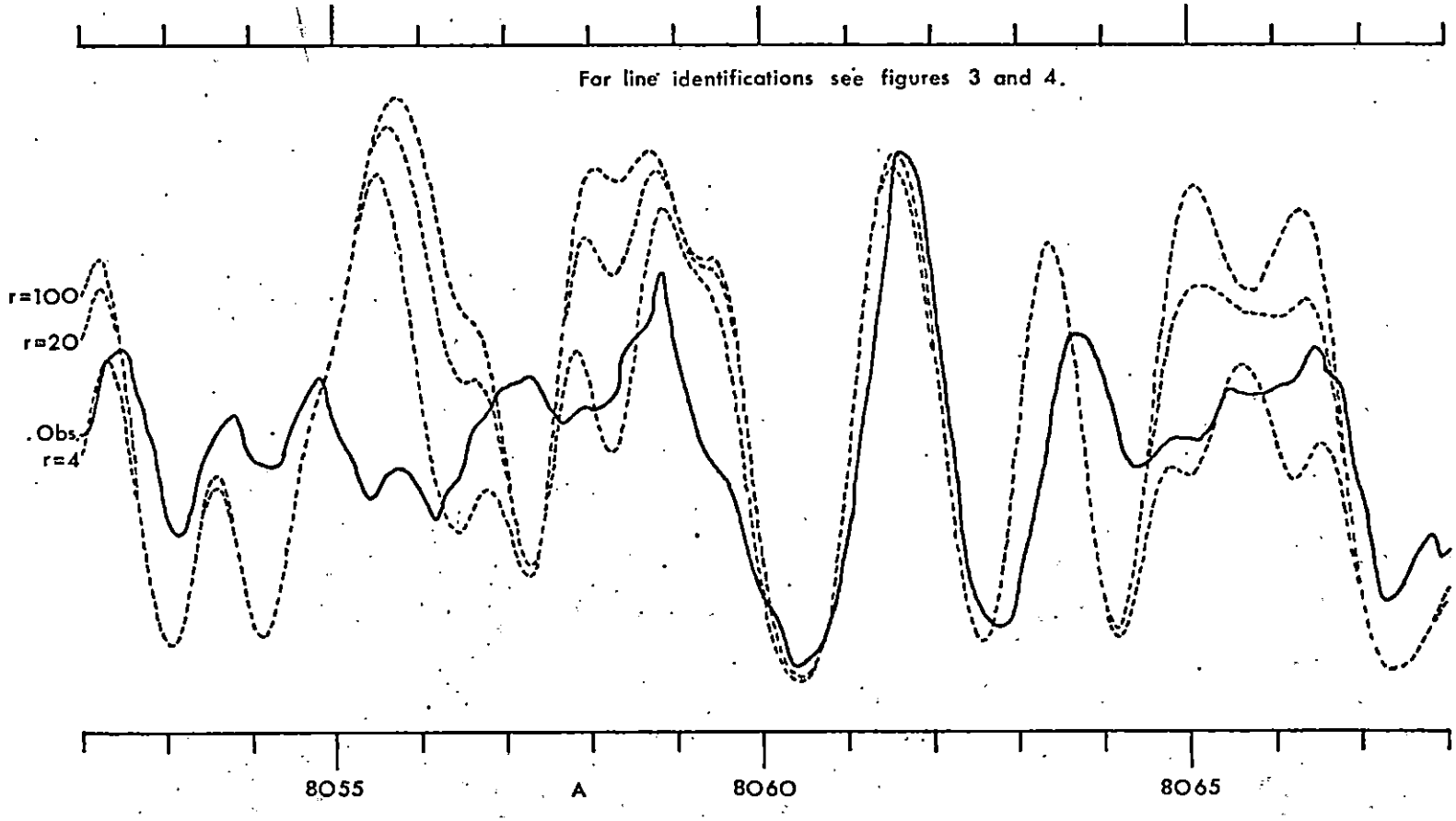

Figure 5. Comparison of instrumentally broadened theoretical profile and observed profile. Theoretical: T = 2800 K, V_t = 9.5 km/sec. Observed: 19. Psc. P: 4970. Dispersion = 12.8 A/mm.

ratio. All were concerned with the possibility of measuring the $C^{13}N^{14}$ lines. As has been mentioned before, two different dispersions were employed in this study. A region of the observed and calculated profiles for 19 Piscium (dispersion =7.9 A/mm) is shown in figure 3. The three theoretical profiles correspond to the three isotope ratios of 4, 20 and 100. The theoretical profile agrees well with the observed profile except that in some places there appears to be added absorption in the observed profile. The cause for this added absorption is that lines of water vapour have been omitted from the theoretical calculations. In figure 4 the same region is compared with the theoretical profile but at a different dispersion of 12.8 A/mm. It is readily seen that at this dispersion many of the expected $C^{13}N^{14}$ lines do not appear. In figure 5 (which covers the same wavelength region) the observed profile is compared with a theoretical profile which has been corrected for instrumental broadening. The agreement betwwen the profiles is better than in figure 4 and the $C^{13}N^{14}$ features are not as distinct on the theoretical tracing. It was therefore thought that for observation of individual $C^{13}N^{14}$ lines in the near infra-red, a dispersion of 7.9 A/mm or better was required.

Fujita (1968a, 1968b) studied the effect of different dispersions ranging from 15 A/mm to 2 A/mm. Although many features were identifiable at 8 A/mm they were more easily observed at 3 A/mm. Since the turbulent velocities (7 km/s) give rise to a Doppler width of approximately 0.2 A, the use of dispersions that resolve to 0.1 A is sufficient. Fujita (1968a) assumed a grain size of 0.02 mm which yields a resolution of 0.1 A for a dispersion of 5 A/mm. Therefore, although the 7.9 A/mm dispersion used in this study resolved lines well, a still higher dispersion would improve the resolution. The use of higher dispersions was impractical because

the exposures required were quite long.

When considering exposure times and quality of the spectrograms, the best dispersion available is 7.9 A/mm. The estimation of grain size in this case may be a little large since one would not expect as good agreement as was obtained betwwen observed and calculated profiles if the resolution were 0.16 A. The plates taken at 12.8 A/mm do not resolve the $C^{13}N^{14}$ lines sufficiently to be of much use. The depths method was applied using instrumental broadening but the results obtained had a large uncertainty. Since spectra of 19 Piscium were obtained at both dispersions a comparison of results was made to determine the inaccuracy introduced by the lower dispersion.

2.13 Effect of additional lines.

When calculating the absorption coefficient the only molecules considered were $C^{12}N^{14}$ and $C^{13}N^{14}$. Other molecules such as $C^{12}C^{12}$ and $C^{12}C^{13}$ were omitted. Although their bands affect the region around λ7800 A (the $C^{12}C^{13}$(3,0) R band head occurs at λ7820.27) and C_2 lines may be found scattered throughout the region, most of these lines are weak when compared to the CN lines. With the method of line depths the amount of absorption added to some of the measured lines cannot be estimated and hence the ratio determined from such a line will be too low. In the empirical pseudo-curve of growth method the lines with added contributions show up readily as a scatter in the points. The lowest points in the graph are those with little or no additional absorptions (see figures 6, 7 and 8). These points may be ignored when comparing the two sets of graphs. Similarly additional absorptions of other elements and telluric molecules may also be omited. It was found for the spectrograms at the lower disper-

sion that not only were some lines over absorbed but also that some lines were filled in. The empirical pseudo-curve of growth method was not used on these spectrograms because the scatter in the points was too great.

Another contribution, which was not included in the calculations, to the observed absorption profile was atmospheric or telluric water vapour. The strength of these lines was dependent on the zenith distance of the star during exposure and on the amount of water vapour in the air. Since the Dominion Astrophysical Observatory is situated quite close to sea level and the long exposures meant following the star until it was far from the zenith, the telluric water vapour lines were quite strong. In addition to the possibility of an unpredictable variation in strength there was also the variable displacement of the telluric lines with respect to the stellar lines.

2.14 Effect of radial velocity on telluric water vapour lines.

The effect of differences in radial velocities on the positions of the telluric H_2O lines has been investigated by Fujita (Fujita and Utsumi, 1963, Fujita, 1963 and 1964). He found that the appearance of the spectrum was greatly changed, even for the same star, when observed at different times of the year. This was due to the variation in the earth's velocity with respect to the star as a result of the earth's rotation on its axis and its revolution about the sun. The variation depended upon the star's coordinates but the variations noted by Fujita (1964) ranged up to 50 km/s, corresponding to a shift of 1.4 A in the near infra-red. When the variation from star to star was considered the difference in wavelength could be as large as 2.0 A. Also the structure of the water vapour spectrum is very complex (since the water vapour molecule

is triatomic) and there are many lines in the region under study (there are 320 lines from λ7800 to λ8300 A).

There were two ways to approach the problem of water vapour. One was to add the water vapour contribution to the summed absorption coefficient for CN, with an appropriate shift for radial velocity. This method was impractical because the amount to be added would have had to been determined by trial and error. Also the amount the lines were to be shifted would have varied for each spectrogram. The second method and the one adopted was to omit any line which appeared to be overly absorbed. As noted earlier this was very simply taken care of in the empirical pseudo-curve of growth method. For the depths method it was possible to omit the $C^{13}N^{14}$ lines so affected by comparing the wavelength with the known wavelength of the telluric H_2O lines.

CHAPTER 3

SUMMARY AND CONCLUSIONS

The results for the four stars are given in table VIII. The results for the empirical pseudo-curve of growth method and depths method are given in columns labled C and D respectively. For two of the spectrograms there is only one value, for the depths method and for a temperature of 2800 K. These two values were obtained by matching an instrumentally broadened theoretical profile to the observed profile. The empirical pseudo-curve of growth method could not be used on these plates for the reason explained in chapter 2. The results for the individual stars are:

19 Piscium (figures 6,7 and 8)

Two spectrograms of 19 Psc were available for this study. However since the results from the lower dispersion spectrogram are subject to a larger uncertainty the value for plate 4970 is given a low weight. The results indicate a C^{12}/C^{13} ratio of less than twenty for all assumed temperatures. On the basis of temperatures published by Utsumi (1970) the isotopic abundance ratio is 6.0 for a temperature of 2800 K.

DS Pegasi (figures 9, 10 and 11)

For the upper and lower limits of temperatures used in this study the C^{12}/C^{13} ratio is near 20 but this is still as low or lower than found by Fujita (1970) for this star. The ratio for the assumed temperature of 2800 K is 8.6, the least amount of C^{13} of the stars in this thesis.

TABLE VIII

Observed C^{12}/C^{13} ratio for assumed temperatures.

Temperature=		3150		2800		2400 K	
Star	Plate	C	D	C	D	C	D
Y CVn	2412	2.8	5.5	2.0	2.4	3.2	6.2
DS Peg	1512	12.6	23.1	7.0	10.1	17.8	26.5
UX Dra	4763				6.4		
19 Psc	1511	15.9	12.4	6.3	5.6	20.0	15.3
19 Psc	4970				5.6		
19 Psc	1511						
(V_t= 7.5 km/s)		13.3	15.3	7.9	6.7	17.8	18.6

C empirical pseudo-curve of growth method

D depths method

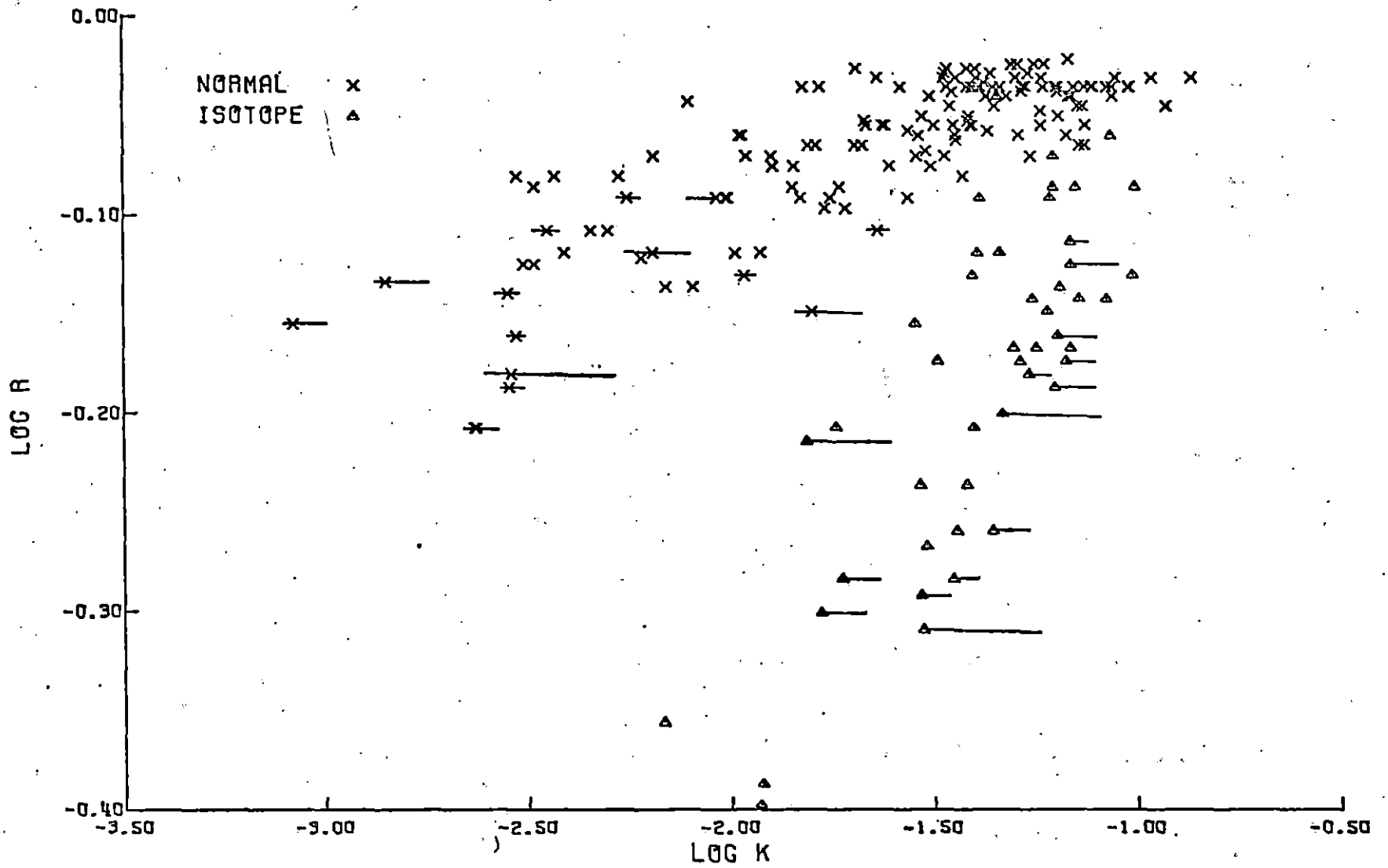

Figure 6. Empirical pseudo-curve of growth method for 19 Psc, plate 1511, with a temperature of 2400 K.

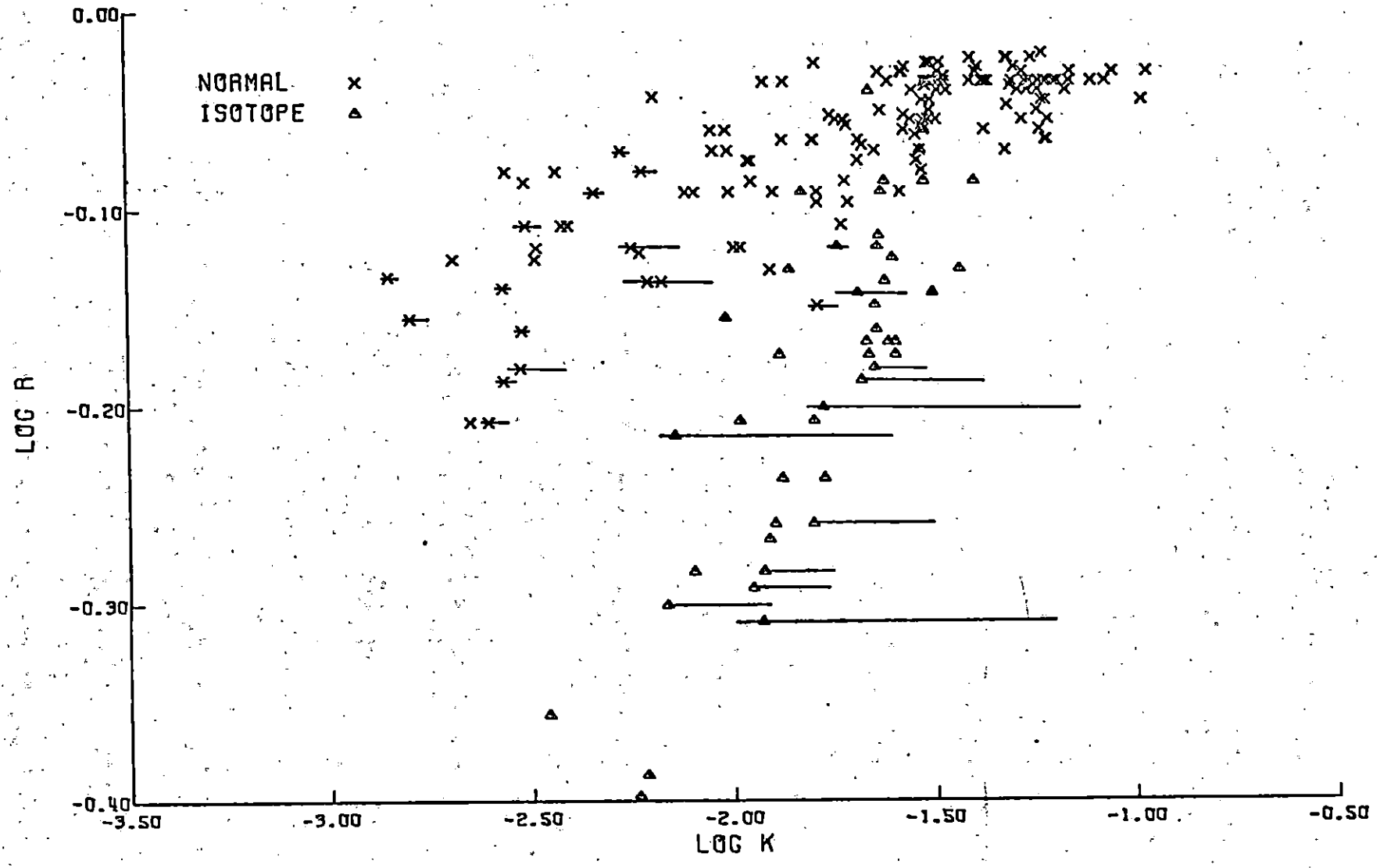

Figure 7. Empirical pseudo-curve of growth method for 19 Psc, plate 1511, with a temperature of 2800 K.

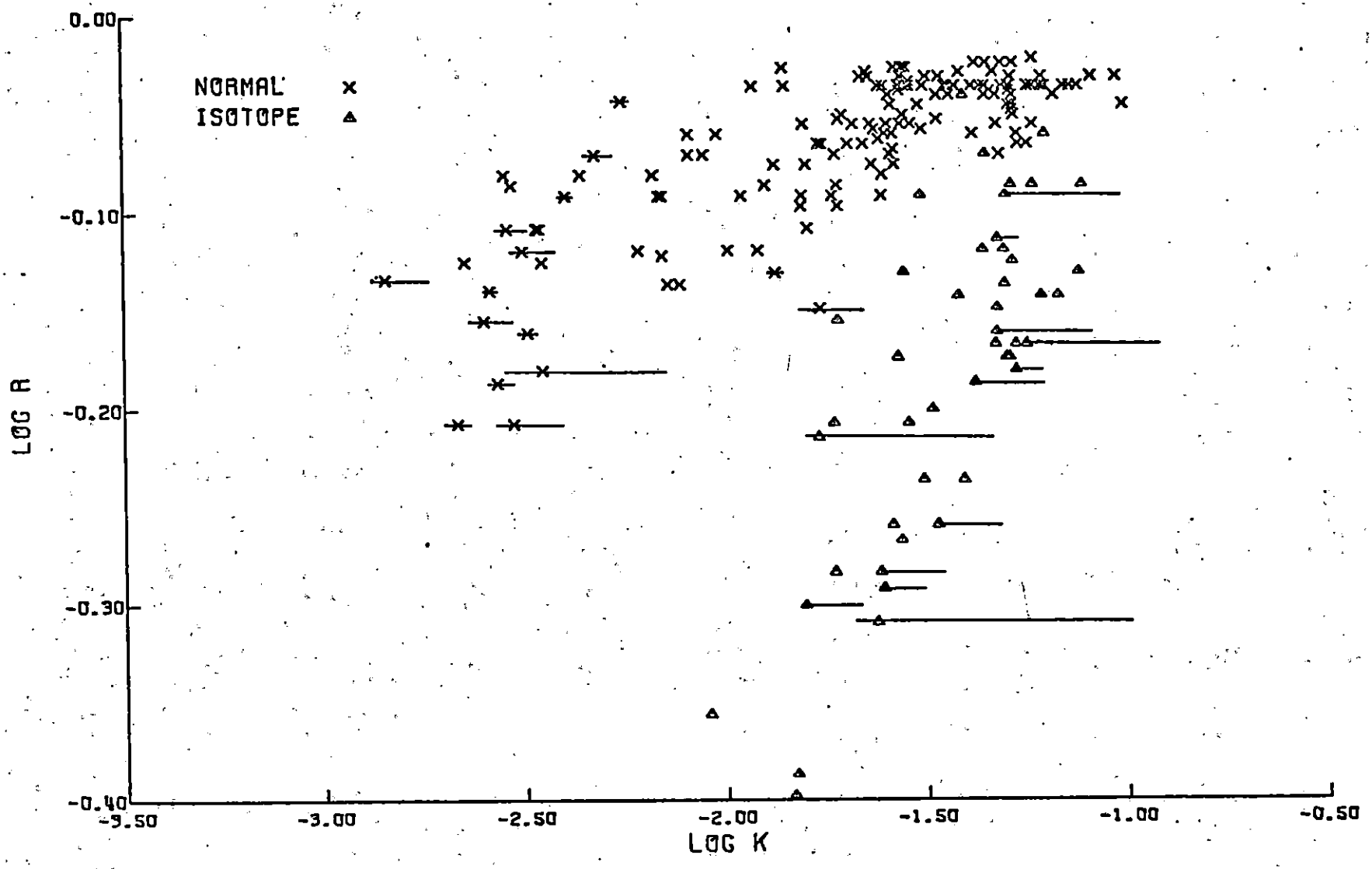

Figure 8. Empirical pseudo-curve of growth method for 19 Psc, plate 1511, with a temperature of 3150 K.

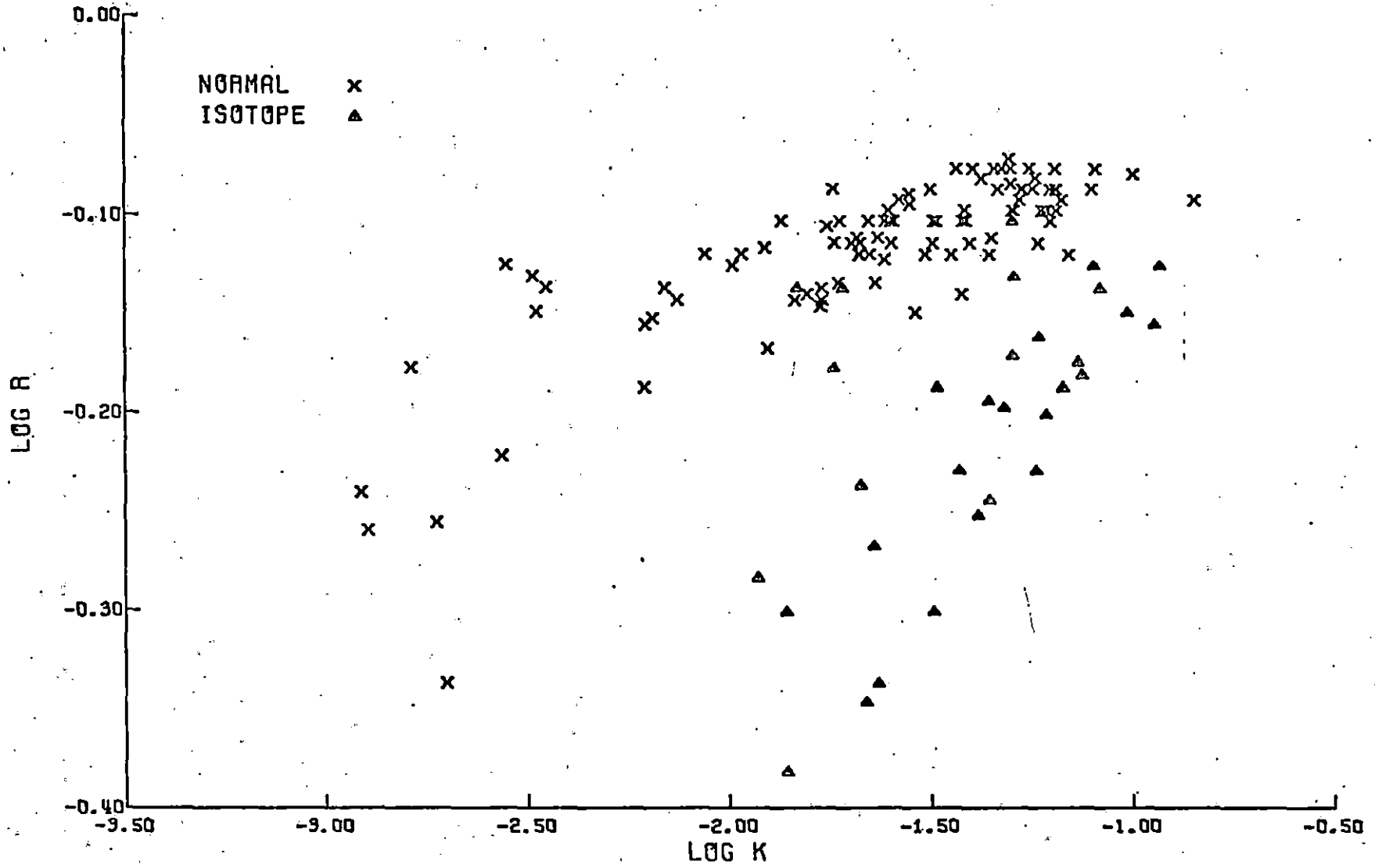

Figure 9. Empirical pseudo-curve of growth method for DS Peg, plate 1512, with a temperature of 2400 K.

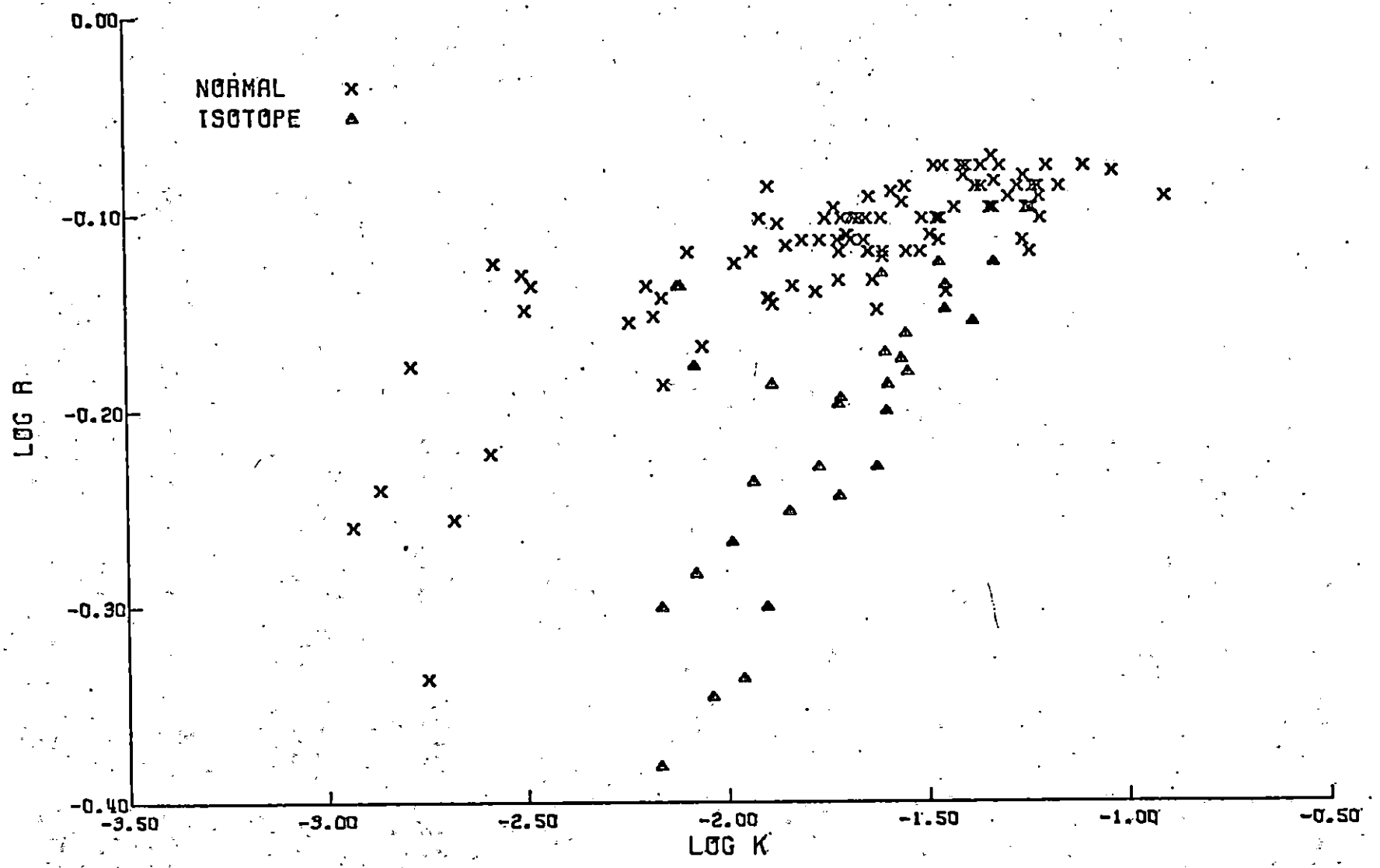

Figure 10. Empirical pseudo-curve of growth method for DS Peg, plate 1512, with a temperature of 2800 K.

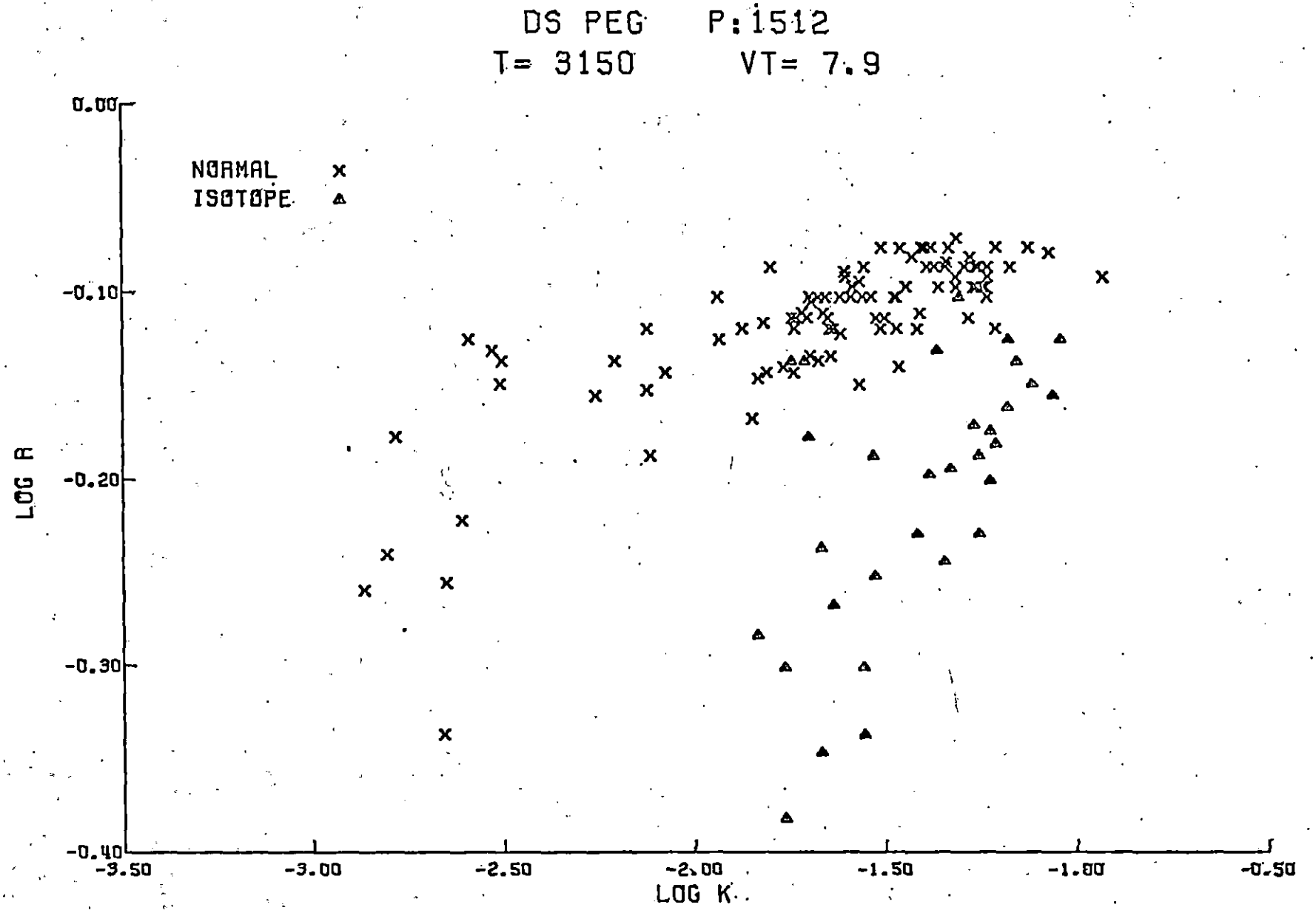

Figure 11. Empirical pseudo-curve of growth method for DS Peg, plate 1512, with a temperature of 3150 K.

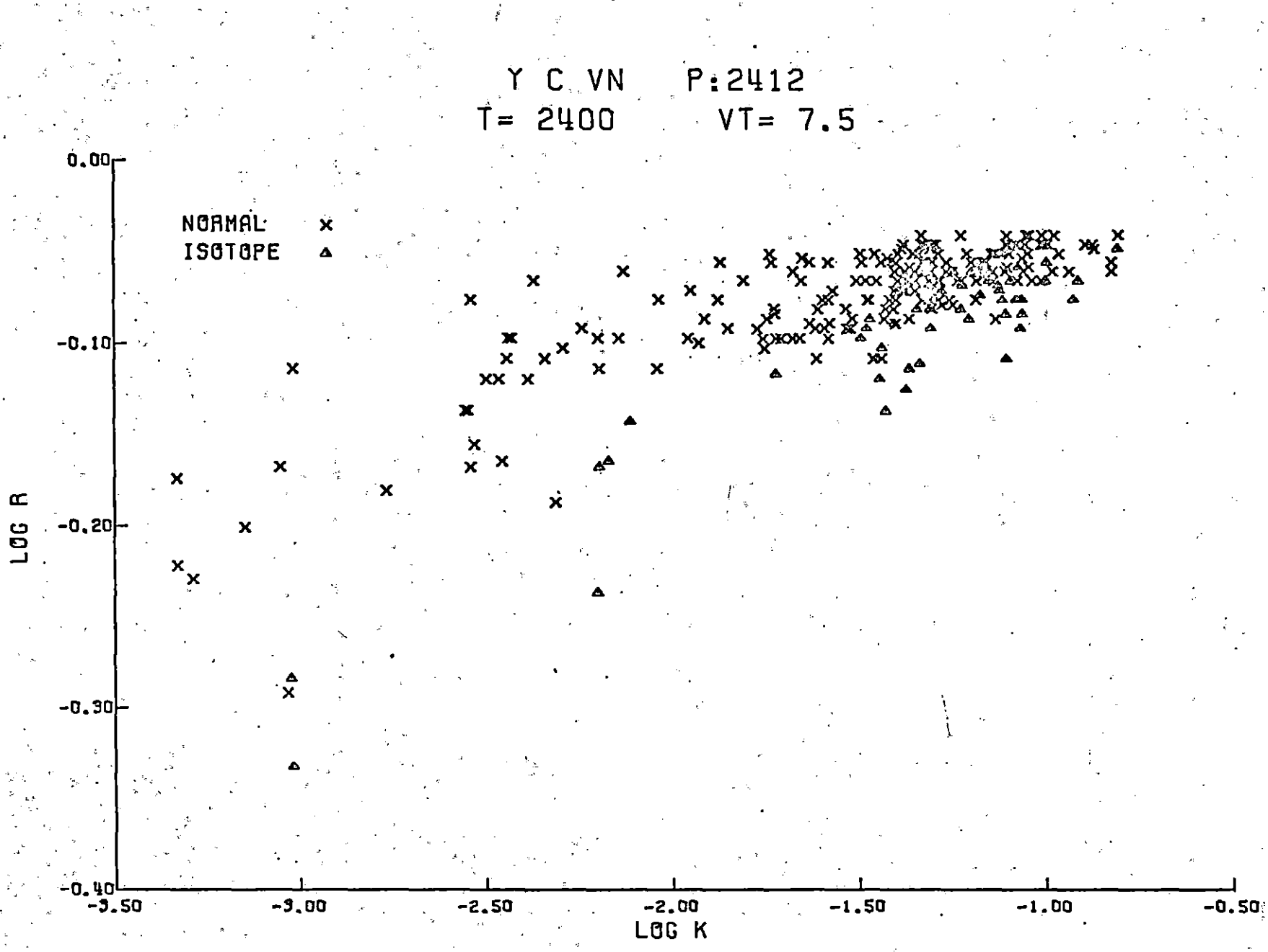

Figure 12. Empirical pseudo-curve of growth method for Y CVn, plate 2412, with a temperature of 2400 K.

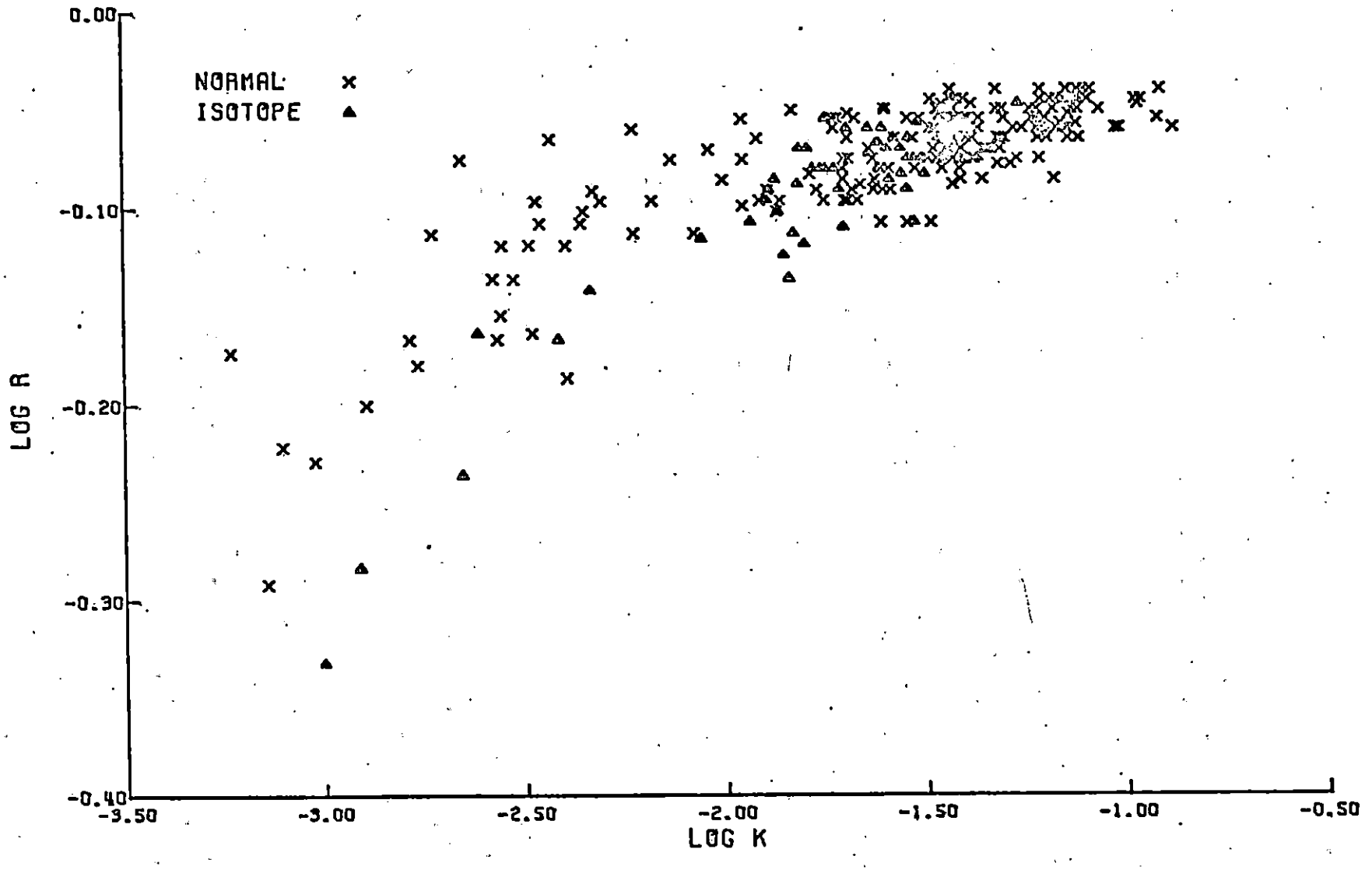

Figure 13. Empirical pseudo-curve of growth method for Y CVn, plate 2412, with a temperature of 2800 K.

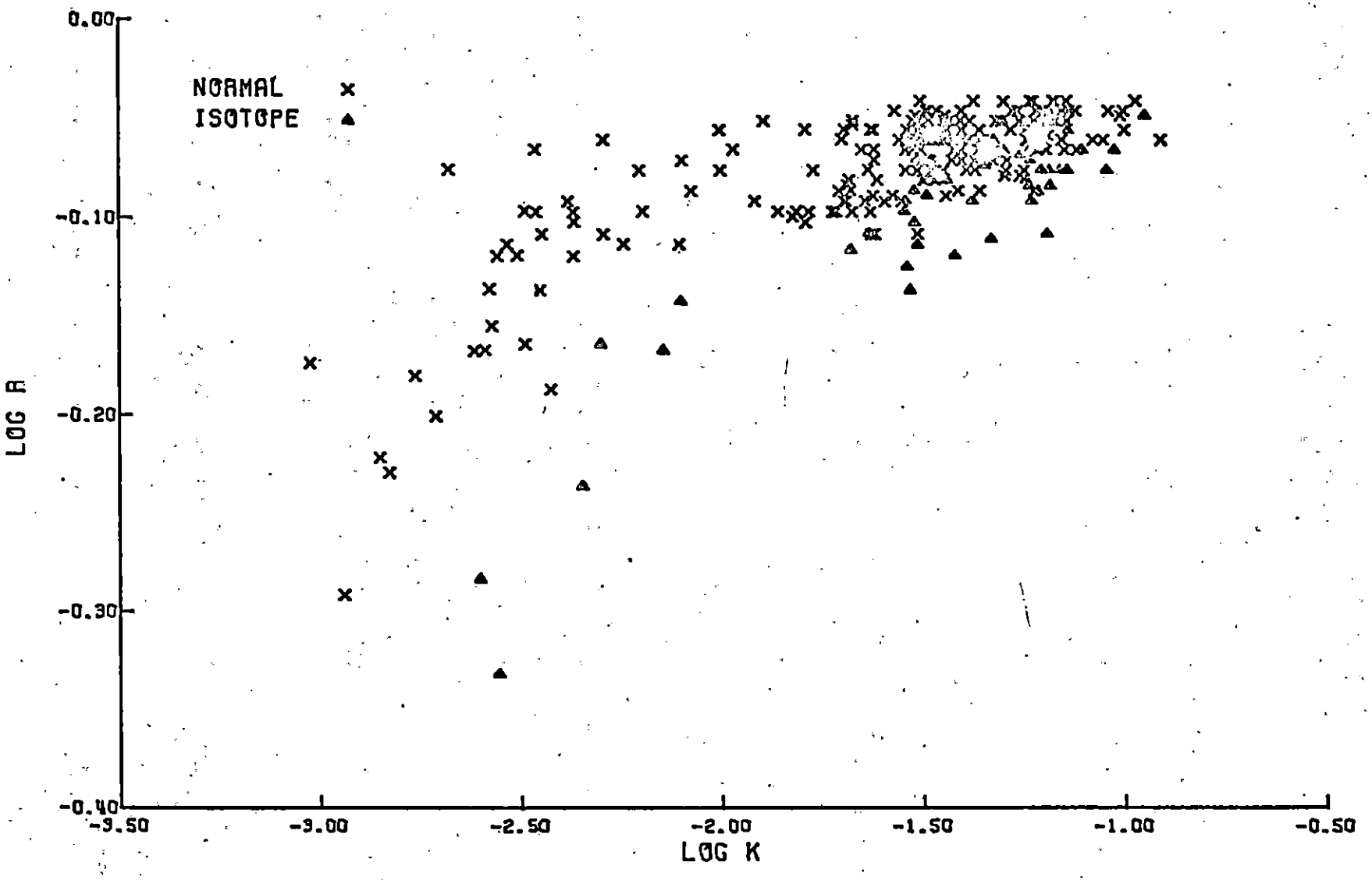

Figure 14. Empirical pseudo-curve of growth method for Y CVn, plate 2412, with a temperature of 3150 K.

Y Canum Venaticorum (figures 12, 13 and 14)

The results indicate a very high abundance of C^{13} in the atmosphere of Y CVn. All investigations of Y CVn show strong evidence of C^{13} (see table I). For the assumed temperature of 3150 K the corresponding carbon ratio is 4.2 . However even for the other two temperatures the ratio is still less than 5 hence Y CVn shows clearly the highest abundance of C^{13} of all the stars in this study.

UX Draconis

The only spectrogram of this star is at the lower dispersion so that the results are subject to a larger uncertainty than those of the other stars. The isotope ratio found is 6.4 for the assumed temperature of 2800 K.

The results for these four stars are in accord with earlier studies, excepting those of Fujita (1970). The empirical pseudo-curve of growth method was found to be superior to the depth method because it was easier to use and made few assumptions. The one drawback is that high dispersion spectrograms are necessary. Finally more work is necessary to determine accurately the molecular excitation temperature of the carbon stars.

APPENDIX A

FORTRAN LISTING OF PROGRAMS

```
C     PROGRAM 'POS & INT'
C
C     TO CALCULATE POSITIONS AND INTENSITIES OF THE CN RED SYSTEM,
C     FOR BOTH NORMAL (C12) AND ISOTOPE (C13) FORMS OF CARBON
C
C     FORMULAS FOR LINE POSITIONS FROM T. FAY, I. MARENIN, AND
C     W. VAN CITTERS,  1970
C
C     FORMULAS FOR HONL-LONDON FACTORS FROM L.T. EARLS, 1935, PHY.
C     REV.  VOL 48, P423.
C
C     INPUT:  FROM CARD READER  'NREAD'                          FORMAT:
C        DESIRED WAVELENGTH REGION 'LAMMIN' TO 'LAMMAX'           1000
C        TEMPERATURE 'T' AND TURBULENT VELOCITY 'VT'              1000
C        PARTITION FUNCTIONS, NORMAL'QN' AND ISOTOPE 'QI'         1010
C        ROTATIONAL AND VIBRATIONAL CONSTANTS FOR NORMAL UPPER &
C        LOWER, ISOTOPE UPPER & LOWER LEVELS (OUTPUT FROM
C        PROGRAM                                                  1030
C        FOR EACH BAND:
C             MINIMUM 'MIN' AND MAXIMUM 'MAX' ROTATIONAL
C             QUANTUM NUMBER N'',  'N'                           1040
C             UPPER, V', AND LOWER, V'', VIBRATIONAL QUANTUM
C             NUMBERS OF BAND ('IVI','IVII')                     1040
C             FRANK CONDON FACTOR                                1010
C
C     OUTPUT:  ON PRINTER  'NPRINT'                              FORMAT:
C        WAVELENGTH REGION 'LAMMIN' TO 'LAMMAX'                   1020
C        VIBRATIONAL BANDS INCLUDED ('IVI','IVII')                1050
C        TOTAL NUMBER OF LINES INCLUDED, NORMAL 'LN', &
C        ISOTOPE 'LI'                                             1060
C
C     OUTPUT:  ON TAPE 'NTAPE1'
C        DATA SET 1      WAVELENGTH AND INTENSITY OF NORMAL CN
C        DATA SET 2      WAVELENGTH AND INTENSITY OF ISOTOPIC CN
C
C     OUTPUT:  ON TEMPORARY SEQUENTIAL DATA SET  'NTAPE2'
C        WAVELENGTH AND INTENSITY OF ISOTOPIC CN
C
C     FOR EACH VIBRATIONAL BAND TO BE INCLUDED THE APPROXIMATE UPPER
C     AND LOWER ROTATIONAL QUANTUM NUMBERS MUST BE SUPPLIED
C     THE BANDS TO BE INCLUDED AND THE MAXIMUM AND MINIMUM ROTATIONAL
C     QUANTUM NUMBER TO BE INCLUDED ARE CHOSEN FROM WAVELENGTH TABLES
C     OF ALL THE BANDS
C
C     BRANCHES IDENTIFIED ACCORDING TO POSITION IN ARRAYS
C       1    2    3    4    5    6    7    8    9   10   11   12
C      P1   P2   Q1   Q2   R1   R2  P12  P21  Q12  Q21  R12  R21
C
C
      DIMENSION CUNS(8,20),CLNS(5,20),CUIS(8,20),CLIS(5,20),CONSUN(8),
```

```
     1  CONSLN(5),CONSUI(8),CONSLI(5),LPOSN(12),LPOSI(12),NPOSN(12),
     2  NPOSI(12),INTN(12),INTI(12)
      DOUBLE PRECISION CUNS,CLNS,CUIS,CLIS,CONSUN,CONSLN,CONSUI,
     1  CONSLI,LPOSN,LPOSI,NPOSN,NPOSI,LAMMIN,LAMMAX,C1N,C1I,C2N,C2I
      REAL INTN,INTI,MAXINT,MININT,NII
C
      DATA NREAD,NPRINT,NTAPE1,NTAPE2/5,6,8,9/
      EXTERNAL SIGLAM,POSITN,INTEN
C
      REWIND NTAPE1
      REWIND NTAPE2
      LN=0
      LI=0
      MAXINT=0.0
C
CC    READ WAVELENGTH REGION
C
      READ(NREAD,1000) LAMMIN,LAMMAX
C
CC    READ TEMPERATURE AND TURBULENT VELOCITY (IN KM/SEC)
C
      READ(NREAD,1000) T,VT
C
CC    READ PARTITION FUNCTIONS FOR NORMAL AND ISOTOPIC CN
C
      READ(NREAD,1010) QN,QI
C
CC    WRITE WAVELENGTH REGION, TEMPERATURE AND TURBULENT VELOCITY
C
      WRITE(NPRINT,1020) LAMMIN,LAMMAX,T,VT
      LAMMIN=LAMMIN-5.
      LAMMAX=LAMMAX+5.
C
CC    READ UPPER AND LOWER ROTATIONAL AND VIBRATIONAL CONSTANTS
CC    FOR NORMAL FORM
C
      DO 100 I=1,20
      READ(NREAD,1030) (CUNS(J,I),J=1,7)
      READ(NREAD,1030) (CLNS(J,I),J=1,5)
  100 CONTINUE
C
CC    READ UPPER AND LOWER ROTATIONAL AND VIBRATIONAL CONSTANTS
CC    FOR ISOTOPIC FORM
C
      DO 110 I=1,20
      READ(NREAD,1030) (CUIS(J,I),J=1,7)
      READ(NREAD,1030) (CLIS(J,I),J=1,5)
  110 CONTINUE
      DO 120 I=1,20
      CUNS(1,I)=CUNS(1,I)+5.*CUNS(3,I)+.111113
```

```
      CLNS(1,I)=CLNS(1,I)+2.*CLNS(3,I)+.093446
      CUIS(1,I)=CUIS(1,I)+5.*CUIS(3,I)+.106504
      CLIS(1,I)=CLIS(1,I)+2.*CLIS(3,I)+.089563
      CUNS(8,I)=CUNS(2,I)/CUNS(3,I)
      CUIS(8,I)=CUIS(2,I)/CUIS(3,I)
  120 CONTINUE
      CONSTN=7.04116337D27/(QN*DSQRT(T/1.5635578D-7+VT*VT*1.D10))
      CONSTI=7.04116337D27/(QI*DSQRT(T/1.62369464D-7+VT*VT*1.0D10))
C
CC    DEFINE SQUARE OF ELECTRONIC TRANSITION MOMENT
      $K=.52*2.5416*2.5416E-36
C
CC    MULTIPLY BY AN ARBITRARY CONSTANT FACTOR SUCH THAT INTENSITIES
C     ARE OF THE ORDER OF UNITY
      $K=$K*1.E16
C
CC    BEGIN CALCULATIONS ON NEXT BAND
CC
CC    READ MINIMUM AND MAXIMUM ROTATIONAL QUANTUM NUMBERS (+1)
C
  130 READ(NREAD,1040,END=240) MIN,MAX
C
CC    READ VIBRATIONAL QUANTUM NUMBERS
CC
      READ(NREAD,1040) IVI,IVII
C
CC    READ FRANK CONDON FACTOR
C
      READ(NREAD,1010) FRANK
C
CC    CALCULATE BAND STRENGTH 'BNDSTR'
      BNDSTR=$K*FRANK
C
CC    COPY CONSTANTS FROM STORAGE INTO ARRAY TO BE USED
C
      DO 140 I=1,8
      CONSUN(I)=CUNS(I,IVI+1)
      CONSUI(I)=CUIS(I,IVI+1)
  140 CONTINUE
      DO 150 I=1,5
      CONSLN(I)=CLNS(I,IVII+1)
      CONSLI(I)=CLIS(I,IVII+1)
  150 CONTINUE
C
CC    WRITE VIBRATIONAL QUANTUM NUMBERS OF BAND
C
      WRITE(NPRINT,1050) IVI,IVII
      DO 230 K=MIN,MAX
      N=K-1
      NII=N
```

```
C
CCC     CALCULATE WAVENUMBERS OF THE 12 BRANCHES FOR N''=N',
CCC     'NPOSN' FOR NORMAL AND 'NPOSI' FOR ISOTOPE
C
        CALL POSITN(NII,CONSUN,CONSLN,NPOSN,C1N,C2N)
        CALL POSITN(NII,CONSUI,CONSLI,NPOSI,C1I,C2I)
C
CCC     CALCULATE HONL-LONDON FACTORS FOR THE 12 BRANCHES
CCC     'INTN' FOR NORMAL AND 'INTI' FOR ISOTOPE
C
        CALL INTEN(NII,CONSUN(8),INTN)
        CALL INTEN(NII,CONSUI(8),INTI)
C
CCC     CONVERT WAVENUMBERS IN VACUO TO WAVELENGTHS IN AIR,
CCC     'LPOSN' FOR NORMAL AND 'LPOSI' FOR ISOTOPE
C
        DO 160 I=1,12
        CALL SIGLAM(NPOSN(I),LPOSN(I))
        CALL SIGLAM(NPOSI(I),LPOSI(I))
  160   CONTINUE
        C1N=DEXP(-C1N*1.43879/T)
        C2N=DEXP(-C2N*1.43879/T)
        C1I=DEXP(-C1I*1.43879/T)
        C2I=DEXP(-C2I*1.43879/T)
C
CCC     CALCULATE INTENSITIES FOR THE 12 BRANCHES
C
        DO 170 I=1,11,2
        INTN(I)=INTN(I)*CONSTN*BNDSTR*C1N
        INTI(I)=INTI(I)*CONSTI*BNDSTR*C1I
        INTN(I+1)=INTN(I+1)*CONSTN*BNDSTR*C2N
        INTI(I+1)=INTI(I+1)*CONSTI*BNDSTR*C2I
  170   CONTINUE
C
CCC     FIND MAXIMUM INTENSITY TO THIS POINT
C
        DO 180 I=1,12
        MAXINT=AMAX1(MAXINT,INTN(I))
  180   CONTINUE
        MININT=MAXINT*1.0E-6
C
CCC     OMIT ANY LINE WHOSE INTENSITY IS 1.0E-6* (MAXIMUM INTENSITY)
C
        DO 190 I=1,12
        IF(MININT.LT.INTN(I)) GO TO 190
        LPOSN(I)=0.0
        LPOSI(I)=0.0
  190   CONTINUE
C
C       OMIT APPROPRIATE BRANCHES FOR LOW ROTATIONAL QUANTUM NUMBER
```

```
C
      IF(N.GT.2) GO TO 200
      LPOSN(7)=0.0
      LPOSI(7)=0.0
      IF(N.GT.1) GO TO 200
      LPOSN(1)=0.0
      LPOSI(1)=0.0
      LPOSN(2)=0.0
      LPOSI(2)=0.0
      LPOSN(9)=0.0
      LPOSI(9)=0.0
      IF(N.GT.0) GO TO 200
      LPOSN(4)=0.0
      LPOSI(4)=0.0
      LPOSN(6)=0.0
      LPOSI(6)=0.0
      LPOSN(8)=0.0
      LPOSI(8)=0.0
      LPOSN(3)=0.0
      LPOSI(3)=0.0
      LPOSN(11)=0.0
      LPOSI(11)=0.0
  200 CONTINUE
C
C     WRITE POSITION (WAVELENGTHS) AND INTENSITIES ONTO TAPE OMITTING
C     ALL LINES OUTSIDE OF REGION 'LAMMIN' TO 'LAMMAX'
C     NORMAL ON 'NTAPE1', ISOTOPE ON 'NTAPE2'
C
      DO 210 I=1,12
      IF(LPOSN(I).LT.LAMMIN.OR.LPOSN(I).GT.LAMMAX) GO TO 210
      LN=LN+1
      WRITE(NTAPE1) LPOSN(I),INTN(I)
  210 CONTINUE
      DO 220 I=1,12
      IF(LPOSI(I).LT.LAMMIN.OR.LPOSI(I).GT.LAMMAX) GO TO 220
      LI=LI+1
      WRITE(NTAPE2) LPOSI(I),INTI(I)
  220 CONTINUE
  230 CONTINUE
      GO TO 130
  240 CONTINUE
      ENDFILE NTAPE1
      ENDFILE NTAPE2
      REWIND NTAPE2
C
C     COPY TEMPORARY DATA SET (ISOTOPE ON 'NTAPE2') ONTO TAPE
C     ('NTAPE1') AS DATA SET 2
C
  250 READ(NTAPE2,END=260) C1N,MININT
      WRITE(NTAPE1) C1N,MININT
```

```
      GO TO 250
C
C     CLOSE AND REWIND ALL DATA SETS
  260 ENDFILE NTAPE1
      REWIND NTAPE1
      REWIND NTAPE2
C
C     WRITE NUMBER OF NORMAL AND ISOTOPE LINES WHICH ARE ON TAPE
C
      WRITE(NPRINT,1060) LN,LI
      STOP
 1000 FORMAT(8F10.5)
 1010 FORMAT(2(1PE15.8))
 1020 FORMAT('1',38X,'LAMBDA MINIMUMUM=',F10.3,5X,'LAMBDA MAXIMUM=',
     1F10.3,/,40X,'TEMPERATURE=',F10.2,5X,'TURBULENT VELOCITY=',
     2F10.2,//,10X,'BANDS INCLUDED')
 1030 FORMAT(16X,7A8)
 1040 FORMAT(3I10)
 1050 FORMAT(' ',12X,'CN(',I2,',',I2,')')
 1060 FORMAT('1',////////////,'0',20X,'THE NUMBER OF LINES ON TAPE IS:
     1NORMAL',I10,/,54X,'ISOTOPE',I9)
      END
```

```
C       SUBROUTINE SIGLAM
C
C       CONVERTS WAVENUMBER 'SIGMA' IN VACUO INTO WAVELENGTH 'LAMBDA' IN
C       AIR (STP).  SIGMA IN CM-1 AND LAMBDA IN ANGSTROMS
C
        SUBROUTINE SIGLAM(SIGMA,LAMBDA)
        DOUBLE PRECISION SIGMA,LAMBDA,DENM,D
        D=SIGMA*SIGMA
        DENM=SIGMA*(1.+2.72643D-4+D*(1.2288D-14+D*3.555D-24))
        LAMBDA=1.D8/DENM
        RETURN
        END
```

```
C     SUBROUTINE POSITN
CCC
CCC   CALCULATES THE ENERGY LEVELS AND WAVE NUMBERS OF THE 12 BRANCHES
C
      SUBROUTINE POSITN(NII,CU,CL,POS,EL1,EL2)
      DIMENSION CU(8),CL(5),POS(12)
      DOUBLE PRECISION CU,CL,POS,P2Q,EL1,EL2,YY1,S,F1,F2,F3,EU1,EU2,
     1  P2Q1,NII1,NII2
      REAL NII
C
      P2Q=.5*CU(6)+CU(7)
      YY1=CU(8)*(CU(8)*.25-1.)
      P2Q1=(1.-.5*CU(8))*P2Q
      NII1=NII*(NII+1.)
CCC
CCC   CALCULATE ENERGY LEVELS FOR LOWER SIGMA STATE INCLUDING
CCC   GAMMA TYPE DOUBLING
C
      EL1=CL(1)+NII1*(CL(3)-NII1*(CL(4)-NII1*CL(5)))+.5*NII*CL(2)
      EL2=EL1-CL(2)*(NII+.5)
CCC
CCC   CALCULATE ENERGY LEVELS:
CCCCC
CCC   FOR R1 AND R21
C
      NII1=(NII+2.)*(NII+2.)
      S=DSQRT(NII1+YY1)
      F1=(P2Q1+CU(7)*(NII+1.)*(NII+3.))*(NII+2.)*.5/S
      F2=P2Q*(NII+1.)*(NII+3.)*.5/S
      F3=P2Q*(NII+2.)*.5
      NII2=(NII+1.5)*(NII+1.5)
      EU1=CU(1)+CU(3)*(NII1-1.-S)-NII2*NII2*(CU(4)-CU(5)*NII2)
      NII2=(NII+2.5)*(NII+2.5)
      EU2=CU(1)+CU(3)*(NII1-1.+S)-NII2*NII2*(CU(4)-CU(5)*NII2)
      POS(5)=EU1-EL1-F1-F2+F3
      POS(12)=EU2-EL1+F1+F2+F3
CCC
CCC   FOR Q1, Q21, R2 AND R21
C
      NII1=(NII+1.)*(NII+1.)
      S=DSQRT(NII1+YY1)
      F1=(P2Q1+CU(7)*NII*(NII+2.))*(NII+1.)*.5/S
      F2=P2Q*NII*(NII+2.)*.5/S
      F3=P2Q*(NII+1.)*.5
      NII2=(NII+.5)*(NII+.5)
      EU1=CU(1)+CU(3)*(NII1-1.-S)-NII2*NII2*(CU(4)-CU(5)*NII2)
      NII2=(NII+1.5)*(NII+1.5)
      EU2=CU(1)+CU(3)*(NII1-1.+S)-NII2*NII2*(CU(4)-CU(5)*NII2)
      POS(3)=EU1-EL1+F1-F2-F3
```

```
      POS(10)=EU2-EL1-F1+F2-F3
      POS(6)=EU2-EL2-F1+F2-F3
      POS(11)=EU1-EL2+F1-F2-F3
C
CC    FOR P1, Q2, Q12 AND P21
C
      NII1=NII*NII
      S=DSQRT(NII1+YY1)
      F1=(P2Q1+CU(7)*(NII1-1.))*NII*.5/S
      F2=P2Q*(NII1-1.)*.5/S
      F3=P2Q*NII*.5
      NII2=(NII-.5)*(NII-.5)
      EU1=CU(1)+CU(3)*(NII1-1.-S)-NII2*NII2*(CU(4)-CU(5)*NII2)
      NII2=(NII+.5)*(NII+.5)
      EU2=CU(1)+CU(3)*(NII1-1.+S)-NII2*NII2*(CU(4)-CU(5)*NII2)
      POS(1)=EU1-EL1-F1-F2+F3
      POS(4)=EU2-EL2+F1+F2+F3
      POS(9)=EU1-EL2-F1-F2+F3
      POS(8)=EU2-EL1+F1+F2+F3
C
CC    FOR P2 AND P12
C
      NII1=(NII-1.)*(NII-1.)
      S=DSQRT(NII1+YY1)
      F1=(P2Q1+CU(7)*(NII-2.)*NII)*(NII-1.)*.5/S
      F2=P2Q*(NII-2.)*NII*.5/S
      F3=P2Q*(NII-1.)*.5
      NII2=(NII-1.5)*(NII-1.5)
      EU1=CU(1)+CU(3)*(NII1-1.-S)-NII2*NII2*(CU(4)-CU(5)*NII2)
      NII2=(NII-.5)*(NII-.5)
      EU2=CU(1)+CU(3)*(NII1-1.+S)-NII2*NII2*(CU(4)-CU(5)*NII2)
      POS(2)=EU2-EL2-F1+F2-F3
      POS(7)=EU1-EL2+F1-F2-F3
      RETURN
      END
```

```
C     SUBROUTINE INTENSITY
CC
CC    SUBROUTINE INTEN
CC
CC    CALCULATES HONL-LONDON FACTORS
C
      SUBROUTINE INTEN(NII,YI,INT)
      REAL INT(12),J,J1,J12,$J,NII
      DOUBLE PRECISION YI
      YI1=YI*(YI-4.)
C
CC    HONL-LONDON FACTORS FOR P12 ('INT(7)') AND P2 ('INT(2)')
C
      J=NII-1.5
      J1=J+J+1.
      J12=J1*J1
      U=1./ SQRT(YI1+J12)
      X=J1*U*(4.*J*(J+1.)+1.-YI-YI)
      $J=.0625/(J+1.)
      INT(7)=(J12-X)*$J
      INT(2)=(J12+X)*$J
C
CC    HONL-LONDON FACTORS FOR P21 ('INT(8)'), P1 ('INT(1)'),
CC    Q2 ('INT(4)') AND Q12 ('INT(9)')
C
      J=NII-.5
      J1=J+J+1.
      J12=J1*J1
      U=1./ SQRT(YI1+J12)
      X=J1*U*(4.*J*(J+1.)-7.+YI+YI)
      $J=.0625/(J+1.)
      INT(8)=(J12-X)*$J
      INT(1)=(J12+X)*$J
      $J=$J/J
      J12=J1*(4.*J*(J+1.)-1.)
      X=J1*U*(J*(-2.+J*(12.+8.*J))+1.-YI-YI)
      INT(4)=(J12+X)*$J
      INT(9)=(J12-X)*$J
C
CC    HONL-LONDON FACTORS FOR R2 ('INT(6)'), R12 ('INT(11)'),
CC    Q1 ('INT(3)') AND Q21 ('INT(10)')
C
      J=NII+.5
      J1=J+J+1.
      J12=J1*J1
      U=1./ SQRT(YI1+J12)
      X=J1*U*(4.*J*(J+1.)-7.+YI+YI)
      $J=.0625/J
      INT(6)=(J12+X)*$J
      INT(11)=(J12-X)*$J
```

```
      $J=$J/(J+1.)
      J12=J1*(4.*J*(J+1.)-1.)
      X=J1*U*(J*(-2.+J*(12.+8.*J))-7.+YI+YI)
      INT(3)=(J12+X)*$J
      INT(10)=(J12-X)*$J
C
CC    HONL-LONDON FACTORS FOR R1 ('INT(5)') AND R21 ('INT(12)')
C
      J=NII+1.5
      J1=J+J+1.
      J12=J1*J1
      U=1./ SQRT(YI1+J12)
      X=J1*U*(4.*J*(J+1.)+1.-YI-YI)
      $J=.0625/J
      INT(5)=(J12+X)*$J
      INT(12)=(J12-X)*$J
      RETURN
      END
```

```
//GO.FT08F001 DD DSNAME=HOLTS1,UNIT=TAPE,LABEL=(1,SL),DISP=(NEW,KEEP), *
// VOLUME=SER=B00071,DCB=(RECFM=VSB,LRECL=16,BLKSIZE=3204,DEN=2)
//GO.FT08F002 DD DSNAME=HOLTS2,UNIT=TAPE,LABEL=(2,SL),DISP=(NEW,KEEP), *
// VOLUME=SER=B00071,DCB=(RECFM=VSB,LRECL=16,BLKSIZE=3204,DEN=2)
//GO.FT09F001 DD UNIT=SYSDA,SPACE=(3204,(50,10)),                      *
// DCB=(RECFM=VSB,LRECL=16,BLKSIZE=3204,OPTCD=C)
```

```
C       PROGRAM 'SORT'
C
        DOUBLE PRECISION A(3000),C1
        REAL B(3000)
        INTEGER TAPE1,TAPE2
        DATA NTAPE,NTAPE1,NTAPE2/8,9,10/
        COMMON A,B
        EXTERNAL SORT,MERGE,SKIP
        NDIM=3000
        IND=0
        REWIND NTAPE
  100   REWIND NTAPE1
        REWIND NTAPE2
        TAPE1=NTAPE1
        TAPE2=NTAPE2
        DO 110 I=1,NDIM
        READ(NTAPE,END=120) A(I),B(I)
  110   CONTINUE
        N=NDIM
        GO TO 130
  120   N=I-1
  130   CALL SORT(N)
        DO 140 I=1,N
        WRITE(NTAPE1) A(I),B(I)
  140   CONTINUE
        ENDFILE NTAPE1
        IF(N.LT.NDIM) GO TO 190
  150   DO 160 I=1,NDIM
        READ(NTAPE,END=170) A(I),B(I)
  160   CONTINUE
        N=NDIM
        GO TO 180
  170   N=I-1
  180   CALL SORT(N)
        CALL MERGE(TAPE1,TAPE2,N)
        IF(N.LT.NDIM) GO TO 190
        GO TO 150
  190   CALL SKIP(NTAPE)
        REWIND TAPE1
  200   READ(TAPE1,END=210) C1,D1
        WRITE(NTAPE) C1,D1
        GO TO 200
  210   ENDFILE NTAPE
        REWIND NTAPE
        IF(IND.EQ.1) GO TO 220
        IND=1
        CALL SKIP(NTAPE)
        GO TO 100
  220   REWIND NTAPE
        REWIND NTAPE1
```

```
      REWIND NTAPE2
      STOP
      END
```

```
C       SUBROUTINE SORT
C
        SUBROUTINE SORT(N)
        DOUBLE PRECISION A(3000),MIN
        REAL B(3000),M1
        COMMON A,B
        M=N-1
        DO 110 I=1,M
        MIN=A(I)
        L=I
        K=I+1
        DO 100 J=K,N
        IF(MIN.LE.A(J)) GO TO 100
        MIN=A(J)
        L=J
  100   CONTINUE
        A(L)=A(I)
        A(I)=MIN
        M1=B(L)
        B(L)=B(I)
        B(I)=M1
  110   CONTINUE
        RETURN
        END
```

```
C       SUBROUTINE SKIP
C       SKIPS TO END OF DATA SET DEFINED BY 'NTAPE'
C
        SUBROUTINE SKIP(NTAPE)
  100   READ(NTAPE,END=110)
        GO TO 100
  110   RETURN
        END
C       SUBROUTINE MERGE
C
        SUBROUTINE MERGE(TAPE1,TAPE2,N)
        INTEGER TAPE1,TAPE2
        DOUBLE PRECISION A(3000),C1
        REAL B(3000)
        COMMON A,B
        REWIND TAPE1
        REWIND TAPE2
        I=1
        READ(TAPE1) C1,D1
  100   IF(C1.GT.A(I)) GO TO 110
        WRITE(TAPE2) C1,D1
        READ(TAPE1,END=120) C1,D1
        GO TO 100
  110   WRITE(TAPE2) A(I),B(I)
        I=I+1
        IF(I.GT.N) GO TO 130
        GO TO 100
  120   WRITE(TAPE2) A(I),B(I)
        I=I+1
        IF(I.GT.N) GO TO 140
        GO TO 120
  130   WRITE(TAPE2) C1,D1
        READ(TAPE1,END=140) C1,D1
        GO TO 130
  140   ENDFILE TAPE2
        REWIND TAPE1
        REWIND TAPE2
        I=TAPE2
        TAPE2=TAPE1
        TAPE1=I
        RETURN
        END
```

```
//GO.FT08F001 DD DSNAME=HOLTS1,UNIT=TAPE,LABEL=(1,SL),DISP=(OLD,KEEP), *
// VOLUME=SER=B00071,DCB=(RECFM=VSB,LRECL=16,BLKSIZE=3204,DEN=2)
//GO.FT08F002 DD DSNAME=HOLTS2,UNIT=TAPE,LABEL=(2,SL),DISP=(OLD,KEEP), *
// VOLUME=SER=B00071,DCB=(RECFM=VSB,LRECL=16,BLKSIZE=3204,DEN=2)
//GO.FT08F003 DD DSNAME=HOLTS3,UNIT=TAPE,LABEL=(3,SL),DISP=(OLD,KEEP), *
// VOLUME=SER=B00071,DCB=(RECFM=VSB,LRECL=16,BLKSIZE=3204,DEN=2)
//GO.FT08F004 DD DSNAME=HOLTS4,UNIT=TAPE,LABEL=(4,SL),DISP=(OLD,KEEP), *
// VOLUME=SER=B00071,DCB=(RECFM=VSB,LRECL=16,BLKSIZE=3204,DEN=2)
//GO.FT09F001 DD UNIT=SYSDA,SPACE=(3204,(50,10)),                      *
// DCB=(RECFM=VSB,LRECL=16,BLKSIZE=3204,OPTCD=C)
//GO.FT10F001 DD UNIT=SYSDA,SPACE=(3204,(50,10)),                      *
// DCB=(RECFM=VSB,LRECL=16,BLKSIZE=3204,OPTCD=C)
```

```
C     PROGRAM 'SIG'
CCCCC
CCCCC PROGRAM TO APPLY VOIGT (HJERTING) FUNCTION TO INTENSITIES AND
CCCCC SUM BOTH ISOTOPE AND NORMAL CN CONTRIBUTIONS BETWEEN WAVELENGTHS
CCCCC 'LAMMIN' AND 'LAMMAX' IN INCREMENTS OF 'STEP'.  ALL LINES WITHIN
CCCCC 'DELLAM' OF WAVELENGTH 'LAM' ARE INCLUDED IN SUMMATION.  INPUT
CCCCC DATA (LINE WAVELENGTHS AND INTENSITIES FOR NORMAL AND ISOTOPE) IS
CCCCC STORED ON 'NTAPEI' AS TWO DATA SETS BEFORE BEING COPIED INTO
CCCCC ARRAYS 'LAMN', 'IHN', 'LAMI' AND 'IHI'.  OUTPUT (WAVELENGTH,
CCCCC NORMAL AND ISOTOPE INTENSITIES) IS ONTO DATA SET DEFINED BY
CCCCC 'NTAPEO'.  PROGRAMS 'POS & INT' AND 'SORT' MUST BE RUN BEFORE
CCCCC 'SIG'.
CCCCC
CCCCC INPUT:  FROM CARD READER  'NREAD'                          FORMAT:
CCCCC    DATA SET SEQUENCE NUMBER 'NTAPEO'                        1000
CCCCC    RATIO OF DAMPING CONSTANT TO DOPPLER WIDTH,
CCCCC    TEMPERATURE AND TURBULENT VELOCITY                       1010
CCCCC    WAVELENGTH RANGE, INCREMENT AND NUMBER OF ANGSTROMS
CCCCC    CALCULATED IN ONE PASS                                   1010
CCCCC
CCCCC INPUT:  FROM TAPE  'NTAPEN' AND 'NTAPEI'
CCCCC    OUTPUT FROM PROGRAM 'SORT' AND CONSITS OF 2 DATA SETS,
CCCCC    THE FIRST IS THE WAVELENGTH & POSITIONS FOR THE NORMAL
CCCCC    FORM OF CN ('NTAPEN') AND THE SECOND IS FOR THE ISOTOPIC
CCCCC    FORM ('NTAPEI').
CCCCC
CCCCC    OUTPUT:  ON TAPE  'NTAPEO'  A SEQUENTIAL DATA SET WHOSE
CCCCC    DATA SET SEQUENCE NUMBER IS DEFINED BY NTAPEO-2
CCCCC    WAVELENGTH 'LAM', SUMMED ABSORPTION COEFFICIENT FOR NORMAL
CCCCC    'SUMIHN' AND ISOTOPE 'SUMIHI'
CCCCC
CCCCC OUTPUT:  ON PRINTER  'NPRINT'                              FORMAT:
CCCCC    ERROR MESSAGE IF NUMBER OF LINES IN A SEGMENT
CCCCC    (DEFINED BY 'STEP1') IS GREATER THAN SIZE OF ARRAY       1020
CCC
      REAL VOIGT(3200),IHN(1500),IHI(1500)
      DOUBLE PRECISION LAMN(1500),LAMI(1500),A,X,H,LAM,LAMMIN,LAMMID,
     1  LAMMAX,IH
C
CCCCC 'CONSTN' & 'CONSTI' ARE 2K/M WHERE M IS THE MASS OF THE NORMAL
CCCCC & ISOTOPE FORM OF CN RESPECTIVELY AND 'C' IS THE VELOCITY OF LIGHT
CCCCC IN KM/SEC
C
      DATA CONSTN/6.395670E-4/, CONSTI/6.158794E-4/, C/299792.5/
      DATA NREAD,NPRINT,NTAPEN,NTAPEI/5,6,1,2/
      COMMON A
      EXTERNAL H
C
CC    READ DATA SET NUMBER FOR OUTPUT DATA
```

```
C
      READ(NREAD,1000) NTAPEO
      NTAPEO=NTAPEO+2
C
CCC   READ RATIO OF DAMPING CONSTANT TO DOPPLER WIDTH 'A', TEMPERATURE
CCC   'T', AND TURBULENT VELOCITY 'VT' IN KM/SEC
C
      READ(NREAD,1010) A,T,VT
C
CCC   DEFINE DOPPLER WIDTH FOR BOTH NORMAL AND ISOTOPE
CCC   THROUGHOUT PROGRAM DIFFERENCES BETWEEN NORMAL AND ISOTOPE
CCC   VARIABLES INDICATED BY ENDING IN N OR I
C
      DPVELN= SQRT(CONSTN*T+VT*VT)/C
      DPVELI= SQRT(CONSTI*T+VT*VT)/C
C
CCC   READ STARTING AND ENDING WAVELENGTHS, 'LAMMIN' & 'LAMMAX',
CCC   'DELLAM', INCREMENT TO WAVELENGTH 'STEP', AND NUMBER OF ANGSTROMS
CCC   CALCULATED IN ONE PASS (USE 30 TO 50), 'STEP1'
C
      READ(NREAD,1010) LAMMIN,LAMMAX,DELLAM,STEP,STEP1
C
CCC   CALCULATE VOIGT PROFILE TO 'DELLAM' FROM LINE CENTER AT WAVELENGTH
CCC   ('LAMMIN' + 'LAMMAX')/2 IN INCREMENTS OF 'DELLAM'/3000 ANGSTROMS.
C
      C1=(LAMMIN+LAMMAX)*DPVELN*1.55E3/DELLAM
      DO 100 I=1,3200
      X=I-1
      X=X/C1
      VOIGT(I)=H(X)
  100 CONTINUE
C
      REWIND NTAPEO
  110 REWIND NTAPEN
      LAMMID=LAMMIN+STEP1
      IF(LAMMID.GE.LAMMAX) LAMMID=LAMMAX
      LAMMIN=LAMMIN-DELLAM-.10
      LAMMID=LAMMID+DELLAM+.10
C
CCC   FIND STARTING NORMAL WAVELENGTH
C
  120 READ(NTAPEN,END=130) LAMN(1),IHN(1)
      IF(LAMN(1).GE.LAMMIN) GO TO 130
      GO TO 120
  130 DO 140 I=2,1500
C
CCC   READ NORMAL WAVELENGTHS BETWEEN 'LAMMIN' AND 'LAMMIN' + 'STEP1'
C
      READ(NTAPEN,END=150) LAMN(I),IHN(I)
      IF(LAMN(I).GT.LAMMID) GO TO 150
```

```
  140 CONTINUE
C
CC      ERROR EXIT
C
        GO TO 280
  150 NN=I-1
C
CC      SKIP TO BEGINNING OF ISOTOPE DATA SET
C
        REWIND NTAPEN
        REWIND NTAPEI
C
CC      FIND STARTING ISOTOPE WAVELENGTH
C
  160 READ(NTAPEI,END=170) LAMI(1),IHI(1)
        IF(LAMI(1).GE.LAMMIN) GO TO 170
        GO TO 160
  170 DO 180 I=2,1500
C
CC      READ ISOTOPE WAVELENGTHS BETWEEN 'LAMMIN' AND 'LAMMIN' + 'STEPI'
C
        READ(NTAPEI,END=190) LAMI(I),IHI(I)
        IF(LAMI(I).GT.LAMMID) GO TO 190
  180 CONTINUE
C
CC      ERROR EXIT
C
        GO TO 280
  190 NI=I-1
        REWIND NTAPEI
        LAMMID=LAMMID-DELLAM-.10
        LAM=LAMMIN+DELLAM+.10
        MN=1
        MI=1
        LN=1
        LI=1
C
CC      SUM CONTRIBUTIONS FOR ALL NORMAL LINES WITHIN 'DELLAM' ANGSTROMS
CC      OF WAVELENGTH 'LAM' USING VOIGT FUNCTION AS STORED IN ARRAY
CC      'VOIGT'
C
  200 SUMIHN=0.0
        SUMIHI=0.0
        DO 220 I=MN,NN
        X=LAMN(I)
        IF(X.LT.LAM-DELLAM) GO TO 210
        IF(X.GT.LAM+DELLAM) GO TO 230
        U=DABS((LAM-X)/(X*DPVELN))
        J=U*C1+1.1
        IH=IHN(I)*VOIGT(J)
```

```
      SUMIHN=SUMIHN+IH
      GO TO 220
  210 LN=I
  220 CONTINUE
C
CC    SUM CONTRIBUTIONS FOR ALL ISOTOPE LINES WITHIN 'DELLAM' ANGSTROMS
CC    OF WAVELENGTH 'LAM' USING VOIGT FUNCTION AS STORED IN ARRAY
C     'VOIGT'
C
  230 DO 250 I=MI,NI
      X=LAMI(I)
      IF(X.LT.LAM-DELLAM) GO TO 240
      IF(X.GT.LAM+DELLAM) GO TO 260
      U=DABS((LAM-X)/(X*DPVELI))
      J=U*C1+1.1
      IH=IHI(I)*VOIGT(J)
      SUMIHI=SUMIHI+IH
      GO TO 250
  240 LI=I
  250 CONTINUE
C
CC    OUTPUT TO TAPE
C
  260 WRITE(NTAPEO) LAM,SUMIHN,SUMIHI
      MN=LN
      MI=LI
      LAM=LAM+STEP
      IF(LAM.GE.LAMMID) GO TO 270
      GO TO 200
  270 LAMMIN=LAMMID+STEP
      IF(LAM.GE.LAMMAX) GO TO 290
      GO TO 110
C
CC    WRITE ERROR MESSAGE
C
  280 WRITE(NPRINT,1020)
C     CLOSE AND REWIND ALL DATA SETS
  290 ENDFILE NTAPEO
      REWIND NTAPEN
      REWIND NTAPEO
      STOP
 1000 FORMAT(I5)
 1010 FORMAT(8F10.3)
 1020 FORMAT('1','ARRAY SIZE TOO SMALL, PROGRAM TERMINATED')
      END
```

```
C      VOIGT FUNCTION (HJERTING FUNCTION)
CCCCCC
CCCCCC
CCCCCC
CCCCCC
CCCCCC
CCCCCC
CCCCCC
CCCCCC
CCCCCC
C
       H(A,U) EXPANDED AS A TAYLOR SERIES IN A  (HARRIS, 1948, AP.J.
       VOL. 108, P112)  TO FIVE TERMS.  FUNCTION F(U) EVALUATED USING
       THREE EXPANSIONS.  THE FIRST AND LAST ARE FROM W.L. MILLER &
       A.R. GORDON 1931, J. PHYS. CHEM., VOL. 35, P2877  WHILE THE
       MIDDLE ONE IS A TERM BY TERM INTEGRATION OF THE FUNCTION.
       THE EXPANSIONS USED ARE:
       F(U)=U*(1-2*U**2/3+4*U**4/15-8*U**6/105+16*U**8/945-...) FOR U<1
            =EXP(-U*U)*(U+U**3/3+U**5/(5*2 )+U**7/(7*3 )+...)   FOR 1<U<5
            =1/(2*U)+1/(4*U**3)+3/(8*U**5)+15/(16*U**7)+
                                           105/(32*U**9)+...    FOR 5<U
C
       TO CHANGE ACCURACY OF F(U) CHANGE DATA ACUR/     / CARD

       DOUBLE PRECISION FUNCTION H(U)
       DOUBLE PRECISION U,A,H0,H1,H2,H3,H4,U2,F,Y,XI,X2,T23,SQRTPI,ACUR
       DATA SQRTPI/1.1283791671      /, T23/.6666666666666666/
       DATA ACUR/1.00-6/
       DATA NPRINT/6/
       COMMON A
       U2=U*U
       IF(U.GE.1.0D0) GO TO 110
       Y=U
       F=U
       IF(U.EQ.0.0) GO TO 160
       X2=U2+U2
       DO 100 I=2,50
       IF(DABS(Y).LT.ACUR*DABS(F)) GO TO 160
       XI=I
       Y=-X2*Y/(XI+XI-1.D0)
       F=F+Y
  100  CONTINUE
C
CC     ERROR RETURN
       GO TO 180
  110  IF(U.LT.5.D0) GO TO 130
       Y=1.D0/(U+U)
       F=Y
       X2=1.D0/(U2+U2)
       DO 120 I=2,200
       IF(DABS(Y).LT.ACUR*DABS(F)) GO TO 160
       XI=I
       Y=Y*(XI+XI-3.D0)*X2
       F=F+Y
  120  CONTINUE
C
CC     ERROR RETURN
       GO TO 180
  130  Y=U
```

```
      F=U
      X2=U2
      DO 140 I=1,2000
      IF(DABS(Y).LT.ACUR*DABS(F)) GO TO 150
      XI=I
      Y=X2*Y/XI
      F=F+Y/(XI+XI+1.D0)
  140 CONTINUE
C
C     ERROR RETURN
      GO TO 180
  150 F=F*DEXP(-U2)
  160 IF(U2.GT.174.) GO TO 170
      H0=DEXP(-U2)
      H1=-SQRTPI*(1.-(U+U)*F)
      H2=(1.D0-U2-U2)*H0
      H3=-SQRTPI*(T23*(1.D0-U2)-(U+U)*(1.D0-T23*U2)*F)
      H4=(5.D-1-U2-U2+T23*U2*U2)*H0
      H=H0+A*(H1+A*(H2+A*(H3+A*H4)))
      RETURN
  170 H1=-SQRTPI*(1.D0-(U+U)*F)
      H3=-SQRTPI*(T23*(1.D0-U2)-(U+U)*(1.D0-T23*U2)*F)
      H=A*(H1+A*A*H3)
      RETURN
C
C     WRITE ERROR MESSAGE (NUMBER OF TERMS IN EXPANSION NOT ENOUGH
C     FOR DESIRED ACCURACY) AND RETURN
C
  180 WRITE(NPRINT,1000) U
      RETURN
 1000 FORMAT(' ',10X,'ACCURACY LOST,  U=',F10.5)
      END
```

```
//GO.FT01F001 DD DSNAME=HOLTS3,UNIT=TAPE,LABEL=(3,SL),DISP=(OLD,KEEP), *
//  VOLUME=SER=B00071,DCB=(RECFM=VSB,LRECL=16,BLKSIZE=3204,DEN=2)
//GO.FT02F001 DD DSNAME=HOLTS4,UNIT=TAPE,LABEL=(4,SL),DISP=(OLD,KEEP), *
//  VOLUME=SER=B00071,DCB=(RECFM=VSB,LRECL=16,BLKSIZE=3204,DEN=2)
//GO.FT09F001 DD DSNAME=HOLTS7,UNIT=TAPE,LABEL=(7,SL),DISP=(OLD,KEEP), *
//  VOLUME=SER=B00007,DCB=(RECFM=VSB,LRECL=20,BLKSIZE=4004)
//GO.FT10F001 DD DSNAME=HOLTS8,UNIT=TAPE,LABEL=(8,SL),DISP=(OLD,KEEP), *
//  VOLUME=SER=B00007,DCB=(RECFM=VSB,LRECL=20,BLKSIZE=4004)
//GO.FT11F001 DD DSNAME=HOLTS9,UNIT=TAPE,LABEL=(9,SL),DISP=(OLD,KEEP), *
//  VOLUME=SER=B00007,DCB=(RECFM=VSB,LRECL=20,BLKSIZE=4004)
//GO.FT12F001 DD DSNAME=HOLT10,UNIT=TAPE,LABEL=(10,SL),DISP=(OLD,KEEP),*
//  VOLUME=SER=B00007,DCB=(RECFM=VSB,LRECL=20,BLKSIZE=4004)
//GO.FT13F001 DD DSNAME=HOLT11,UNIT=TAPE,LABEL=(11,SL),DISP=(OLD,KEEP),*
//  VOLUME=SER=B00007,DCB=(RECFM=VSB,LRECL=20,BLKSIZE=4004)
//GO.FT14F001 DD DSNAME=HOLT12,UNIT=TAPE,LABEL=(12,SL),DISP=(OLD,KEEP),*
//  VOLUME=SER=B00007,DCB=(RECFM=VSB,LRECL=20,BLKSIZE=4004)
//GO.FT15F001 DD DSNAME=HOLT13,UNIT=TAPE,LABEL=(13,SL),DISP=(OLD,KEEP),*
//  VOLUME=SER=B00007,DCB=(RECFM=VSB,LRECL=20,BLKSIZE=4004)
//GO.FT16F001 DD DSNAME=HOLT14,UNIT=TAPE,LABEL=(14,SL),DISP=(OLD,KEEP),*
//  VOLUME=SER=B00007,DCB=(RECFM=VSB,LRECL=20,BLKSIZE=4004)
//GO.FT17F001 DD DSNAME=HOLT15,UNIT=TAPE,LABEL=(15,SL),DISP=(OLD,KEEP),*
//  VOLUME=SER=B00007,DCB=(RECFM=VSB,LRECL=20,BLKSIZE=4004)
//GO.FT18F001 DD DSNAME=HOLT16,UNIT=TAPE,LABEL=(16,SL),DISP=(OLD,KEEP),*
//  VOLUME=SER=B00007,DCB=(RECFM=VSB,LRECL=20,BLKSIZE=4004)
//GO.FT19F001 DD DSNAME=HOLT17,UNIT=TAPE,LABEL=(17,SL),DISP=(OLD,KEEP),*
//  VOLUME=SER=B00007,DCB=(RECFM=VSB,LRECL=20,BLKSIZE=4004)
//GO.FT20F001 DD DSNAME=HOLT18,UNIT=TAPE,LABEL=(18,SL),DISP=(OLD,KEEP),*
//  VOLUME=SER=B00007,DCB=(RECFM=VSB,LRECL=20,BLKSIZE=4004)
```

```
C      PROGRAM 'PLOT'
CCC
CCC    CALCULATES AND PLOTS PROFILES
CCC    PLOT IS 5" HIGH, EVERY ANGSROM IS MARKED WITH WAVELENGTH
CCC    EVERY 10 ANGSTROMS.  THREE PROFILES ARE PRODUCED CORRESPONDING
CCC    TO THE THREE ABUNDANCE RATIOS INPUT
CCC    TRACING IS LABELLED WITH DATA SET SEQUENCE NUMBER, STRENGTH
CCC    AND DISPERSION.
CCC
CCC    INPUT:  FROM CARD READER  'NREAD'                          FORMAT:
CCC       DATA SET SEQUENCE NUMBER 'NTAPE'                         1000
CCC       THREE C12/C13 RATIOS  'R1', 'R2' AND 'R3'                1010
CCC       STRENGTH CONSTANT FOR PLOT 'STRCN'                       1010
CCC       DISPERSION 'DISP' IN INCHES PER ANGSTROM AND MAXIMUM
CCC       LINE DEPTH 'RC'                                          1010
CCC       WAVELENGTH LIMITS 'LAMMIN' TO 'LAMMAX' AND MINIMUM
CCC       WAVELENGTH ON TAPE 'START'                               1010
CCC
CCC    INPUT:  ON TAPE 'NTAPE' A SEQUENTIAL DATA SET WHOSE DATA
CCC       SET SEQUENCE NUMBER IS DEFINED BY NTAPE-2
CCC       POSITION 'POS', ABSORPTION COEFFICIENTS FOR NORMAL
CCC       'IHC12N(I)' AND ISOTOPE 'IHC13N(I)'
CCC
CCC    OUTPUT:  CALCOMP PLOTTER VIA TAPE
CC
       REAL X(203),Y1(203),Y2(203),Y3(203),AXL(33),AYL(33),AYU(33),
      1  IHC12N(200),IHC13N(200)
       DOUBLE PRECISION LAMMIN,LAMMAX,START,POS
       INTEGER IBUF(1000)
       COMMON IBUF,XY
C
CC     INTIALIZE ARRAYS FOR PLOTTING AXIS
       DATA AYU/5.0,5.28,5.0,5.0,5.14,5.0,5.0,5.14,5.0,5.0,5.14,5.0,5.0,
      1  5.14,5.0,5.0,5.28,5.0,5.0,5.14,5.0,5.0,5.14,5.0,5.0,5.14,5.0,
      2  5.0,5.14,5.0,5.0,0.0,1.0/
       DATA AYL/0.0,-.28,0.0,0.0,-.14,0.0,0.0,-.14,0.0,0.0,-.14,0.0,0.0,
      1  -.14,0.0,0.0,0.0,-.28,0.0,0.0,0.0,-.14,0.0,0.0,-.14,0.0,0.0,-.14,0.0,
      2 0.0,-.14,0.0,0.0,0.0,1.0/
       DATA NREAD,NPRINT/5,6/
       COFGF(TA)=TA*RC/(RC+TA)
C
CCC    READ DATA SET SEQUENCE NUMBER AND CALCULATE DATA SET
CCC    REFERENCE NUMBER
C
       READ(NREAD,1000) NTAPE
       NTAPE=NTAPE+2
       REWIND NTAPE
C
C      READ ISOTOPIC TO NORMAL CN ABUNDANCE RATIOS
```

```
C
      READ(NREAD,1010) R1,R2,R3
C
CC    READ STRENGTH CONSTANT
C
      READ(NREAD,1010) STRCN
C
CC    READ DISPERSION AND MAXIMUM LINE DEPTH
C
      READ(NREAD,1010) DISP,RC
C
CC    READ WAVELENGTH REGION AND MINIMUM ON TAPE
C
      READ(NREAD,1010) LAMMIN,LAMMAX,START
C
      XN=NTAPE-2
C
CC    PREPARE TO PLOT AND IDENTIFY TRACING
      CALL ASSIGN(X,Y1,Y2,Y3,DISP,STRCN,XN,AXL,AYL,AYU)
      IF(LAMMIN.LE.START) GO TO 110
      LAMMIN=LAMMIN-.06
C
C     FIND STARTING WAVELENGTH ON TAPE
  100 READ(NTAPE,END=140) POS
      IF(POS.GE.LAMMIN) GO TO 110
      GO TO 100
C
CC    READ POSITION AND ABSORPTION COEFFICIENTS FOR NORMAL AND
CC    ISOTOPIC FORM
C
  110 DO 120 I=1,200
      READ(NTAPE,END=140) POS,IHC12N(I),IHC13N(I)
  120 CONTINUE
C
CC    STOP IF MAXIMUM WAVELENGTH REACHED
      IF(POS.GE.LAMMAX) GO TO 140
C
CC    COMPUTE PROFILES USING THE THREE ISOTOPIC ABUNDANCE RATIOS
C     FOR 10 ANGSTROMS
      DO 130 I=1,200
      J=I+1
      Y1(J)=COFGF((IHC12N(I)+R1*IHC13N(I))*STRCN)
      Y2(J)=COFGF((IHC12N(I)+R2*IHC13N(I))*STRCN)
      Y3(J)=COFGF((IHC12N(I)+R3*IHC13N(I))*STRCN)
  130 CONTINUE
      START=POS-9.95
C
C     DRAW UPPER AND LOWER HORIZONTAL AXIS WITH TICS EVERY ANGSTROM
      CALL LINE(AXL,AYU,31,1,0,0)
      CALL LINE(AXL,AYL,31,1,0,0)
```

```
C
C       PLOT THE THREE LINE PROFILES
        CALL LINE(X,Y1,201,1,0,0)
        CALL LINE(X,Y2,201,1,0,0)
        CALL LINE(X,Y3,201,1,0,0)
C
C       LABEL WAVELENGTH ON AXIS
        CALL NUMBER(-.5,-.5,.14,START,0.0,2)
C
C       MOVE ORIGIN 10 ANGSTROMS
        CALL PLOT(XY,0.0,-3)
        Y1(1)=Y1(201)
        Y2(1)=Y2(201)
        Y3(1)=Y3(201)
        GO TO 110
C
C       CLOSE AND REWIND ALL DATA SETS
  140   CALL PLOT(15.0,0.0,999)
        REWIND NTAPE
        STOP
 1000   FORMAT(I5)
 1010   FORMAT(8F10.5)
        END
```

```
C       SUBROUTINE ASSIGN
C
C       INITIALIZES ARRAYS, SETS UP FOR PLOTTING AND LABELS TRACING
C
        SUBROUTINE ASSIGN(X,Y1,Y2,Y3,DISP,STRCN,XN,AXL,AYL,AYU)
        COMMON IBUF,XY
        INTEGER IBUF(1000)
        REAL X(203),Y1(203),Y2(203),Y3(203),AXL(33),AYL(33),AYU(33)
C
C       SET UP FOR PLOTTING
        CALL PLOTS(IBUF,1000,6)
C
C       IDENTIFY TRACING
        CALL SYMBOL(0.0,3.0,.28,'HOLTS',0.0,5)
C
C       LABEL DATA SET SEQUENCE NUMBER
        CALL SYMBOL(2.0,4.0,.14,'TAPE=',0.0,5)
        CALL NUMBER(2.7,4.0,.14,XN,0.0,-1)
C
C       INDICATE STRENGTH CONSTANT USED AND DISPERSION
        CALL SYMBOL(2.0,3.0,.14,'STR=',0.0,4)
        CALL NUMBER(2.56,3.0,.14,STRCN,0.0,0)
        CALL SYMBOL(2.0,2.0,.14,'DISP=',0.0,5)
        CALL NUMBER(2.70,2.0,.14,DISP,0.0,3)
C
C       REDEFINE ORIGIN
        CALL PLOT(4.0,1.0,-3)
C
C       DRAW VERTICAL AXIS
        CALL AXIS(0.0,0.0,'RL',2,5.0,90.0,1.0,-.2)
C
C       INITIALIZE INFORMATION FOR PLOTTING SUBROUTINES
        Y1(1)=0.0
        Y2(1)=0.0
        Y3(1)=0.0
        X(202)=0.0
        Y1(202)=1.0
        Y2(202)=1.0
        Y3(202)=1.0
        X(203)=20.0
        Y1(203)=-.2
        Y2(203)=-.2
        Y3(203)=-.2
C
C       CALCULATE HORIZONTAL AXIS WITH INPUT DISPERSION
        DO 100 I=1,201
        X(I)=(I-2)*DISP
  100   CONTINUE
        XY=10.*DISP
        DO 110 I=1,3
```

```
      AXL(I)=0.0
      AXL(I+3)=DISP
      AXL(I+6)=2.*DISP
      AXL(I+9)=3.*DISP
      AXL(I+12)=4.*DISP
      AXL(I+15)=5.*DISP
      AXL(I+18)=6.*DISP
      AXL(I+21)=7.*DISP
      AXL(I+24)=8.*DISP
      AXL(I+27)=9.*DISP
  110 CONTINUE
      AXL(31)=10.*DISP
      AXL(32)=0.0
      AXL(33)=1.0
      RETURN
      END
```

```
//GO.PLOTTAPE DD DSNAME=UVIC,UNIT=TAPE,DISP=(NEW,KEEP),                    *
//  LABEL=(,SL),VOLUME=SER=B00036,DCB=(DEN=2)
//GO.FT09F001 DD DSNAME=HOLTS7,UNIT=TAPE,LABEL=(7,SL),DISP=(OLD,KEEP),    *
//  VOLUME=SER=B00007,DCB=(RECFM=VSB,LRECL=20,BLKSIZE=4004)
//GO.FT10F001 DD DSNAME=HOLTS8,UNIT=TAPE,LABEL=(8,SL),DISP=(OLD,KEEP),    *
//  VOLUME=SER=B00007,DCB=(RECFM=VSB,LRECL=20,BLKSIZE=4004)
//GO.FT11F001 DD DSNAME=HOLTS9,UNIT=TAPE,LABEL=(9,SL),DISP=(OLD,KEEP),    *
//  VOLUME=SER=B00007,DCB=(RECFM=VSB,LRECL=20,BLKSIZE=4004)
//GO.FT12F001 DD DSNAME=HOLT10,UNIT=TAPE,LABEL=(10,SL),DISP=(OLD,KEEP),   *
//  VOLUME=SER=B00007,DCB=(RECFM=VSB,LRECL=20,BLKSIZE=4004)
//GO.FT13F001 DD DSNAME=HOLT11,UNIT=TAPE,LABEL=(11,SL),DISP=(OLD,KEEP),   *
//  VOLUME=SER=B00007,DCB=(RECFM=VSB,LRECL=20,BLKSIZE=4004)
//GO.FT14F001 DD DSNAME=HOLT12,UNIT=TAPE,LABEL=(12,SL),DISP=(OLD,KEEP),   *
//  VOLUME=SER=B00007,DCB=(RECFM=VSB,LRECL=20,BLKSIZE=4004)
//GO.FT15F001 DD DSNAME=HOLT13,UNIT=TAPE,LABEL=(13,SL),DISP=(OLD,KEEP),   *
//  VOLUME=SER=B00007,DCB=(RECFM=VSB,LRECL=20,BLKSIZE=4004)
//GO.FT16F001 DD DSNAME=HOLT14,UNIT=TAPE,LABEL=(14,SL),DISP=(OLD,KEEP),   *
//  VOLUME=SER=B00007,DCB=(RECFM=VSB,LRECL=20,BLKSIZE=4004)
//GO.FT17F001 DD DSNAME=HOLT15,UNIT=TAPE,LABEL=(15,SL),DISP=(OLD,KEEP),   *
//  VOLUME=SER=B00007,DCB=(RECFM=VSB,LRECL=20,BLKSIZE=4004)
//GO.FT18F001 DD DSNAME=HOLT16,UNIT=TAPE,LABEL=(16,SL),DISP=(OLD,KEEP),   *
//  VOLUME=SER=B00007,DCB=(RECFM=VSB,LRECL=20,BLKSIZE=4004)
//GO.FT19F001 DD DSNAME=HOLT17,UNIT=TAPE,LABEL=(17,SL),DISP=(OLD,KEEP),   *
//  VOLUME=SER=B00007,DCB=(RECFM=VSB,LRECL=20,BLKSIZE=4004)
//GO.FT20F001 DD DSNAME=HOLT18,UNIT=TAPE,LABEL=(18,SL),DISP=(OLD,KEEP),   *
//  VOLUME=SER=B00007,DCB=(RECFM=VSB,LRECL=20,BLKSIZE=4004)
```

```
C     PROGRAM  'INSTR'
C
C     CALCULATES PROFILE; APPLIES INSTRUMENTAL PROFILE AND PLOTS
C     INSTRUMENTAL PROFILE IS INPUT AS LINE DEPTHS AT INTERVALS
C     CORRESPONDING TO STEP SIZE DEFINED IN PROGRAM 'SIG'
C     MAXIMUM WIDTH IS 30*STEP
C
C     PLOT IS 5" HIGH, EVERY ANGSROM IS MARKED WITH WAVELENGTH
C     EVERY 10 ANGSTROMS.  THREE PROFILES ARE PRODUCED CORRESPONDING
C     TO THE THREE ABUNDANCE RATIOS INPUT
C     TRACING IS LABELLED WITH INSTRUMENTAL PROFILE NAME, DATA SET
C     SEQUENCE NUMBER, STRENGTH AND DISPERSION
C
C      INPUT:  FROM CARD READER  'NREAD'                          FORMAT:
C         DATA SET SEQUENCE NUMBER 'NTAPE'                         1000
C         THREE C12/C13 RATIOS  'R1', 'R2' AND 'R3'                1010
C         STRENGTH CONSTANT FOR PLOT 'STRCN'
C         DISPERSION 'DISP' IN INCHES PER ANGSTROM AND MAXIMUM
C         LINE DEPTH 'RC'                                          1010
C         WAVELENGTH LIMITS 'LAMMIN' TO 'LAMMAX' AND MINIMUM
C         WAVELENGTH ON TAPE 'START'                               1010
C         INSTRUMENTAL PROFILE NAME  'TITLE'                       1020
C         INSTRUMENTAL PROFILE 'INPRO'                             1010
C
C       INPUT:  ON TAPE 'NTAPE' A SEQUENTIAL DATA SET WHOSE DATA
C          SET SEQUENCE NUMBER IS DEFINED BY NTAPE-2
C          POSITION 'POS', ABSORPTION COEFFICIENTS FOR NORMAL
C          'SIGIH' AND ISOTOPE 'SIGIHI'
C
C       OUTPUT:  CALCOMP PLOTTER VIA TAPE
C
      REAL RLR1S(230),RLR2S(230),RLR3S(230),INPRO(31),X(203),Y1(203),
     1  Y2(203),Y3(203),AXL(33),AYL(33),AYU(33),TITLE(10)
      DOUBLE PRECISION LAMMIN,LAMMAX,START,POS
      INTEGER FILEN,IBUF(1000)
      COMMON IBUF,XY
      COMMON /CINPRO/ INPRO,AREA
C
C     INTIALIZE ARRAYS FOR PLOTTING AXIS
      DATA AYU/5.0,5.28,5.0,5.0,5.14,5.0,5.0,5.14,5.0,5.0,5.14,5.0,5.0,
     1  5.14,5.0,5.0,5.28,5.0,5.0,5.14,5.0,5.0,5.14,5.0,5.0,5.14,5.0,
     2  5.0,5.14,5.0,5.0,0.0,1.0/
      DATA AYL/0.0,-.28,0.0,0.0,-.14,0.0,0.0,-.14,0.0,0.0,-.14,0.0,0.0,
     1  -.14,0.0,0.0,-.28,0.0,0.0,-.14,0.0,0.0,-.14,0.0,0.0,-.14,0.0,
     2 0.0,-.14,0.0,0.0,0.0,1.0/
      DATA NREAD,NPRINT,NDISK/5,6,8/
      COFGF(TA)=TA*RC/(RC+TA)
C
C
```

```
C     DEFINE DIRECT AXIS DATA SET TO STORE COMPUTED PROFILES
      DEFINE FILE 8(1000,20,L,FILEN)
      FILEN=1
C
CC    READ DATA SET SEQUENCE NUMBER AND CALCULATE DATA SET
CC    REFERENCE NUMBER
C
      READ(NREAD,1000) NTAPE
      NTAPE=NTAPE+2
      REWIND NTAPE
C
CC    READ ISOTOPIC TO NORMAL CN ABUNDANCE RATIOS
C
      READ(NREAD,1010) R1,R2,R3
C
CC    READ STRENGTH CONSTANT
C
      READ(NREAD,1010) STRCN
C
CC    READ DISPERSION AND MAXIMUM LINE DEPTH
C
      READ(NREAD,1010) DISP,RC
C
CC    READ WAVELENGTH REGION AND MINIMUM ON TAPE
C
      READ(NREAD,1010) LAMMIN,LAMMAX,START
C
CC    READ TITLE OF PROFILE
C
      READ(NREAD,1020) TITLE
C
CC    READ INSTRUMENTAL PROFILE
C
      READ(NREAD,1010) INPRO
C
CC    APPLY SIMPSON'S RULE COEFFICIENTS
      DO 100 I=2,28,2
      INPRO(I)=4.*INPRO(I)
      INPRO(I+1)=2.*INPRO(I+1)
  100 CONTINUE
      INPRO(30)=4.*INPRO(30)
C
C     SUM COEFFICIENTS IN INPRO  (FOR NORMALIZATION )
      AREA=0.0
      DO 110 I=1,31
      AREA=AREA+INPRO(I)
  110 CONTINUE
      XN=NTAPE-2
C
C     PREPARE TO PLOT AND IDENTIFY TRACING
```

```
      CALL ASSIGN(X,Y1,Y2,Y3,DISP,STRCN,XN,AXL,AYL,AYU,TITLE)
      LAMMAX=LAMMAX+.75
      LAMMIN=LAMMIN-.75
      IF(LAMMIN.LE.START) LAMMIN=START+9.25
      LAMMIN=LAMMIN-.06
C
C     FIND STARTING WAVELENGTH ON TAPE
  120 READ(NTAPE,END=140) POS,SIGIH,SIGIHI
      IF(POS.GE.LAMMIN) GO TO 130
      GO TO 120
C
C     COMPUTE PROFILES USING THE THREE ISOTOPIC ABUNDANCE RATIOS
C     AND STORE ON DIRECT ACCESS DATA SET
  130 READ(NTAPE,END=140) POS,SIGIH,SIGIHI
C
C     STOP IF MAXIMUM WAVELENGTH REACHED
      IF(POS.GT.LAMMAX) GO TO 140
      RLR1=COFGF((SIGIH+R1*SIGIHI)*STRCN)
      RLR2=COFGF((SIGIH+R2*SIGIHI)*STRCN)
      RLR3=COFGF((SIGIH+R3*SIGIHI)*STRCN)
      WRITE(NDISK'FILEN) POS,RLR1,RLR2,RLR3
      GO TO 130
  140 MAXFIL=FILEN-5
      FIND(NDISK'1)
C
C     CALCULATE PROFILE WITH INSTRUMENTAL PROFILE & PLOT
  150 IF(FILEN+31.GE.MAXFIL) GO TO 170
      DO 160 I=1,230
      READ(NDISK'FILEN) POS,RLR1S(I),RLR2S(I),RLR3S(I)
  160 CONTINUE
      FILEN=FILEN-30
      FIND(NDISK'FILEN)
C
C     APPLY INSTRUMENTAL PROFILES
      CALL INSTR(RLR1S,Y1)
      CALL INSTR(RLR2S,Y2)
      CALL INSTR(RLR3S,Y3)
      XN=POS-10.7
C
C     DRAW UPPER AND LOWER HORIZONTAL AXIS WITH TICS EVERY ANGSTROM
      CALL LINE(AXL,AYU,31,1,0,0)
      CALL LINE(AXL,AYL,31,1,0,0)
C
C     PLOT THE THREE LINE PROFILES
      CALL LINE(X,Y1,201,1,0,0)
      CALL LINE(X,Y2,201,1,0,0)
      CALL LINE(X,Y3,201,1,0,0)
C
C     LABEL WAVELENGTH ON AXIS
      CALL NUMBER(-.5,-.5,.14,XN,0.0,2)
```

```
C
C       MOVE ORIGIN 10 ANGSTROMS
        CALL PLOT(XY,0.0,-3)
        Y1(1)=Y1(201)
        Y2(1)=Y2(201)
        Y3(1)=Y3(201)
        GO TO 150
C
C       CLOSE AND REWIND ALL DATA SETS
  170 CALL PLOT(15.0,0.0,999)
        REWIND NTAPE
        STOP
 1000 FORMAT(I5)
 1010 FORMAT(8F10.5)
 1020 FORMAT(10A4)
        END
```

```
C       SUBROUTINE INSTR
C
C       APPLIES INSTRUMENTAL PROFILE TO CALCULATED THEORETICAL PROFILE
C
        SUBROUTINE INSTR(DM1,DM2)
        REAL DM1(230),DM2(203),D(31),INPRO(31)
        COMMON /CINPRO/ INPRO,AREA
        DO 110 I=16,215
        D(1)=DM1(I-15)*INPRO(1)
        D(2)=DM1(I-14)*INPRO(2)
        D(3)=DM1(I-13)*INPRO(3)
        D(4)=DM1(I-12)*INPRO(4)
        D(5)=DM1(I-11)*INPRO(5)
        D(6)=DM1(I-10)*INPRO(6)
        D(7)=DM1(I-9)*INPRO(7)
        D(8)=DM1(I-8)*INPRO(8)
        D(9)=DM1(I-7)*INPRO(9)
        D(10)=DM1(I-6)*INPRO(10)
        D(11)=DM1(I-5)*INPRO(11)
        D(12)=DM1(I-4)*INPRO(12)
        D(13)=DM1(I-3)*INPRO(13)
        D(14)=DM1(I-2)*INPRO(14)
        D(15)=DM1(I-1)*INPRO(15)
        D(16)=DM1(I)*INPRO(16)
        D(17)=DM1(I+1)*INPRO(17)
        D(18)=DM1(I+2)*INPRO(18)
        D(19)=DM1(I+3)*INPRO(19)
        D(20)=DM1(I+4)*INPRO(20)
        D(21)=DM1(I+5)*INPRO(21)
        D(22)=DM1(I+6)*INPRO(22)
        D(23)=DM1(I+7)*INPRO(23)
        D(24)=DM1(I+8)*INPRO(24)
        D(25)=DM1(I+9)*INPRO(25)
        D(26)=DM1(I+10)*INPRO(26)
        D(27)=DM1(I+11)*INPRO(27)
        D(28)=DM1(I+12)*INPRO(28)
        D(29)=DM1(I+13)*INPRO(29)
        D(30)=DM1(I+14)*INPRO(30)
        D(31)=DM1(I+15)*INPRO(31)
        T=0.0
        DO 100 J=1,31
        T=T+D(J)
  100   CONTINUE
        DM2(I-14)=T/AREA
  110   CONTINUE
        RETURN
        END
```

```
C       SUBROUTINE ASSIGN
C
C       INITIALIZES ARRAYS, SETS UP FOR PLOTTING AND LABELS TRACING
C
        SUBROUTINE ASSIGN(X,Y1,Y2,Y3,DISP,STRCN,XN,AXL,AYL,AYU,TITLE)
        COMMON IBUF,XY
        INTEGER IBUF(1000)
        REAL X(203),Y1(203),Y2(203),Y3(203),AXL(33),AYL(33),AYU(33)
       1,TITLE(10)
C
C       SET UP FOR PLOTTING
        CALL PLOTS(IBUF,1000,6)
C
C       IDENTIFY TRACING
        CALL SYMBOL(0.0,3.0,.28,'HOLTS',0.0,5)
C       WRITE INSTRUMENTAL PROFILE NAME ON TRACING
C
        CALL SYMBOL(3.0,3.0,.14,TITLE,0.0,40)
        CALL PLOT(6.0,0.0,-3)
C
C       LABEL DATA SET SEQUENCE NUMBER
        CALL SYMBOL(2.0,4.0,.14,'TAPE=',0.0,5)
        CALL NUMBER(2.7,4.0,.14,XN,0.0,-1)
C
C       INDICATE STRENGTH CONSTANT USED AND DISPERSION
        CALL SYMBOL(2.0,3.0,.14,'STR=',0.0,4)
        CALL NUMBER(2.56,3.0,.14,STRCN,0.0,2)
        CALL SYMBOL(2.0,2.0,.14,'DISP=',0.0,5)
        CALL NUMBER(2.70,2.0,.14,DISP,0.0,3)
C
C       REDEFINE ORIGIN
        CALL PLOT(4.0,1.0,-3)
C
C       DRAW VERTICAL AXIS
        CALL AXIS(0.0,0.0,'RL',2,5.0,90.0,1.0,-.2)
C
C       INITIALIZE INFORMATION FOR PLOTTING SUBROUTINES
        Y1(1)=0.0
        Y2(1)=0.0
        Y3(1)=0.0
        X(202)=0.0
        Y1(202)=1.0
        Y2(202)=1.0
        Y3(202)=1.0
        X(203)=20.0
        Y1(203)=-.2
        Y2(203)=-.2
        Y3(203)=-.2
C
C       CALCULATE HORIZONTAL AXIS WITH INPUT DISPERSION
```

```
      DO 100 I=1,201
      X(I)=(I-2)*DISP
  100 CONTINUE
      XY=10.*DISP
      DO 110 I=1,3
      AXL(I)=0.0
      AXL(I+3)=DISP
      AXL(I+6)=2.*DISP
      AXL(I+9)=3.*DISP
      AXL(I+12)=4.*DISP
      AXL(I+15)=5.*DISP
      AXL(I+18)=6.*DISP
      AXL(I+21)=7.*DISP
      AXL(I+24)=8.*DISP
      AXL(I+27)=9.*DISP
  110 CONTINUE
      AXL(31)=10.*DISP
      AXL(32)=0.0
      AXL(33)=1.0
      RETURN
      END
```

```
//GO.PLOTTAPE DD DSNAME=UVIC,UNIT=TAPE,DISP=(NEW,KEEP),                    *
//  LABEL=(,SL),VOLUME=SER=B00071,DCB=(DEN=2)
//GO.FT08F001 DD UNIT=SYSDA,DISP=(NEW,DELETE),                            *
//  SPACE=(20,(1000),RLSE,CONTIG),DCB=(OPTCD=C,RECFM=F)
//GO.FT09F001 DD DSNAME=HOLTS7,UNIT=TAPE,LABEL=(7,SL),DISP=(OLD,KEEP),    *
//  VOLUME=SER=B00007,DCB=(RECFM=VSB,LRECL=20,BLKSIZE=4004)
//GO.FT10F001 DD DSNAME=HOLTS8,UNIT=TAPE,LABEL=(8,SL),DISP=(OLD,KEEP),    *
//  VOLUME=SER=B00007,DCB=(RECFM=VSB,LRECL=20,BLKSIZE=4004)
//GO.FT11F001 DD DSNAME=HOLTS9,UNIT=TAPE,LABEL=(9,SL),DISP=(OLD,KEEP),    *
//  VOLUME=SER=B00007,DCB=(RECFM=VSB,LRECL=20,BLKSIZE=4004)
//GO.FT12F001 DD DSNAME=HOLT10,UNIT=TAPE,LABEL=(10,SL),DISP=(OLD,KEEP),   *
//  VOLUME=SER=B00007,DCB=(RECFM=VSB,LRECL=20,BLKSIZE=4004)
//GO.FT13F001 DD DSNAME=HOLT11,UNIT=TAPE,LABEL=(11,SL),DISP=(OLD,KEEP),   *
//  VOLUME=SER=B00007,DCB=(RECFM=VSB,LRECL=20,BLKSIZE=4004)
//GO.FT14F001 DD DSNAME=HOLT12,UNIT=TAPE,LABEL=(12,SL),DISP=(OLD,KEEP),   *
//  VOLUME=SER=B00007,DCB=(RECFM=VSB,LRECL=20,BLKSIZE=4004)
//GO.FT15F001 DD DSNAME=HOLT13,UNIT=TAPE,LABEL=(13,SL),DISP=(OLD,KEEP),   *
//  VOLUME=SER=B00007,DCB=(RECFM=VSB,LRECL=20,BLKSIZE=4004)
//GO.FT16F001 DD DSNAME=HOLT14,UNIT=TAPE,LABEL=(14,SL),DISP=(OLD,KEEP),   *
//  VOLUME=SER=B00007,DCB=(RECFM=VSB,LRECL=20,BLKSIZE=4004)
//GO.FT17F001 DD DSNAME=HOLT15,UNIT=TAPE,LABEL=(15,SL),DISP=(OLD,KEEP),   *
//  VOLUME=SER=B00007,DCB=(RECFM=VSB,LRECL=20,BLKSIZE=4004)
//GO.FT18F001 DD DSNAME=HOLT16,UNIT=TAPE,LABEL=(16,SL),DISP=(OLD,KEEP),   *
//  VOLUME=SER=B00007,DCB=(RECFM=VSB,LRECL=20,BLKSIZE=4004)
//GO.FT19F001 DD DSNAME=HOLT17,UNIT=TAPE,LABEL=(17,SL),DISP=(OLD,KEEP),   *
//  VOLUME=SER=B00007,DCB=(RECFM=VSB,LRECL=20,BLKSIZE=4004)
//GO.FT20F001 DD DSNAME=HOLT18,UNIT=TAPE,LABEL=(18,SL),DISP=(OLD,KEEP),   *
//  VOLUME=SER=B00007,DCB=(RECFM=VSB,LRECL=20,BLKSIZE=4004)
```

REFERENCES

GENERAL

Aller, L. H. Astrophysics: The Atmospheres of the Sun and Stars. Second edition. New York: Ronald Press Company, 1963.

Davis, S. P. and Phillips, J. G. The Red System ($A^2\Pi$-$X^2\Sigma$) of the CN Molecule. Berkeley and Los Angeles: University of California Press, 1963.

Fujita, Y. Interpretation of Spectra and Atmospheric Structure in Cool Stars. Tokyo: University of Tokyo Press, 1970.

Herzberg, G. Spectra of Diatomic Molecules. New York: Van Nostrand Book Company, 1950.

Jevons, W. Band Spectra of Diatomic Molecules. London: Physical Society, 1932.

Johnson, R. C. An Introduction to Molecular Spectra. London: Methuen and Company, 1949.

Kaplan, W. Advanced Calculus. Reading: Addison-Wesley Publishing Company, 1952.

Kovacs, I. Rotational Structure of Diatomic Molecules. London: A. Hilger, 1969.

Mihalas, D. Stellar Atmospheres. San Francisco: W. H. Freeman and Company, 1970.

Moore, C. E., Minnaert, M. G. J. and Houtgast, J. The Solar Spectrum 2935 A to 8770 A. Washington: National Bureau of Standards, 1966.

Wright, K. O. Astronomical Techniques. Volume 2 of Stars and Stellar Systems. Edited by W. A. Hiltner. Third edition. Chicago: University of Chicago Press, 1966.

PAPERS

Arnold, J. O., Whiting, E. E. and Lyle, G. C. 1969, J.Q.S.R.T., 9, 775

Bracewell, R. N. 1955, J. Opt. Soc. Am., 45, 873

Caughlan, G. R.	1965, Ap. J., 141, 688
Caughlan, G. R. and Fowler, W. A.	1962, Ap. J., 136, 453
Climenhaga, J. L.	1960, Pub. Dom. Ap. Obs., 11, No. 16
	1966, Colloquium on Late-Type Stars, 54
Climenhaga, J. L., Holts, J. T. and Smolinski, J.	1971, B.A.A.S., 3, 9
Dieke, G. H.	1935, Phys. Rev., 47, 661
Earls, L. T.	1935, Phys. Rev., 48, 423
Eddington, A. S.	1913, M.N.R.A.S., 73, 359
Faÿ, T., Marenin, I. and Van Citters, W.	1971, J.Q.S.R.T., 11, 1203
Finn, G. D. and Mugglestone, D.	1965, M.N.R.A.S., 129, 221
Fujita, Y.	1962, J.R.A.S.C., 56, 1
	1963, Proc. Jap. Acad., 39, 48
	1964, ibid., 40, 332
	1965, Vistas in Astr., 7, 71
	1966, I. A. U. Symp., 24, 21
	1967a, Proc. Jap. Acad., 43, 472
	1967b, ibid., 43, 966
	1968a, ibid., 44, 495
	1968b, Bull. Astr. Inst. Czech., 19, 274
Fujita, Y. and Tsuji, T.	1964, Proc. Jap. Acad., 40, 404
	1965, Pub. Dom. Ap. Obs., 12, 339
	1966, I. A. U. Symp., 26, 307
Fujita, Y. and Utsumi, K.	1963, Proc. Jap. Acad., 39, 358
Fujita, Y. and Yamashita, Y.	1960, Publ. Astr. Soc. Japan, 12, 267

Fujita, Y. and Yamashita, Y.	1963, Pub. Dom. Ap. Obs., 12, 117
Fujita, Y., Tsuji, T. and Maehara, H.	1966a, Proc. Jap. Acad., 42, 765
	1966b, Colloquium on Late-Type Stars, 75
	1969, Proc. Jap. Acad., 45, 484
Fujita, Y., Yamashita, Y. and Tsuji, T.	1964, Proc. Jap. Acad., 40, 664
Fujita, Y., Yamashita, Y., Kamijo, F., Tsuji, T. and Utsumi, K.	1965, Pub. Dom. Ap. Obs., 12, 293
Harris, D. L.	1948, Ap. J. 108, 112
Hayashi, C.	1964, Private communication to Fujita.
Hirai, M.	1969, Publ. Astr. Soc. Japan, 21, 91
Hjerting, F.	1938, Ap. J., 88, 508
McKellar, A.	1936, Pub. Astr. Soc. Pac., 48, 216
	1948, Pub. Dom. Ap. Obs., 7, 396
	1949, Contri. Dom. Ap. Obs., No. 20 235
	1952, ibid., No. 28, 156
Mannino, G.	1958, Mem. Soc. Ital. Astr., XXIX, 1
Mendoza, E. E. and Johnson, H. L.	1965, Ap. J., 141, 161
Menzel, D. H.	1930, Pub. Astr. Soc. Pac., 42, 34
	1936, Ap. J., 105, 126
Miller, L. W. and Gordan, A. R.	1931, J. Phys. Chem., 35, 2874
Minnaert, M.	1935, Zs. f. Ap., 10, 40
Mulliken, R. and Christy, A.	1931, Phys. Rev., 38, 87
Poletto, G. and Rigutti, M.	1965, Nuovo. Cim., 39, 519
Posener, D. W.	1959, Aust. J. of Phy., 12, 184
Richarson, E. H.	1968, J.R.A.S.C., 62, 313
Sanford, R. F.	1929, Pub. Astr. Soc. Pac., 41, 271

Sanford, R. F.	1932, ibid., 44, 246
	1940, ibid., 52, 203
Shajn, G.	1942, Observatory, 64, 255
Spindler, R. J.	1965, J.Q.S.R.T., 5, 165
Tatum, J. B.	1966, Pub. Dom. Ap. Obs., 13, 1
	1967, Ap. J. Supp., 14, 21
Tsuji, T.	1966, Proc. Jap. Acad., 42, 258
Utsumi, K.	1963, Pub. Astr. Soc. Japan, 15, 482
	1967, ibid., 19, 342
	1970, ibid., 22, 93
Wyller, A. A.	1957, Ap. J., 125, 177
	1958, ibid., 127, 763
	1959, A. J., 64, 57
	1960, Ast. Nor., 7, 13
Yamashita, Y.	1967, Pub. Dom. Ap. Obs., 13, 67

VITA

Surname: Holts Given Names: John Thomas

Place of Birth: Victoria, British Columbia

Date of Birth: April 13, 1947

Educational Institutions Attended, with Dates of Entering and Leaving:

University of Victoria 1965 to 1972

Degrees, Diplomas, Etc., Awarded, with Dates and Names of Institutions:

B. Sc. 1969 University of Victoria

Honours and Awards:

University of Victoria Graduate Scholarship 1969 - 1970

University of Victoria Graduate Scholarship 1970 - 1971

National Research Council Bursary 1971 - 1972

PARTIAL COPYRIGHT LICENSE

I hereby grant the right to lend my thesis or dissertation (the title of which is shown below) to users of the University of Victoria Library, and to make single copies only for such users or in response to a request from the library of any other university, or similar institution, on its behalf or for one of its users. I further agree that permission for extensive copying of this thesis for scholarly purposes may be granted by me or a member of the University designated by me. It is understood that copying or publication of this thesis for financial gain shall not be allowed without my written permission.

Title of Thesis/Dissertation

C^{12}/C^{13} Ratio from CN Bands in the Near Infra-Red Spectra of Some Carbon Stars.

Author [redacted]

signature

John Thomas Holts

name

Feb 12 / 1975

date